الجمهورية الجزائرية الديمقراطية الشعبية

People's democratic Republic of Algeria

وزارة التعليم العالي والبحث العلمي

Ministry of Higher Education and Scientific Research

جامعة الشهيد الشيخ العربي التبسي – تبسة

Echahid Cheikh Larbi Tebessi University -Tebessi -

Faculty of science and Technology

Civil Engineering Department

Master's Thesis

Presented for obtaining the Academic Master's degree

In: Civil Engineering

Specialty: Geotechnic

By: Serradj Chaima

Title

Load Bearing Capacity of Cohesive-Frictional Soils Reinforced with Full-Wraparound Geotextiles: A Numerical Investigation

before the jury

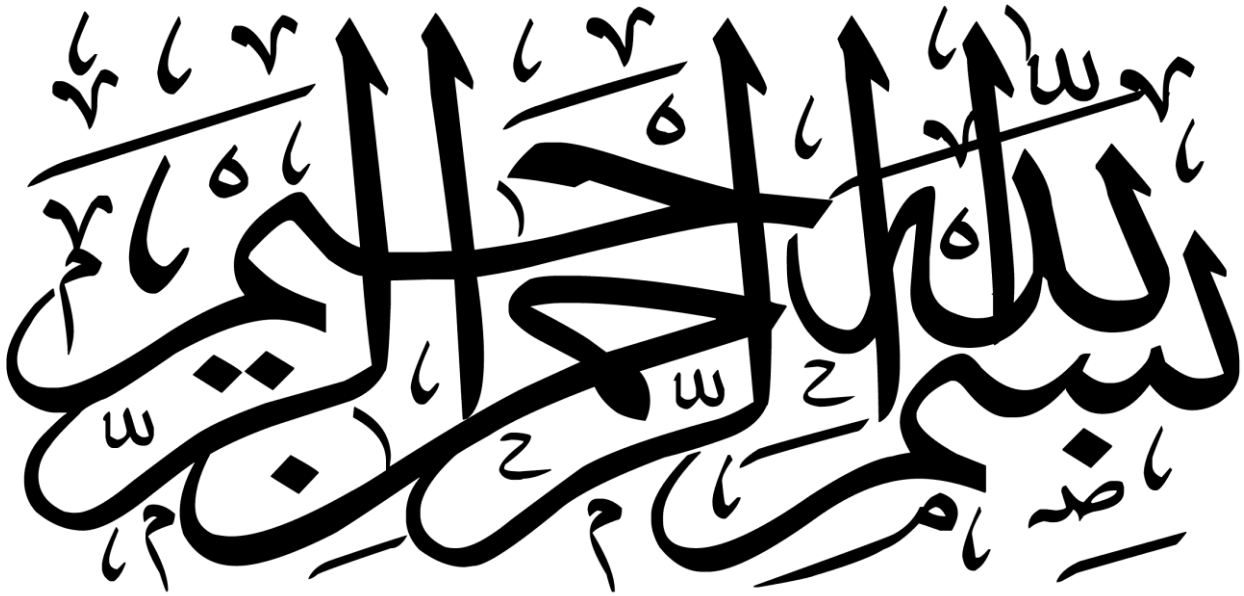
Presented and supported publicly, the 10/06/2025

composed of:

M/ Abdelkader Houam	Full Professor	President
M/ Rafik Boufarh	Lecturer –A-	supervisor
M/ Rachida Malaoui	Lecturer –B-	Examiner

Academic Year

2024/2025


بسم الله الرحمن الرحيم

Acknowledgment

In the Name of Allah, the Most Gracious, Most Merciful.

I would like to express my sincere gratitude, appreciation, and respect to my supervisor, ***Dr. Rafik Boufarh****, who guided this research and generously devoted his time and expertise to support it. I am truly thankful for his encouragement, patience, and understanding throughout this journey.*

I would also like to extend my deep gratitude to the members of the jury committee who dedicated their valuable time to read and evaluate my work.

My heartfelt thanks go to all the esteemed teachers whom I deeply respect and appreciate for their continuous efforts and dedication over the years.

A special appreciation goes to everyone who supported me, contributed to my growth, and positively impacted my academic path.

Finally, and most importantly, I would like to thank all those who believed in me and stood by my side throughout this endeavor.

Dedication

*To the one whose prayers were the secret behind my success, whose kind gaze gave me strength in difficult times… to **my father**, my first support and eternal safety.*

*And to the source of tenderness, my companion through every stage of life… to **my mother**, who embraced my weakness and pushed me forward no matter what.*

To my beloved sisters, the companions of my heart and laughter, and to my dear brothers, the protectors of my back and soul… thank you for always being there and for your priceless love.

To my dearest friends, those who were the light in darkness, the laughter in exhaustion, and the push when I felt I couldn't go on… thank you for being the most beautiful part of this journey.

And finally, I dedicate this work to myself…

To the girl who stumbled but stood again, who cried but kept going, who was afraid but still faced it all.

To you — my strength, my pride, and the beginning of all that's yet to come, God willing.

Abstract

This numerical study aims to enhance the bearing capacity of shallow foundations built over weak soils by investigating different soil types and geotextile reinforcement configurations using PLAXIS 2D software. The research focuses on two main techniques: a simple horizontal reinforcement layout and a full wraparound method, where geotextile fully surrounds the soil including lateral and top sides, and is filled with soil from the inside and additionally covered from the top. Several key parameters were analyzed, including the embedment depth of the top geotextile layer (U), the width of the reinforcement (W), the vertical spacing between layers (H), and the number of geotextile layers (N). The results showed that the full wraparound configuration significantly outperformed the simple horizontal reinforcement in terms of bearing capacity improvement. The study also identified optimal ranges for the dimensionless parameters U/B, W/B, H/B, and N. These findings offer practical insights into cost-effective and performance-optimized design strategies for reinforced soil foundations.

Keywords

Bearing capacity, Cohesive-Frictional soils, geosynthetics, full-wraparound reinforcement, numerical modeling, PLAXIS 2D, parametric study.

Résumé

Cette étude numérique vise à améliorer la capacité portante des fondations superficielles construites sur des sols faibles en examinant différents types de sols et configurations de renforcement par géotextile à l'aide du logiciel PLAXIS 2D. La recherche se concentre sur deux techniques principales : une disposition de renforcement horizontal simple et une méthode d'enveloppement complet, où le géotextile entoure complètement le sol, y compris les côtés latéraux et le côté supérieur, et est rempli de sol de l'intérieur et additionnellement recouvert du dessus. Plusieurs paramètres clés ont été analysés, notamment la profondeur d'encastrement de la couche de géotextile supérieure (U), la largeur du renforcement (W), l'espacement vertical entre les couches (H), et le nombre de couches de géotextile (N). Les résultats ont montré que la configuration d'enveloppement complet surpassait significativement le renforcement horizontal simple en termes d'amélioration de la capacité portante. L'étude a également identifié des plages optimales pour les paramètres adimensionnels U/B, W/B, H/B, et N. Ces résultats offrent des perspectives pratiques pour les stratégies de conception optimisées en termes de coût et de performance pour les fondations en sol renforcé.

Mots-clés

Capacité portante, sols cohésifs-frictionnels, géosynthétiques, renforcement enveloppant complet, modélisation numérique, PLAXIS 2D, étude paramétrique.

الملخص

تهدف هذه الدراسة العددية إلى تعزيز قدرة التحمل للأساسات السطحية المُنشأة على تربة ضعيفة، من خلال دراسة أنواع مختلفة من التربة وتكوينات تدعيم بالجيوتكستيل، باستخدام برنامج PLAXIS 2D. يرتكز البحث على تقنيتين رئيسيتين: ترتيب أفقي بسيط للجيوتكستيل، وطريقة اللف الكامل Full) (Wraparound، حيث يُحيط الجيوتكستيل بالتربة بشكل كامل من الجوانب ومن الأعلى، ويتم ملؤه بالتربة من الداخل وتغطيته بطبقة إضافية من الأعلى.

تم تحليل عدة معلمات رئيسية، من بينها عمق إدراج طبقة الجيوتكستيل العلوية(U) ، عرض التدعيم (W)، المسافة الرأسية بين الطبقات(H) ، وعدد طبقات الجيوتكستيل .(N) أظهرت النتائج أن تكوين اللف الكامل تفوّق بشكل ملحوظ على التكوين الأفقي البسيط من حيث تحسين قدرة التحمل. كما حدّدت الدراسة نطاقات مثلى للمعاملات اللابعديةU/B ، W/B، H/B، و .Nوتُقدّم هذه النتائج رؤى عملية نحو استراتيجيات تصميم فعّالة من حيث التكلفة ومحسّنة من حيث الأداء لتدعيم الأساسات على التربة.

الكلمات المفتاحية

قدرة التحمل، التربة التماسكية-الاحتكاكية، الجيوسينتيتيك، التدعيم باللف الكامل، النمذجة العددية، بلاكسيس D2، الدراسة البارامترية.

List of Figures

Figure Ⅰ-1 Basic Structural Components: From Foundation Soil to Superstructure. 4
Figure Ⅰ-2 Foundation Bearing Capacity and Settlement Patterns Under Different Loading Conditions. 6
Figure Ⅰ-3 Failure mechanism for Terzhagi's bearing capacity solution.[5] 8
Figure Ⅰ-4 Stress Distribution and Failure Zones Beneath a Shallow Foundation.[1] 8
Figure Ⅰ-5 Bearing capacity factors for different ϕ[4] 10
Figure Ⅰ-6 Terzaghi's Bearing Capacity Factors for different ϕ.[4] 10
Figure Ⅰ-7 Terzaghi's Modified Bearing Capacity Factors[1] 11
Figure Ⅰ-8 Meyerhof's bearing capacity coefficients.[1] 13
Figure Ⅰ-9 Identification of items in Hansen's bearing capacity equation.[1] 15
Figure Ⅰ-10 Groundwater effects below base of footing.[7] 15
Figure Ⅰ-11 Plate load Test Setup. [1] 17
Figure Ⅰ-12 Typical plate load test arrangement with counterweights and measurement drvices.[7] 18
Figure Ⅱ-1 Dynamic Compaction of Soil. [9] 22
Figure Ⅱ-2 Application of Dynamic Compaction. [11] 25
Figure **Ⅱ-3** Dynamic Compaction Grid. [11] 26
Figure **Ⅱ-4** Methodology of building stone columns. [16] 30
Figure **Ⅱ-5** Reinforcement function of geosynthetics: a tensile member; and b tensioned membrane.[17] 31
Figure **Ⅱ-6** Variation in ultimate bearing capacity of the foundation bed with and without geosynthetics.[20] 32
Figure **Ⅱ-7** Geogrids used for soil reinforcement [19] 33
Figure **Ⅱ-8** Membrane mechanism [20] 34
Figure **Ⅱ-9** Geonets used for soil reinforcement. [17] 34
Figure Ⅱ-10 Geomembranes used for soil reinforcement. [15] 35
Figure Ⅱ-11 Geosynthetic clay liners used for soil reinforcement. [20] 35
Figure Ⅱ-12 Geotextile-encased used for soil reinforcement. [17] 36
Figure Ⅱ-13 Photograph of the geocell: a folded; b expanded. [20] 36
Figure Ⅱ-14 Different applications of geocells. [20] 37
Figure **Ⅱ-15** Geofoam used for soil reinforcement. [15] 37
Figure Ⅱ-16 Geocomposites used for soil reinforcement. [16] 38
Figure Ⅱ-17 Geotextiles used for soil reinforcement. [17] 39
Figure Ⅱ-18 Reinforcement. [20] 39
Figure Ⅱ-19 Filtration. [20] 40
Figure Ⅱ-20 Separation functions of geosynthetics. [20] 40

Figure Ⅱ-21 Drainage.[20] 41
Figure Ⅱ -22 Classification of Geosynthetics and Their Types.[19] 44
FigureⅢ-1 Geometry of a strip footing resting on a sand layer. 47
Figure Ⅲ-2 Model geometry in the input. 48
Figure Ⅲ-3 Grain size distribution curves of all soil mixtures.[21] 49
Figure Ⅲ-4 the liquid limit, plastic limit, and plasticity index for all the soil mixtures. [21] 49
Figure Ⅲ-5 relationship between the soil strength parameters (friction angle and cohesion) and the amount of clay in the soil. [21] 50
Figure Ⅲ-6 Input window for general soil data information. 51
FigureⅢ-7 Input window for mechanical soil data information. 51
Figure**Ⅲ-9** Generation of boundary conditions. 53
FigureⅢ-10 prescribed vertical displacement 53
FigureⅢ-11 Position of nodes and stress points in soil elements. 54
FigureⅢ-12 Mesh generation. 55
FigureⅢ-13 hydraulic conditions. 55
FigureⅢ-14 Set the current model phase to the initial phase. 56
Figure Ⅲ-15 Set the current model phase to the calculated phase. 57
Figure Ⅲ-16 Deformed mesh. 58
Figure Ⅲ-17 Total displacements U_x. 58
Figure Ⅲ-18 Total displacements U_y. 59
FigureⅢ-19 Calculation information. 59
Figure Ⅲ-20 Load–settlement curve of the footing (PLAXIS 2D) 60
FigureⅣ-1 Ultimate Bearing Capacity vs. Soil Type. 65
Figure Ⅳ-2: Distribution of deformation for different soil types. 67
Figure Ⅳ-3 Reinforcement layout configurations for numerical investigations.[21] 68
Figure **Ⅳ-4** Relationship between bearing stress with various parameters of (U/B). 68
Figure Ⅳ-5 Relationship between bearing stress and S/B ratio with various parameters of U/B 69
Figure Ⅳ-6 effect of U/B ratio on stress distribution below the footing. 70
Figure Ⅳ-7 Relationship between bearing stress with various parameters of (W/B). 71
FigureⅣ-8 Relationship between bearing stress and S/B ratio with various parameters of W/B 72
Figure Ⅳ-9 Effect of geotextile length (W/B) on deformation patterns in reinforced soil. 72
FigureⅣ-10 Relationship between bearing stress with various parameters of (H/B). 73
Figure Ⅳ-11 Relationship between bearing stress and S/B ratio with various parameters of H/B 74
FigureⅣ-12 effect of H/B ratio on stress distribution below the footing. 74
Figure Ⅳ-13 Relationship between bearing stress with various parameters of (N). 75
FigureⅣ-14 effect of number of geotextile layer (N) on soil reinforcement efficiency. 76

FigureⅣ-15 Simulated bearing stress results of strip footing resting on different soils reinforced with different reinforcing (Series C)**.**..... 78
Figure Ⅳ-16 Simulated bearing stress results of strip footing resting on different soils reinforced with different reinforcing (SeriesD). 80
Figure Ⅳ-17 Simulated bearing stress results of strip footing resting on different soils reinforced with different reinforcing (SeriesE)..... 82
Figure **Ⅳ-18** Simulated bearing stress results of strip footing resting on different soils reinforced with different reinforcing (SeriesF) 84
Figure **Ⅳ-19** Simulated stress distribution results are presented for three cases. 85
Figure Ⅳ-20 simulated stress distribution results are shown for the following cases 86
Figure Ⅳ-21 simulated stress distribution results are shown for the following cases 87
Figure Ⅳ-22 simulated stress distribution results are shown for the following cases. 88
Figure Ⅳ-23 simulated stress distribution results are shown for the following cases 89
Figure Ⅳ-24 simulated stress distribution results are shown for the following cases 90

List of Tables

Table Ⅰ- 1 *The bearing capacity factors are graphically.* 14
Table *Ⅱ-1 Suitability of Dynamic Compaction with soil type along with Degree of Saturation.* 24
Table **Ⅲ-1** properties of soils. 50
Table **Ⅲ-2** Geotextile characteristics. 52
Table Ⅲ-8 Input window for geotextile data information. 52
Table Ⅲ-3 Comparison between Numerical and Analytical Bearing Capacities for Unreinforced Soil. **61**
Table Ⅳ-1 Details of numerical programs 64
Table Ⅳ-2 Ultimate Bearing Capacity vs Soil Type. 65

List of Symbols and acronyms

Symbol / Acronym	Description	Unit
q_a	Allowable bearing pressure	kPa
q_s	Safe bearing capacity	kPa
q_n	Net ultimate bearing capacity	kPa
q_u	Ultimate bearing capacity	kPa
γ	Unit weight of soil	kN/m³
γ_{sat}	Saturated unit weight of soil	kN/m³
γw	Unit weight of water	kN/m³
c	Soil cohesion	kPa
φ	Internal friction angle	°
ψ	Dilatancy angle	°
E	Young's modulus	kN/m²
ν	Poisson's ratio	–
K_o	Coefficient of earth pressure at rest	–
FS	Factor of safety	–
Nc	Bearing capacity factor related to cohesion	–
Nq	Bearing capacity factor related to surcharge	–
$N\gamma$	Bearing capacity factor related to unit weight	–
Sc	Shape factor related to cohesion	–
Sq	Shape factor related to surcharge	–
$S\gamma$	Shape factor related to unit weight	–
dc	Depth factor related to cohesion	–
dq	Depth factor related to surcharge	–
$d\gamma$	Depth factor related to unit weight	–
ic	Inclination factor related to cohesion	–
iq	Inclination factor related to surcharge	–
$i\gamma$	Inclination factor related to unit weight	–
B	Width of the foundation	m
D	Depth of foundation	m
GCL	Geosynthetic Clay Liner	–

SPT	Standard Penetration Test	–

Table of contents

Acknowledgment

Dedication

Abstract

Résumé

الملخص

List of figures

List of Tables

List of Symbols and acronyms

Table of contents

Introduction

Chapter Ⅰ: bearing capacity of Shallow foundation

Ⅰ-1 Introduction 4

Ⅰ-2- Definitions 4

Ⅰ-2-1-Bearing capacity 4

Ⅰ-2-2- ultimate Bearing Capacity (q_U) 5

Ⅰ-2-3-Net ultimate Bearing Capacity (q_n) 5

Ⅰ-2-4-Safe Bearing Capacity (q_s) 5

Ⅰ-2-5-Allowable Bearing Pressure (q_a) 5

Ⅰ-2-6-Foundation 5

Ⅰ-3-Bearing capacity failure 6

Ⅰ-4Ultimate Bearing Capacity Equations 7

Ⅰ-4-1 Terzaghi's Bearing Capacity equation 7

Ⅰ-4-1-1Assumptions 7

Ⅰ-4-1-2Limitations 8

Ⅰ-4-1-3Concept 9

Ⅰ-4-1-4-A Modified Bearing Capacity Factors 10

Ⅰ-4-1-5 Effect of shape of Foundation 12

Ⅰ-4-2Meyerhof's Bearing Capacity equation 12

Ⅰ-4-3Brinch Hansen's Bearing Capacity equation 14

Ⅰ-5Effect of Water Table fluctuation 15

Ⅰ-6Factor of safety or safety factor (F_S) 16

Ⅰ-7Determination of Bearing Capacity from field tests 16
Ⅰ-7-1. Plate Loading Test:..... 16
Ⅰ-7-1-1Procedure: 16
Ⅰ-7-2Standard Penetration Test (SPT): 18
Ⅰ-8Conclusion:..... 20

Chapter Ⅱ:Soil Reinforcement Techniquesiel et mèthod

Ⅱ-1Introduction 22
Ⅱ-2-Definition Reinforced soil..... 22
Ⅱ-3-Traditional Soil Reinforcement Techniques 22
Ⅱ-3-1-Dynamic Compaction 22
Ⅱ-3-1-1-Definition..... 23
Ⅱ-3-1-2 Suitability..... 23
Ⅱ-3-1-3 Execution Method of Dynamic Compaction 24
Ⅱ-3-1-4 Applications in Various Industries..... 26
Ⅱ-3-1-5 Advantages..... 26
Ⅱ-3-1-6 Disadvantages 27
Ⅱ-3-2- Soil Replacement 27
Ⅱ-3-2-1 Definition 27
Ⅱ-3-2-2 Applications..... 27
Ⅱ-3-2-3 Application Procedure of Soil Replacement 28
Ⅱ-3-2-4 Advantages 29
Ⅱ-3-2-5 Limitations..... 29
Ⅱ-4 Modern Soil Reinforcement Techniques 29
Ⅱ-4-1 Stone Columns 29
Ⅱ-4-1-1 Definition..... 29
Ⅱ-4-1-2 Construction Methodology 29
Ⅱ-4-1-3 Key Features and Benefits 30
Ⅱ-4-2 Geosynthetics 31
Ⅱ-4-2-1 Definition..... 31
Ⅱ-4-2-2 The Functions Of Geo-Synthetics..... 31

Ⅱ-4-2-3 Reinforcement..... 31
Ⅱ-4-2-4 Filtration..... 32
Ⅱ-4-2-5 Separation 32
Ⅱ-4-2-6 Drainage..... 32
Ⅱ-4-2-7Erosion Control..... 32
Ⅱ-4-2-8 Barrier/Protection..... 33
Ⅱ-4-3 Geo synthetics classified..... 33
Ⅱ-4-3-1 Geogrids..... 33
Ⅱ-4-3-2 Geonets 34
Ⅱ-4-3-3Geomembranes 34
Ⅱ-4-3-4Geosynthetic clay liners (GCLs)..... 35
Ⅱ-4-3-5Geotextile-encased..... 35
Ⅱ-4-3-6 Geocells 36
Ⅱ-4-3-7 Geofoam..... 37
Ⅱ-4-3-8Geocomposites..... 38
Ⅱ-4-3-9 Geotextiles 38
Ⅱ-4-3-9-1 Functions of Geotextiles..... 39
Ⅱ-4-3-9-1-1 Reinforcement..... 39
Ⅱ-4-3-9-1-2 Filtration..... 40
Ⅱ-4-3-9-1 -3 Separation..... 40
Ⅱ-4-3-9-1 -4 Drainage 40
Ⅱ-4-3-9-1 -5Erosion Control..... 41
Ⅱ-4-3-9-1 -6 Barrier/Protection..... 41
Ⅱ-4-3-9-2 Types of Geotextiles..... 41
Ⅱ-4-3-9-2-1Woven Geotextiles..... 41
Ⅱ-4-3-9-2-2 Non-Woven Geotextiles..... 41
Ⅱ-4-3-9-2-3Knitted Geotextiles..... 42
Ⅱ-4-3-9-3Applications of Geotextiles in Engineering 42
Ⅱ-4-3-9-4 Properties of Geotextiles 42
Ⅱ-4-3-9-4-1 Physical Properties..... 42

Ⅱ-4-3-9-4-2Mechanical Properties 42
Ⅱ-4-3-9-4-3 Hydraulic Properties 43
Ⅱ-4-3-9-4-4 Durability 43
Ⅱ-5 Conclusion 45

Chapter III: Numerical analysis

Ⅲ-1Introduction 47
Ⅲ-2 Geometry 47
Ⅲ-3Materials 48
Ⅲ-3-1 Soil Samples 48
Ⅲ-3-2Reinforcement Geotextile 51
Ⅲ-4Boundary Conditions (Conditions aux limites) 52
Ⅲ-5Loading (Chargement) 53
Ⅲ-6Meshing 54
Ⅲ-7 Hydraulic Conditions (Conditions hydrauliques) 55
Ⅲ-8 Calculation phases 56
Ⅲ-8-1 Initial Phase 56
Ⅲ-8-2Type of Analysis – Plastic Calculation 56
Ⅲ-8-3Analysis of Mesh Deformation 57
Ⅲ-8-3-1Mesh Deformation 57
Ⅲ-8-3-2Total Horizontal Displacement (Ux): 58
Ⅲ-8-3-3Total Vertical Displacement (Uy): 58
Ⅲ-9Bearing Capacity 59
Ⅲ-10Validation by Comparing Plaxis and Terzaghi Results 60
Ⅲ-11Conclusion 61

Chapter Ⅳ: Parametric study

Ⅳ-1Introduction: 63
Ⅳ-2Effect of Soil Nature (Series A): 65
Ⅳ-2-1Results and Discussion : 65
Ⅳ-3Effect of Reinforcement – Series B: 67
Ⅳ-3-2Effect of Geotextile Width (W) (Series B2) : 71

Ⅳ-3-2-1Results and Discussion: 71
Ⅳ-3-3Effect of Vertical Spacing Between Reinforcement Layers (H/B) -Series B3 : 73
Ⅳ-3-3-1Results and Discussion: 73
Ⅳ-4 Serie c: 76
Ⅳ-4-1-1Results and Discussion: 77
Ⅳ-5 Serie D: 79
Ⅳ-5-11Results and Discussion: 80
Ⅳ-6 Serie E (Full Wraparound with B0 Core): 81
Ⅳ-6-1 Results and Discussion: 82
Ⅳ-7 Series F (Full Wraparound with Full Encapsulation) : 83
Ⅳ-7-1Results and Discussion: 84
Ⅳ-8Conclusion 91
Conclusion ***92***
References ***94***

Introduction

In recent decades, the world has witnessed a significant rise in population density, which has led to intensive urban expansion to meet the growing demand for housing and infrastructure. This increasing pressure has driven the need to utilize all available types of land, including those with weak geotechnical characteristics that are not naturally suitable for direct construction. In this context, the concept of bearing capacity becomes crucial, as it represents the soil's ability to support structural loads without undergoing failure or excessive settlement.

Through bearing capacity analysis, engineers can evaluate the suitability of soils and classify them accordingly, determining whether they require improvement. While some soils are inherently strong and stable, others are weak and prone to collapse, necessitating treatment before any construction work. As a result, soil reinforcement has emerged as a key discipline in geotechnical engineering, with various techniques developed to improve the mechanical performance of soil, whether through chemical stabilization, physical modification, or reinforcement using geosynthetic materials such as geotextiles.

These reinforcement methods vary, including both vertical techniques (e.g., columns or piles) and horizontal ones using reinforcement layers. Since the shallow foundation is the interface between the structure and the ground, its stability directly depends on the behavior of the underlying soil. Consequently, ensuring sufficient soil improvement becomes essential, particularly for sensitive or high-load projects.

Although traditional horizontal reinforcement techniques have shown some effectiveness, they do not always deliver optimal results, especially in very weak soils or under heavy loading. This has led to the exploration of enhanced or alternative methods. One such method is the Full Wraparound technique, a relatively new and not widely adopted approach that involves fully enclosing the soil beneath and around the foundation using geotextile layers—both from the sides and from the top. This improves the confinement effect and increases the area of interaction between the reinforcement and the surrounding soil.

While this technique has been the subject of limited experimental studies in the past, the present work is distinguished by its numerical evaluation using advanced modeling, along with a personalized approach to optimize and adapt the method to different soil conditions.

This research is divided into three main parts:

- **The first part** includes two theoretical chapters that provide a comprehensive literature review of the concepts related to bearing capacity, as well as a classification and assessment of the main soil reinforcement methods used in civil engineering.
- **The second part** focuses on numerical modeling using PLAXIS 2D software, analyzing the behavior of various types of unreinforced soils and comparing the results with traditional calculations based on Terzaghi's method.
- **The third part** presents a detailed parametric study aimed at evaluating the performance of soils reinforced with geotextiles, comparing the horizontal simple method with the Full Wraparound technique. This part also identifies the key influencing parameters (such as the number of layers, depth, and extension length) in order to determine the most efficient solutions, with careful consideration of the economic aspect.

Chapter I :

Bearing Capacity of Shallow Foundation

Ⅰ-1 Introduction

In any construction project, the foundation plays a crucial role as it is the structural element that transfers loads from the structure to the ground. Although this component may not always be visible, its importance cannot be ignored. Without a proper foundation, no building can remain stable or safe.

The stability of a foundation depends largely on the bearing capacity of the soil beneath it. If the ground is too weak, it will not be able to support the structure, which may lead to settlement or even failure. Therefore, understanding and evaluating the soil's bearing capacity is a fundamental step in the design process.

In this chapter, we will study different methods used to estimate the bearing capacity of soil. This includes theoretical approaches as well as practical considerations that help engineers ensure the stability and safety of structures.

Ⅰ-2- Definitions

Ⅰ-2-1-Bearing capacity

Is the ability of foundation soil to support forces from the superstructure without experiencing shear failure or excessive settlement. Foundation soil refers to the portion of ground subjected to additional stresses when foundations and superstructures are constructed upon it. Below are several important terminologies related to soil bearing capacity.

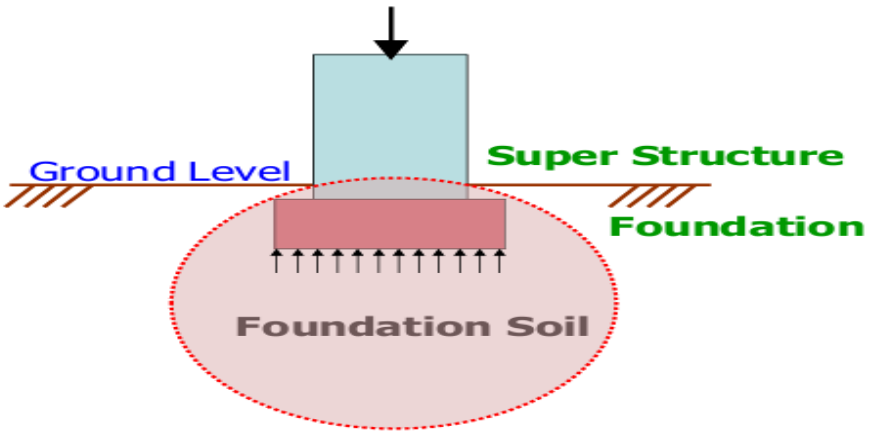


Figure Ⅰ**-1** Basic Structural Components: From Foundation Soil to Superstructure.[1]

Ⅰ-2-2- Ultimate Bearing Capacity (q_U)

It is the maximum pressure that a foundation soil can withstand without undergoing shear failure.

Ⅰ-2-3-Net ultimate Bearing Capacity (q_n)

It is the maximum extra pressure (in addition to initial overburden pressure) that a foundation soil can withstand without undergoing shear failure.

$$q_n = q_u - q_0$$

Here, q_0 represents the overburden pressure at foundation level and is equal to γD for level ground without surcharge where γ is the unit weight of soil and D is the depth to foundation bottom from Ground Level.[1]

Ⅰ-2-4-Safe Bearing Capacity (q_s)

It is the safe extra load the foundation soil is subjected to in addition to initial overburden pressure.

$$q_s = \frac{q_n}{F_S} + q_0$$

Here. **Fs** represent the factor of safety.

Ⅰ-2-5-Allowable Bearing Pressure (q_a)

It is the maximum pressure the foundation soil is subjected to considering both shear failure and settlement.

$$q_a = \frac{q_u}{F_S}$$

Ⅰ-2-6-Foundation

Foundations are simply the bottom part of any structure that touches the ground. When a building stands tall, the foundation is what spreads all that weight into the soil below. [1] It's like the building's footprint, making sure the soil doesn't get stressed beyond what it can

handle. The foundation keeps everything stable - no sliding sideways or tipping over. Geotechnical engineers focus on making sure both the foundation and the soil beneath it stay strong and don't sink too much over time. By the way, you'll often hear people use "footing" and "foundation" to mean the same thing.

Ⅰ-3-Bearing capacity failure

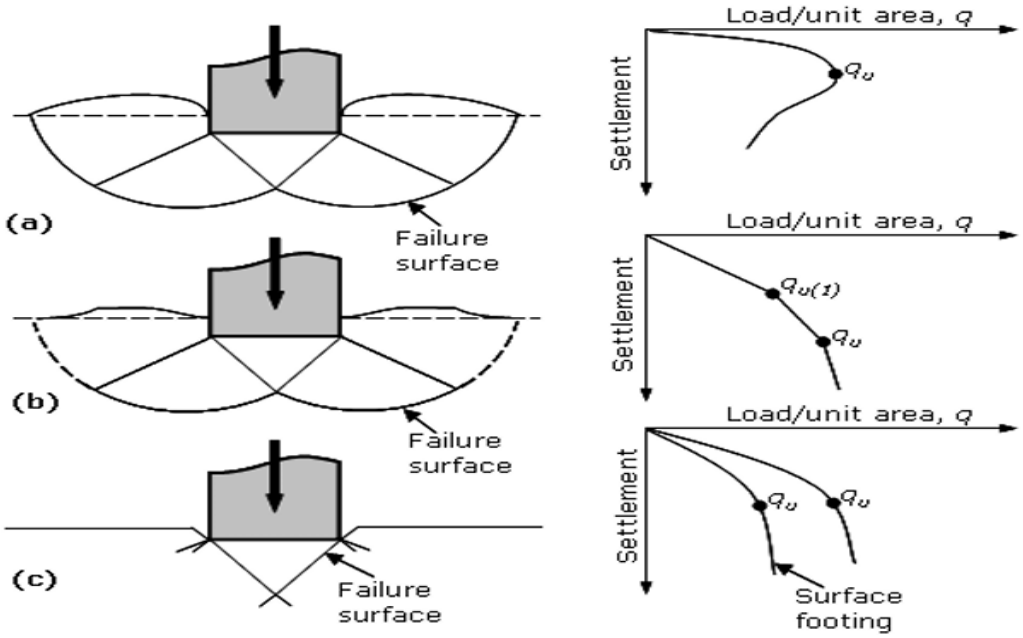


Figure Ⅰ**-2** Types Of Shear Failure: A) The General Shear Failure, B) The Local Shear Failure, C) The Case Of Punching Shear Failure [2].

Relative density of the soil and size of the foundation are among the major factors that affect the mode of bearing failure likely to occur. The modes of bearing failure are generally separated into three categories: The general shear failure (FigureI-2 a) is usually associated with soils of low compressibility such as dense sand and stiff cohesive soils. In this case, if load is gradually applied to the foundation, settlement will increase. At a certain point – when the applied load per unit area equals to the ultimate load qu – a sudden failure in the soil supporting the foundation will take place. The failure surface in the soil will extend to the ground surface and full shear resistance of the soil is developed along the failure surface. Bulging of the soil near the footing is usually apparent. [2]

For the local shear failure (FigureI-2 b), which is common in sands and clays of medium compaction, the failure surface will gradually extend outward from the foundation but will not reach the ground surface as shown by the solid segment in FigureI-2 b. The shear

resistance is fully developed over only part of the failure surface (solid segment of the line). There is a certain degree of bulging of the soil. [1]

In the case of punching shear failure (FigureI-2 c) , a condition common in loose and very compressible soils, considerable vertical settlement may take place with the failure surfaces restricted to vertical planes immediately adjacent to the sides of the foundation; the ground surface may be dragged down. After the first yield has occurred the load-settlement curve will be steep slightly, but remain fairly flat.[2]

Ⅰ-4Ultimate Bearing Capacity Equations

Ⅰ-4-1 Terzaghi's Bearing Capacity Equation

When we talk about the pioneers in soil mechanics, we can't overlook Karl von Terzaghi. He was really the first person to give us a solid, comprehensive theory about how to evaluate bearing capacity for rough shallow foundations.

Terzaghi initially suggested that we should consider a foundation "shallow" if it doesn't go deeper than it is wide. Though interestingly, researchers who came after him found that foundations could still be considered shallow even when they go down to three or four times their width. [3]

Back in 1943, Terzaghi developed this method for figuring out bearing capacity when dealing with general shear failure. What made his approach so valuable was how comprehensive it was—he took into account everything from soil cohesion and friction to the pressure from the soil above and even the weight of the soil itself. It was quite revolutionary for its time and still forms the basis of many calculations we use today. [4]

Ⅰ-4-1-1Assumptions

1) Soil is homogeneous and Isotropic.

2) The shear strength of soil is represented by Mohr Coulombs Criteria.

3) The footing is strip footing type with rough base. It is essentially a two dimensional plane strain problem.

4) Elastic zone has straight boundaries inclined at an angle equal to the horizontal.

5) Failure zone is not extended above, beyond the base of the footing. Shear resistance of soil above the base of footing is neglected.[5]

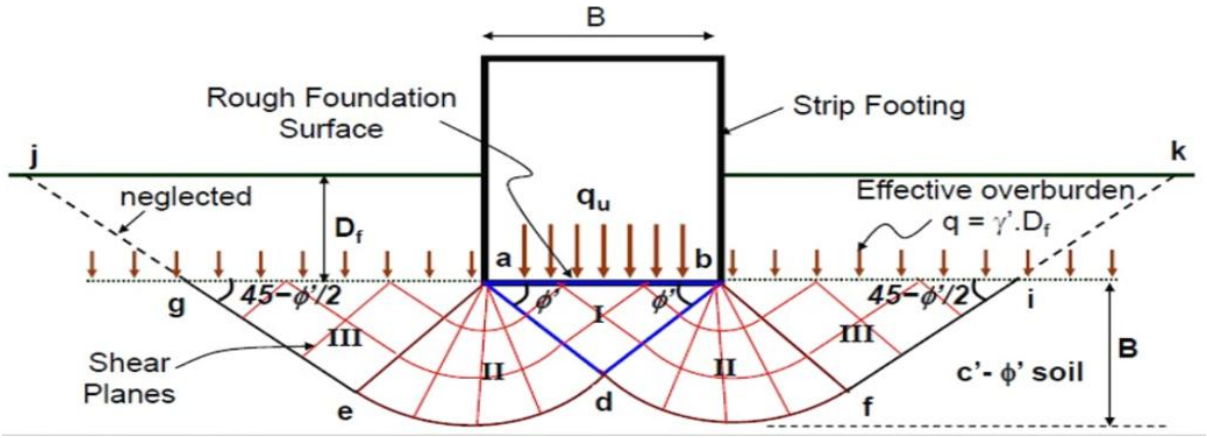


Figure Ⅰ-3 Failure Mechanism for Terzaghi's Bearing Capacity Solution.[5]

Ⅰ-4-1-2Limitations

1. The theory is applicable to shallow foundations

2. As the soil compresses, Φ increases which is not considered. Hence fully plastic zone may not develop at the assumed Φ.

3. All points need not experience limit equilibrium condition at different loads. 4. Method of superstition is not acceptable in plastic conditions as the ground is near failure zone.[5]

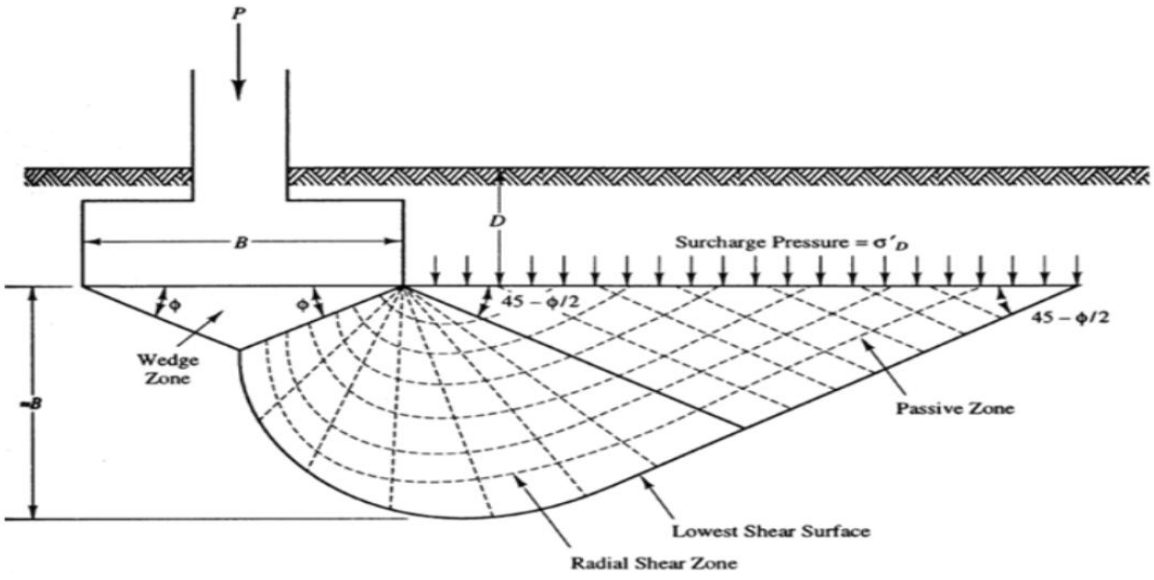


Figure Ⅰ-4 4 Stress Distribution and Failure Zones Beneath a Shallow Foundation.[1]

Ⅰ-4-1-3Concept

A strip footing of width B gradually compresses the foundation soil underneath due to the vertical load from superstructure. Let q_U be the final load at which the foundation soil experiences failure due to the mobilization of plastic equilibrium. The foundation soil fails along the composite failure surface and the region is divided in to five zones, Zone 1 which is elastic, two numbers of Zone 2 which are the zones of radial shear and two zones of Zone 3 which are the zones of linear shear. Considering horizontal force equilibrium and incorporating empirical relation, the equation for ultimate bearing capacity is obtained as follows.[1]

Ultimate bearing capacity: $q_u = cN_c + \gamma DN_q + 0.5\gamma BN\gamma$

If the ground is subjected to additional surcharge load q, then

$$q_u = cN_c + (\gamma D + q)N_q + 0.5\gamma BN\gamma$$

Net ultimate bearing capacity

$$q_n = cN_c + \gamma DN_q + 0.5\gamma BN\gamma - \gamma D$$

$$q_n = cN_c + \gamma D(N_q - 1) + 0.5\gamma BN_\gamma$$

Safe bearing capacity

$$q_s = \left[cN_c + \gamma D(N_q - 1) + 0.5\gamma BN_\gamma\right]\frac{1}{F} + \gamma D$$

Here, F = Factor of safety (usually 3)

c = cohesion

γ = unit weight of soil

D = Depth of foundation

q = Surcharge at the ground level

B = Width of foundation

N_C, Nq, Nγ = Bearing Capacity factors.

ϕ'	N_c	N_q	N_γ[a]	ϕ'	N_c	N_q	N_γ[a]
0	5.70	1.00	0.00	26	27.09	14.21	9.84
1	6.00	1.10	0.01	27	29.24	15.90	11.60
2	6.30	1.22	0.04	28	31.61	17.81	13.70
3	6.62	1.35	0.06	29	34.24	19.98	16.18
4	6.97	1.49	0.10	30	37.16	22.46	19.13
5	7.34	1.64	0.14	31	40.41	25.28	22.65
6	7.73	1.81	0.20	32	44.04	28.52	26.87
7	8.15	2.00	0.27	33	48.09	32.23	31.94
8	8.60	2.21	0.35	34	52.64	36.50	38.04
9	9.09	2.44	0.44	35	57.75	41.44	45.41
10	9.61	2.69	0.56	36	63.53	47.16	54.36
11	10.16	2.98	0.69	37	70.01	53.80	65.27
12	10.76	3.29	0.85	38	77.50	61.55	78.61
13	11.41	3.63	1.04	39	85.97	70.61	95.03
14	12.11	4.02	1.26	40	95.66	81.27	115.31
15	12.86	4.45	1.52	41	106.81	93.85	140.51
16	13.68	4.92	1.82	42	119.67	108.75	171.99
17	14.60	5.45	2.18	43	134.58	126.50	211.56
18	15.12	6.04	2.59	44	151.95	147.74	261.60
19	16.56	6.70	3.07	45	172.28	173.28	325.34
20	17.69	7.44	3.64	46	196.22	204.19	407.11
21	18.92	8.26	4.31	47	224.55	241.80	512.84
22	20.27	9.19	5.09	48	258.28	287.85	650.67
23	21.75	10.23	6.00	49	298.71	344.63	831.99
24	23.36	11.40	7.08	50	347.50	415.14	1072.80
25	25.13	12.72	8.34				

Figure Ⅰ-5 Bearing Capacity Factors for Different Φ [4]

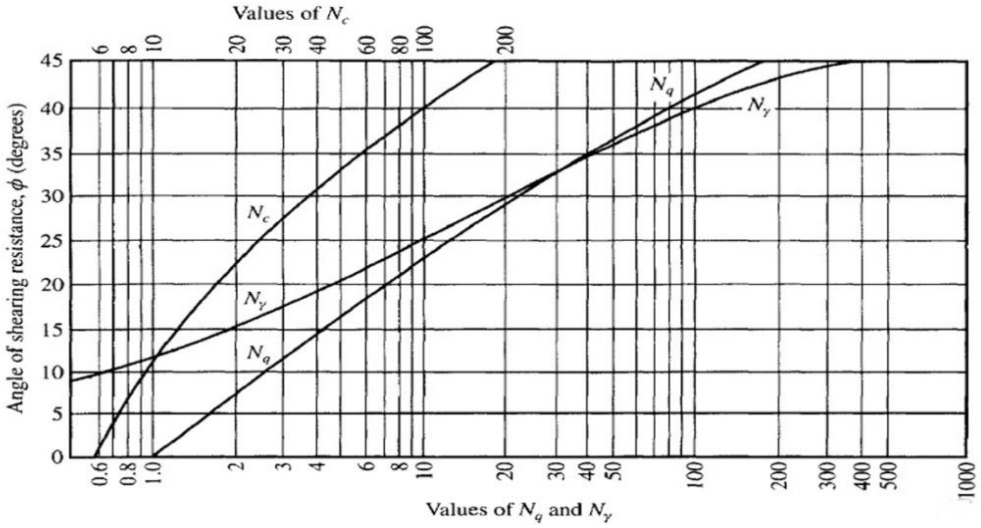


Figure Ⅰ-6 Terzaghi's Bearing Capacity Factors for different ϕ. [4]

Ⅰ-4-1-4-A Modified Bearing Capacity Factors

The classical Terzaghi bearing capacity factors assume general shear failure in homogeneous soil. However, in practical applications, especially for non-standard soil conditions or partially drained states, modified factors are often used. The table below provides modified

values of the bearing capacity factors, and as a function of the internal friction angle, which are suitable for more accurate bearing capacity assessments.

ϕ'	N'_c	N'_q	N'_γ	ϕ'	N'_c	N'_q	N'_γ
0	5.70	1.00	0.00	26	15.53	6.05	2.59
1	5.90	1.07	0.005	27	16.30	6.54	2.88
2	6.10	1.14	0.02	28	17.13	7.07	3.29
3	6.30	1.22	0.04	29	18.03	7.66	3.76
4	6.51	1.30	0.055	30	18.99	8.31	4.39
5	6.74	1.39	0.074	31	20.03	9.03	4.83
6	6.97	1.49	0.10	32	21.16	9.82	5.51
7	7.22	1.59	0.128	33	22.39	10.69	6.32
8	7.47	1.70	0.16	34	23.72	11.67	7.22
9	7.74	1.82	0.20	35	25.18	12.75	8.35
10	8.02	1.94	0.24	36	26.77	13.97	9.41
11	8.32	2.08	0.30	37	28.51	15.32	10.90
12	8.63	2.22	0.35	38	30.43	16.85	12.75
13	8.96	2.38	0.42	39	32.53	18.56	14.71
14	9.31	2.55	0.48	40	34.87	20.50	17.22
15	9.67	2.73	0.57	41	37.45	22.70	19.75
16	10.06	2.92	0.67	42	40.33	25.21	22.50
17	10.47	3.13	0.76	43	43.54	28.06	26.25
18	10.90	3.36	0.88	44	47.13	31.34	30.40
19	11.36	3.61	1.03	45	51.17	35.11	36.00
20	11.85	3.88	1.12	46	55.73	39.48	41.70
21	12.37	4.17	1.35	47	60.91	44.45	49.30
22	12.92	4.48	1.55	48	66.80	50.46	59.25
23	13.51	4.82	1.74	49	73.55	57.41	71.45
24	14.14	5.20	1.97	50	81.31	65.60	85.75
25	14.80	5.60	2.25				

Figure I-7 Terzaghi's Modified Bearing Capacity Factors [1]

These modified factors are particularly useful when accounting for partial mobilization of shear strength or non-linear stress-strain behavior of real soils.

When to use this table:

- When modeling real soil behavior that deviates from ideal conditions (e.g. non-associated flow, reduced mobilization of φ).
- When using numerical models (e.g. FEM software) that incorporate more realistic soil mechanics assumptions.
- For partially saturated or variably saturated soils.
- When guided by references or studies that employ these modified values.

When *not* to use this table:

- For classical Terzaghi analysis under ideal, dry or fully saturated conditions with general shear failure.
- When using alternative bearing capacity theories (e.g. Meyerhof, Vesic).

- For local shear failure, where reductions are made to φ and c instead of using modifiedN_c, N_q, and N_γ.

Use this table only if your analytical or numerical approach explicitly supports or requires these modified values.[6]

Ⅰ-4-1-5 Effect of Shape of Foundation

The shape of footing influences the bearing capacity. Terzaghi and other contributors have suggested the correction to the bearing capacity equation for shapes other than strip footing based on their experimental findings. The following are the corrections for circular, square and rectangular footings.

Circular footing: $q_u = 1.3cN_c + \gamma DN_q + 0.3\gamma BN_\gamma$

Square footing: $q_u = 1.3cN_c + \gamma DN_q + 0.4\gamma BN_\gamma$

Rectangular footing: $q_u = (1 + 0.3\frac{B}{L})cN_c + \gamma DN_q + (1 - 0.2\frac{B}{L})\gamma BN_\gamma$

Where Nc, Nq and Nγ are called the bearing capacity factors and are obtained as follows:

$N_q = \frac{e^{(3\pi/2-\varphi')\tan\varphi'}}{2\cos(45+\varphi'/2)}$ $N_c = cot\varphi'(Nq - 1)$ $N_\gamma = \frac{1}{2}\tan\varphi'(\frac{Kp\gamma}{cos^2\varphi'} - 1)$

Figure I-6 shows the variation of the bearing capacity factors provided by Terzaghi. Based on this figure, Aysen (2002) proposed the following equation to obtain the value of Kpγ in the Nγ equation:

$Kp\gamma = (8\varphi'^2 - 4\varphi' + 3.8)tan^2(60 + \varphi'/2)$

Where ' ϕ in the first term is in radians. In the undrained conditions (cu and φ_u=0):

N_q=1, $N_c = \left(\frac{3}{2}\pi + 1\right) = 5.71$, $N_\gamma = 0$

Ⅰ-4-2Meyerhof's Bearing Capacity Equation

Meyerhof (1951) developed a bearing capacity equation by extending Terzhagi's failure mechanism and taking into account the effects of footing shape, load inclination and footing depth by adding the corresponding factors of s, d, and i. [2]

For a rectangular footing of L by B (L > B) and inclined load:

$$q_u = c' N_c \, sc \, ic \, dc + \gamma D N_q sq \, iq \, dq + 0.5 \, B \, \gamma \, N_\gamma s\gamma \, i\gamma \, d\gamma$$

For vertical load, $ic = iq = i\gamma = 1$.

The bearing capacity factors: $N_\gamma = (Nq - 1) \, tan(1.4\varphi')$

$$N_q = exp(\pi \, tan \, \varphi') \tan(45 + \frac{\varphi'}{2})$$

$$N_c = cot \, \varphi' (Nq - 1)$$

In the undrained conditions (cu and $\varphi_u = 0$):

$N_q = 1 \quad N_c = 5.71 \quad N_\gamma = 0$

φ°	N_c	N_q	N_γ
0	5.14	1.00	0.00
2	5.63	1.20	0.01
4	6.19	1.43	0.04
6	6.81	1.72	0.11
8	7.53	2.06	0.21
10	8.34	2.47	0.37
12	9.28	2.97	0.60
14	10.37	3.59	0.92
16	11.63	4.34	1.37
18	13.10	5.26	2.00
20	14.83	6.40	2.87
22	16.88	7.82	4.07
24	19.32	9.60	5.72
26	22.25	11.85	8.00
28	25.80	14.72	11.19
30	30.14	18.40	15.67
32	35.49	23.18	22.02
34	42.16	29.44	31.15
36	50.59	37.75	44.43
38	61.35	48.93	64.08
40	75.32	64.20	93.69
42	93.71	85.38	139.32
44	118.37	115.31	211.41
46	152.10	158.51	328.74
48	199.27	222.31	526.47
50	266.89	319.07	873.89

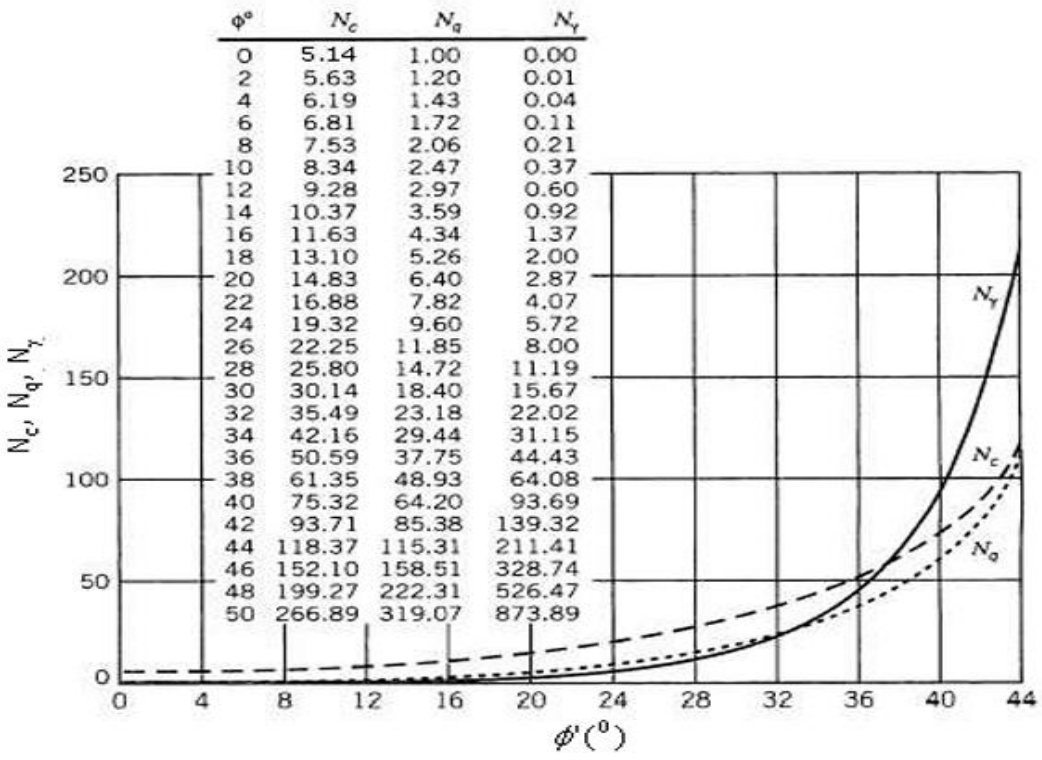


Figure Ⅰ-8 Meyerhof's Bearing Capacity Coefficients.[1]

The bearing capacity factors:

$N_q = \exp(\pi \tan \varphi')tan^2(45 + \varphi'/2)$, $N_c = cot\varphi'(Nq - 1)$, $N_\gamma = (Nq - 1)\tan(1.4\varphi')$

In the undrained conditions (c_u and $\varphi_u = 0$):

N_q=1, N_c=(π+2)=5.71 , N_γ=0

The bearing capacity factors are graphically presented in FigureI-8. The shape, inclination and depth factors are according to:

Table I- 1 The Bearing Capacity Factors Are Graphically. **[2]**

	Shape	Depth	Inclination
Any φ′	Sc = 1 + 0.2 K_p (B / L)	d_c= dγ = 1 + 0.2 $\sqrt{K_p}$ (D / B)	$i_c = i_q$ = (1 - α⁰ / 90⁰)²
For φ′ = 0	Sq=Sγ=1	d_q = dγ = 1	iγ = 0
For φ′ ≥ 10°	Sq= Sγ = 1 + 0.1 Kp (B / L)	d_q = dγ = 1 + 0.1 √Kp (D / B)	iγ = (1 - α⁰ / φ⁰)²

Kp = tan² (45 + φ′ / 2)

α = angle of resultant measured from vertical axis.

When triaxial φ′ is used for plane strain φ′ adjust it as:

$\varphi' = (1.1 - 0.1\ B / L) \times \varphi'_{triaxial}$

Ⅰ-4-3Brinch Hansen's Bearing Capacity equation

As mentioned in previous section, bearing capacity depends on many factors and Terzaghi's bearing capacity equation doers not take in to consideration all the factors. Brinch Hansen and several other researchers have provided a comprehensive equation for the determination bearing capacity called Generalized Bearing Capacity equation considering the almost all the factors mentioned above. The equation for ultimate bearing capacity is as follows from the comprehensive theory.

$$q_u = cN_c\ sc\ ic\ dc + qN_q sq\ iq\ dq + 0.5\ B\ \gamma\ N_\gamma\ \ s\gamma\ i\gamma\ d\gamma$$

Here, the bearing capacity factors are given by the following expressions which depend on φ.

$$N_\gamma = 1.(Nq - 1)tan\varphi$$

$$Nq = exp(\pi\, tan\, \varphi)\tan(45 + \frac{\varphi}{2})$$

$$N_c = cot\ \varphi(Nq - 1)$$

Equations are available for shape factors (s_c, s_q, s_γ), depth factors (d_c, d_q, d_γ) and load inclination factors (i_c, i_q, i_γ). The effects of these factors are to reduce the bearing capacity.[1]

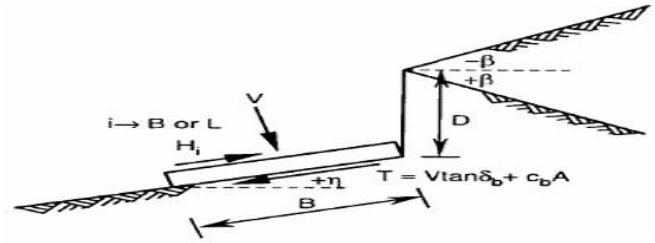


Figure Ⅰ-9 Identification of Items in Hansen's Bearing Capacity Equation.[1]

Ⅰ-5Effect of Water Table fluctuation

For all the bearing capacity equations, you will have to make some adjustments for the groundwater condition. The term D γ in the bearing capacity equations refers to the vertical stress of the soil above the base of the footing. The last term B γ refers to the vertical stress of a soil mass of thickness B, below the base of the footing. You need to check which one of the three groundwater situations is applicable to your project.[2]

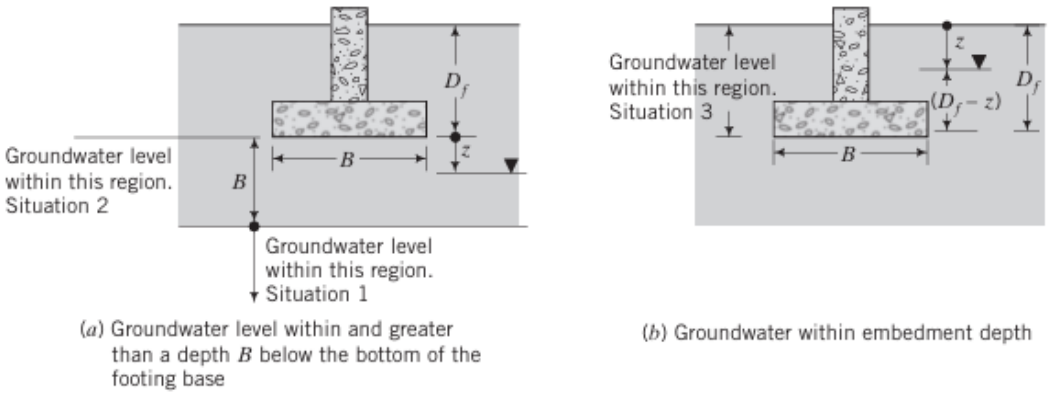


Figure Ⅰ-10 Groundwater Effects Below Base of Footing.[7]

Situation 1: If the groundwater level is at a depth greater than or equal to B below the bottom of the footing base (FigureI-10 a), no correction is required.

Situation 2: If the groundwater level is within a depth B below the bottom of the footing base such that 0<z < B (FigureI-10 a), then the term γ_B is $\gamma z + (\gamma_{sat} - \gamma_w)$ (B- z) or $\gamma_{sat} z + (\gamma sat - \gamma w)$ (B- z). The latter equation is used if the soil above the groundwater level is saturated. Note that z is measured from the bottom of the footing base. γDf remains unchanged.

Situation 3: If the groundwater level is within the embedment depth such that 0 <z < Df (FigureI-10 b), then the term γ_{Df} is γ_z 1 $(\gamma_{sat} - \gamma_w)$ (Df -z) or $\gamma_{sat} z$ 1 $(\gamma_{sat} - \gamma_w)$ $(D_f - z)$ if the soil above the ground water level is saturated. Note that z is measured from the ground surface; $\Gamma b = (\gamma_{sat} - \gamma_w)$ B. [7]

Ⅰ-6Factor of safety or safety factor (F_S)

Is the ratio of the ultimate net bearing capacity to the allowable net bearing capacity or to the applied maximum net vertical stress? In geotechnical engineering, a factor of safety between 2 and 5 is used to calculate the allowable bearing capacity. [7]

$$FS = qf/qa$$

Ⅰ-7Determination of Bearing Capacity from field tests

It is difficult to obtain undisturbed coarse-grained samples for laboratory testing and one has to use results from field tests to determine the bearing capacity of shallow foundations. Some field tests are:

Ⅰ-7-1 Plate Loading Test:

The plate loading test is carried out to estimate the bearing capacity of single footings. The plates (made of steel) dimensions are ⇒ 25 mm thick and 150 mm to 762 mm in diameter. In practice a circular plate of 300 mm is commonly used. Square plates that are 300 mm×300 mm are also used.

Ⅰ-7-1-1Procedure*:*

Step 1: Excavate bore hole with a minimum diameter 4BP [B_p = plate diameter] to a depth of D (D = depth of the proposed foundation).

Step 2: Then place the plate at the center of the hole.

Step 3: Apply initial setting load to make the proper contact of the plate with the ground.

Step 4: set the dial gages reading as the initial readings.

Step 5: Apply the first load approximately equal to 1/5th of the anticipated ultimate load

Step 6: Keep this load constant till the settlement of the plate under this load ceases (where the settlement is about 0.3mm/hr., it is supposed that the settlement is almost stopped.)

If this situation is achieved before 1hr, the load has to kept applied for an hr. If this situation is achieved after 2hrs, then the load has to kept constantly applied for 2hrs

Step 7: Record the settlement dial gage readings.

Difference of initial & final reading gives settlement of the plate

Step 8: change the next load=2*1/5*ultimate load repeat as the pervious steps. [1]

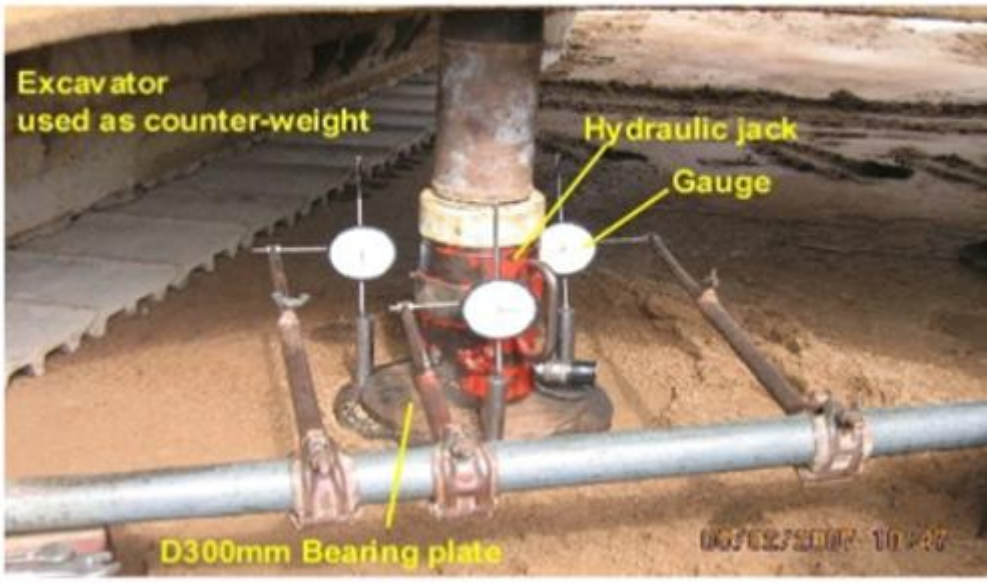


Figure Ⅰ-11 Plate Load Test Setup. [1]

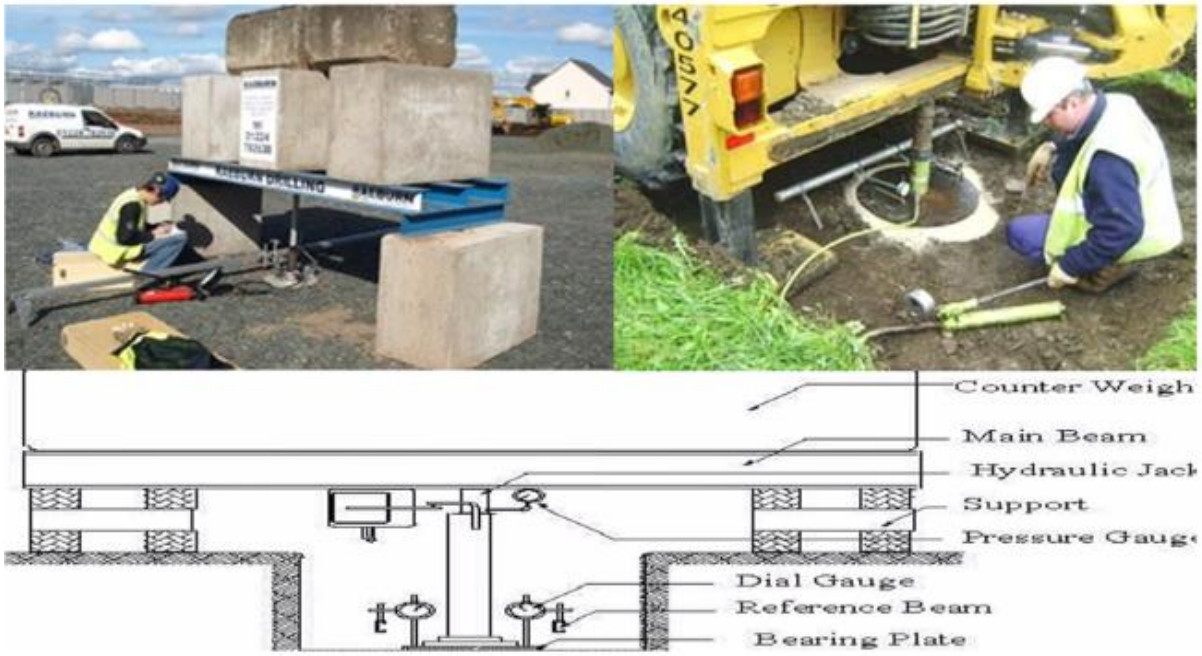


Figure Ⅰ-12 Typical Plate Load Test Arrangement with Counterweights and Measurement Devices.[7]

For tests in clay: $qu(F) = qu(p)$

For tests in sandy soil: $qu(F) = qu(p)\frac{B_F}{B_P}$

Where

⇒ $q_{u(F)}$ and $q_{u(P)}$ are ultimate bearing capacity of foundation and plate, and B_F and B_P stand for width of foundation and plate

For cohesion less soil: $s_F = s_p[(B(bp + 0.3)/(bp\ (B + 0.3))]\text{^}2$

For cohesive soil:$S_F = S_P * \frac{B}{b_p}$ [7]

Ⅰ-7-2Standard Penetration Test (SPT):

The Standard Penetration Test (SPT) is used to determine the allowable bearing capacity of cohesion less coarse-grained soils such as sands. The N values obtained from SPT are usually corrected for various effects such as overburden pressure and energy transfer. The following are two of the most commonly used methods in practice for correcting the N values.[7]

$c_N = \left(\frac{95.8}{\sigma'_{Z0}}\right)$; $C_N \leq 2$ (Liao and Whitman, 1985)

$C_N = 0.77 \log_{10}\left(\frac{1916}{\sigma'_{Z0}}\right)$; $C_N \leq 2$, $\sigma'_{Z0} > 24KPa$ (Peck et al., 1974)

Where c_N is a correction factor for overburden pressure, and σ'_{Z0} is the effective overburden pressure in kPa. A further correction factor is imposed on N values if the groundwater level is within a depth B below the base of the footing. The ground water corr3ection factor Is:

$$c_W = \frac{1}{2} + \frac{z}{2(D+B)}$$

Where z is the depth to the groundwater table, and D and B are the footing depth and width. If the depth of the groundwater table is beyond B from the f8ooting base Cw $= 1$. The corrected N value is:

$$N_{cor} = c_N c_w N$$

Meyerhof (1956, 1974) proposed the following equations to determine the allowable bearing capacity qa from SPT values.

$q_a = \frac{12}{25} s_e N_{cor} k_d \qquad B \leq 1.22\ m$

$q_a = \frac{8}{25} s_e N_{cor} \left(\frac{B+0.305}{B}\right)^2 K_d \qquad B > 1.22\ m$

Where S_e is the elastic settlement of the layer in mm and $kd = 1 + 0.33D/B \leq 1.33$.

In practice, each value of N is a soil layer up to a depth B below the footing base is corrected and an average value of $Ncor$ is used in Eqn. (2.43). Bowles (1996) modified Meyerhof's equations by 50% increase in the allowable bearing capacity. Bowles's equations are:

$q_a = \frac{20}{25} s_e N_{cor} k_d \qquad B \leq 1.22\ m$

$q_a = \frac{12.5}{25} s_e N_{cor} \left(\frac{B+0.305}{B}\right)^2 K_d \qquad B > 1.22\ m$

Ⅰ-8 Conclusion:

As is well known, foundations are a crucial element to ensure the stability of structures, as their performance quality heavily depends on their bearing capacity. Due to the importance of this factor, several methods have been developed to analyze bearing capacity, among which the most common is the traditional method (Terzaghi's method). However, despite the widespread use of this method, it relies on simplified assumptions that may not always reflect the soil behavior accurately. Therefore, since the soil is responsible for transferring loads to greater depths, and it is necessary to distinguish between weak and strong soils, improving soil properties is considered an effective way to increase bearing capacity. In this context, we will present below the main techniques used to strengthen the soil in order to improve its behavior under foundations.

Chapter Ⅱ:

Soil Reinforcement Techniques

Ⅱ-1Introduction

It is well known that in some cases, the soil's bearing capacity is so weak that no structures can be built on it. This poses a significant challenge in construction projects. In such cases, foundations cannot be constructed in the usual way, so it is necessary to search for methods to improve the soil's quality and make it capable of bearing loads. In this chapter, we will explore the various techniques and methods that contribute to soil improvement, enabling us to build foundations on it with confidence and without any risks.

Ⅱ-2-Definition Reinforced soil

Reinforced soil refers to a composite material made by combining natural soil with linear reinforcement elements, such as strips or layers, which are capable of withstanding significant tensile stresses. These reinforcements enhance the mechanical behavior of the soil by allowing it to resist tensile forces that it would not be able to sustain on its own. The main mechanism behind this improvement is the frictional interaction between the soil and the reinforcement, through which the stresses are effectively transferred from the soil to the reinforcing elements.

Ⅱ-3-Traditional Soil Reinforcement Techniques

Ⅱ-3-1-Dynamic Compaction



Figure Ⅱ-1 Dynamic Compaction of Soil. [9]

Ⅱ-3-1-1-Definition

The technique dates back to the mid-20th century and has evolved significantly. Initially used for military airstrips, DC's effectiveness soon led to its adoption in civil engineering projects worldwide. Today, it stands as a reliable method for ground improvement, favored for its cost-efficiency and versatility.[9]

Dynamic Compaction, often referred to as DC, is a powerful ground improvement method used to increase soil density. It involves dropping heavy weights from a considerable height to compact the underlying in situ soil. This process creates a shock wave that rearranges soil particles, reducing voids and increasing density.[9]

Ⅱ-3-1-2 Suitability

Dynamic compaction is suitable for the following conditions:

- Loose and partially saturated fills
- Saturated free-drained soils
- Silts with plasticity index less than 8
- Clayey soil with a low degree of saturation (moisture content lower than plastic limit)

Dynamic compaction is generally not recommended for clayey soil with high plasticity index (greater than 8) and high degree of saturation. However, this method has been used to improve clayey soils in some countries (Han, 1998; Liang and Xu,2011).

Dynamic compaction has been used to improve problematic geomaterials by increasing bearing capacity, reducing settlement, minimizing collapsible potential, and mitigating liquefaction for commercial and residential buildings, storage tanks, highways and railways, airports, and harbors.

There are some recommendations regarding the general soil type with their degree of saturation and the suitability of the dynamic compaction to treat them given by Martin Larisch and Tim Pervan, Fletcher construction private Ltd. [10]

General Soil type	Degree of Saturation	Suitability of DC
Granular deposits in the grain size range of boulders to sand with 0% passing the 0.074mm sieve	High or Low	Excellent
Granular deposits containing not more than 35% silts	High	Good
	Low	Excellent
Semi-permeable soil deposits, generally silty soils containing some sands but less than 25% clay with PI<8	High	Fair
	Low	Good
Impermeable soil deposits generally clayey soils where PI>8	High	Not Recommended
	Low	Fair-minor improvements water content should be less than plastic limit
Miscellaneous fill including paper, organic deposits, metal and wood	Low	Fair-long term settlement anticipated due to decomposition. Limit use to embankments
Highly organic deposits peat-organic silts	High	Not recommended unless sufficient energy applied to mix granular with organic soils

Table Ⅱ-1 Suitability of Dynamic Compaction with Soil Type Along with Degree of Saturation.

Ⅱ-3-1-3 Execution Method of Dynamic Compaction

- **Site Investigation**

- Analyze the soil type, depth of weak layers, and void ratio.
- Determine whether the site conditions are appropriate (preferably granular soils or loose fill).

➢ **Selection of Drop Weight and Height**

- Choose the appropriate weight (typically 10 to 40 tons).
- Set the drop height (from 10 to 30 meters).
- The impact energy is calculated as: $E = m \times g \times h$.

➢ **Grid Pattern Layout**

- Impact points are arranged in a grid pattern (square or triangular).

➢ **Grid Pattern Layout**

- Spacing between points typically ranges from 3 to 10 meters, depending on the soil and objectives.

➢ **Execution of Drop Sequences**

- Drop the weight at each point several times (usually 5 to 10 drops per point).
- Allow short intervals between drops to permit energy dissipation.
- Multiple passes may be performed, with adjustments in spacing or energy.

➢ **Surface Leveling**

- After compaction, the surface is leveled, and any craters are filled.
- Light surface compaction may be applied to improve uniformity.

➢ **Post-Compaction Testing**

- Conduct in-situ tests such as CPT (Cone Penetration Test) or SPT (Standard Penetration Test).
- Compare results with pre-compaction data to evaluate effectiveness.[11]

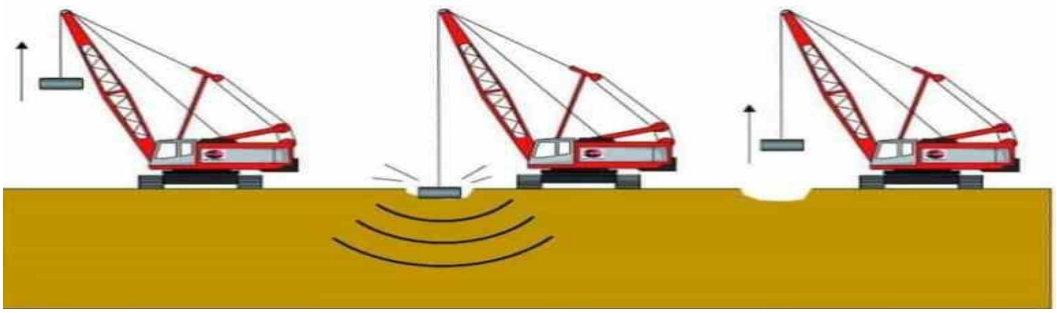


Figure Ⅱ-2 Application of Dynamic Compaction. [11]

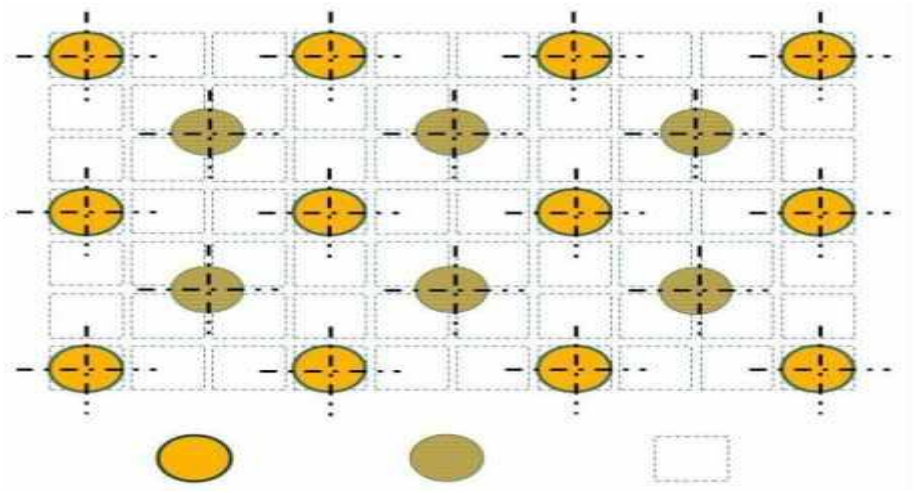


Figure Ⅱ**-3** Dynamic Compaction Grid. [11]

Ⅱ-3-1-4 Applications in Various Industries

- **Construction:** DC is valuable for preparing sites for commercial and industrial buildings.
- **Road Building:** Ensures the ground beneath highways and roads is stable, preventing future settlement issues.
- **Land Reclamation:** Used to improve the stability of reclaimed land, making it suitable for development, especially in coastal areas.[9]

Ⅱ-3-1-5 Advantages

- Densify and compact soil to a depth of 12m
- Effective in various soil conditions
- Cost effective
- Dramatic cost savings in excess of deep foundations and most undercut and replace options
- Accelerate schedules
- Mitigate soil liquefaction
- Improves bearing capacity of soil
- Decreases the volume of landfill waste
- Reduces post-construction settlements

- Environmentally friendly. [12]

Ⅱ-3-1-6 Disadvantages

- It cannot be used within 30m from buildings and 15m from underground services.
- Dynamic compaction is not appropriate if water depth is less than 1.5m.
- It cannot be applied if soft cohesive soils are located in the upper part of the compaction.
- Dynamic compaction is not effective when soils have fines content in excess of 20%.
- Requires an intensive in situ testing program to examine the result of compaction.[12]

Ⅱ-3-2- Soil Replacement

Ⅱ-3-2-1 Definition

Soil replacement is one of the oldest and most basic techniques used to improve weak soil conditions. The idea is simple: remove the poor-quality soil, such as organic layers or soft clay, and replace it with stronger materials like sand, gravel, or crushed stone. Although most soils can be used as fill, some are harder to compact properly. By placing a good-quality soil layer under a shallow foundation, it is possible to reduce settlement and increase the bearing capacity. Since the most stressed zone under a shallow foundation is limited in depth—usually about one to one and a half times the foundation's width—only that part needs to be replaced with better material to improve the foundation performance.

There are two main types:

Partial Replacement: Only the upper weak layers are removed and replaced.

Full Replacement: The entire weak stratum is excavated down to a competent soil layer.[13]

Ⅱ-3-2-2 Applications

The soil replacement method is applicable for soft soil. There are two primary techniques for soil replacement: removal and replacement of the soil and soil displacement.

The former is suitable for any soft or weak soil, provided that the soft soil layer is near the surface, groundwater can be lowered economically or the soil layer is located above groundwater, and the weak soil thickness is not greater than 9 m.

It involves the removal of soft soil and replacing it with structural fill during grading operations. Soil displacement includes overloading very soft soil until it shears and is displaced by firmer fill.[14]

Ⅱ-3-2-3 Application Procedure of Soil Replacement

- **Initial Soil Investigation**

Conduct geotechnical studies to identify the depth and characteristics of the weak soil.

Ensure the soft layer is shallow enough (typically ≤ 3–4 m) for economic feasibility.

- **Selection of Replacement Type**
- **Partial Replacement**: Used when only the upper layer is weak.
- **Full Replacement**: Applied when the entire weak stratum must be removed down to competent soil.
- **Excavation and Removal**

Excavate the unsuitable soil using manual or mechanical methods, depending on the depth.

Dispose of or treat the removed material appropriately.

- **Selection of Fill Material**

Use well-graded sand, gravel, or engineered fill with favorable mechanical properties (strength, low compressibility).

- **Placement and Compaction**

Place the fill in thin layers (typically 20–30 cm thick).

Compact each layer thoroughly using appropriate compaction equipment (e.g., plate compactors, rollers).

- **Quality Control and Testing**

Perform field tests (such as in-situ density tests or penetration tests) to verify compaction quality.

Adjust the process if target specifications are not met.[15]

Ⅱ-3-2-4 Advantages

- Immediate results—no waiting period like preloading.
- Effective for shallow problematic soils.
- Allows selection of engineered fill material with desired properties.

Ⅱ-3-2-5 Limitations

- Not economical for deep weak layers.
- Requires excavation, disposal, and compaction logistics.
- Can disturb surrounding structures if not properly managed.

Ⅱ-4 Modern Soil Reinforcement Techniques

Ⅱ-4-1 Stone Columns

Ⅱ-4-1-1 Definition

Stone columns, also known as ballasted columns (colonnes ballastées), are a technique I chose to include because of their practical use in improving weak soils. The idea is to insert compacted gravel or crushed stone vertically into the ground to create columns. This method helps make the soil stronger, improves drainage, and limits settlement problems, especially when dealing with compressible layers.

Ⅱ-4-1-2 Construction Methodology

The construction of stone columns typically involves:

1. Installation Equipment: A vibrating probe or ramming probe is used to create vertical holes in the soil. This equipment can either feed stone from the surface or inject it from below, depending on the specific method employed.

2. Compaction Process: The stone is placed in lifts (usually around 2 feet thick), with each layer compacted using the vibrating probe until the desired density and column dimensions are achieved.

3. Grid Pattern Arrangement: Stone columns are installed in a triangular or square grid pattern to ensure effective reinforcement across the area being treated.[16]

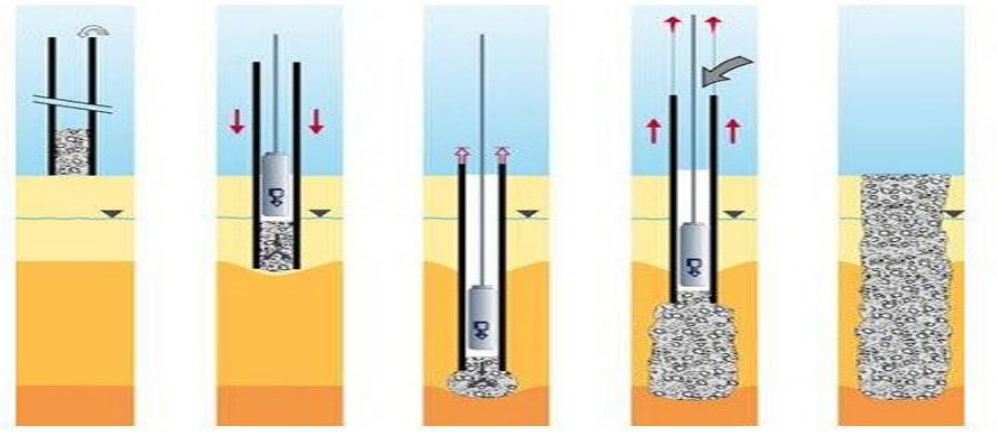


Figure Ⅱ-4 Methodology of Building Stone Columns. [16]

Ⅱ-4-1-3 Key Features and Benefits

- Load-Bearing Capacity: Stone columns significantly increase the soil's load-bearing capacity, allowing for the use of shallower foundations instead of deep ones. This is crucial for structures that would otherwise require extensive foundational work due to weak underlying soils.
- Settlement Reduction: By reinforcing the soil, stone columns help minimize both total and differential settlement. This is especially important in construction projects where uneven settling could lead to structural issues.
- Soil Consolidation: The granular material within stone columns facilitates accelerated soil consolidation by acting as drainage points, which helps relieve pore water pressure and enhances overall soil stability.
- Liquefaction Mitigation: In areas prone to liquefaction during seismic events, stone columns can reinforce the soil, reducing the risk of damage by increasing its shear strength and creating a non liquefiable crust above weaker layers.

Ⅱ-4-2 Geosynthetics

Ⅱ-4-2-1 Definition

The term geosynthetic combines two parts: “geo”, which relates to the earth, and “synthetic”, which refers to something man-made. In general, geosynthetics are polymer-based materials that come in a flat (planar) form. They are used in direct contact with soil, rock, or other geotechnical materials, and they serve as essential components in many engineered structures and systems.

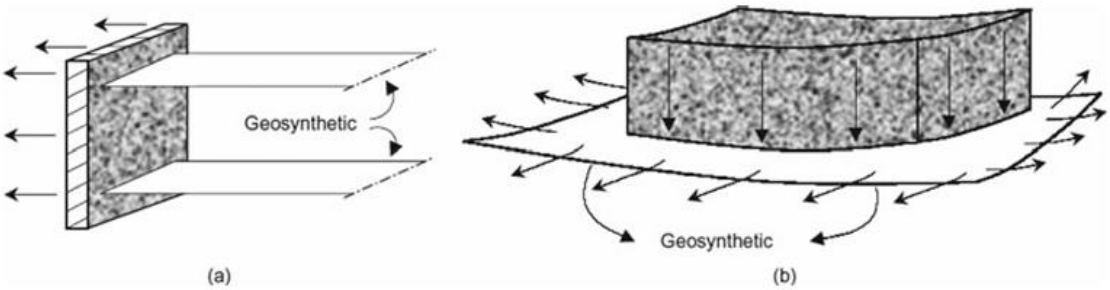


Figure II-5 Reinforcement Function of Geosynthetics: A Tensile Member; And B Tensioned Membrane.[17]

Ⅱ-4-2-2 The Functions of Geo-Synthetics

- Reinforcement
- Filtration
- Separation
- Drainage
- Erosion Control
- Barrier/Protection

Ⅱ-4-2-3 Reinforcement

Reduction of Stress Intensity (Concentration) through Wider Distribution the stresses over the subgrade are higher in unreinforced flexible pavements than in geo-synthetic-reinforced pavement due to stress distribution factor

Reinforcement Mechanisms Induced by Geo-synthetics:

(a) Lateral Restraint

(b) Increased Bearing Capacity; and

(c) Membrane Tension Support

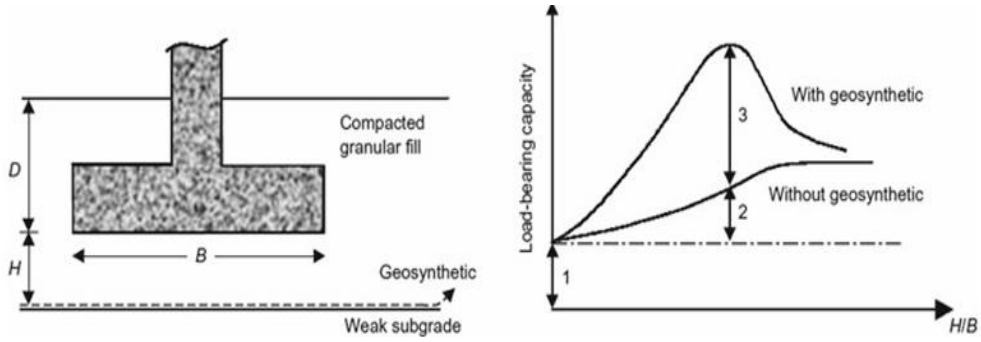


Figure **II-6** Variation in ultimate bearing capacity of the foundation bed with and without geosynthetics.[20]

Ⅱ-4-2-4 Filtration

Retaining soil particles subjected to hydraulic forces which allow the passage of liquids/gases. This function is often partnered with separation.

Ⅱ-4-2-5 Separation

a. Preventing intermixing of soil types or soil/aggregate to maintain the integrity of each material yet still allow the free passage of liquids/gases. Commonly used in between sub-base/subgrade and around drainage materials.

b. Contamination of the base course layers leads to a reduction of strength, stiffness and drainage characteristics, promoting distress and early failure of roadway.

Ⅱ-4-2-6 Drainage

Allowing fluids and gases to flow both through the plan of the material. Commonly used as components in geo-composites used for surface water runoff or for gas collection under membranes.

Ⅱ-4-2-7Erosion Control

Protecting and reinforcing slopes and drainage channels from erosive agents whilst allowing the establishment of vegetation cover.

Ⅱ-4-2-8 Barrier/Protection

Preventing or limiting localized damage to an adjacent material, usually a geomembrane used to line a lagoon or a landfill. Thick geotextiles prevent puncture or excessive strain in the membrane.[17]

Ⅱ-4-3 Geo synthetics classified

Geo synthetics are classified as follows:

- Geotextiles
- Geogrids
- Geonets
- Geo-membranes
- Geo-synthetic clay liners
- Geocells/geo web members
- Geofoam Geo-composites

Ⅱ-4-3-1 Geogrids

They have open grid like configuration i.e. they have large aperture between individual ribs. They have Low strain and stretch about 2% under load. Strength is more that other common geotextiles. Function: Used exclusively for reinforcement.[18]



Figure **II-7** Geogrids used for soil reinforcement [19]

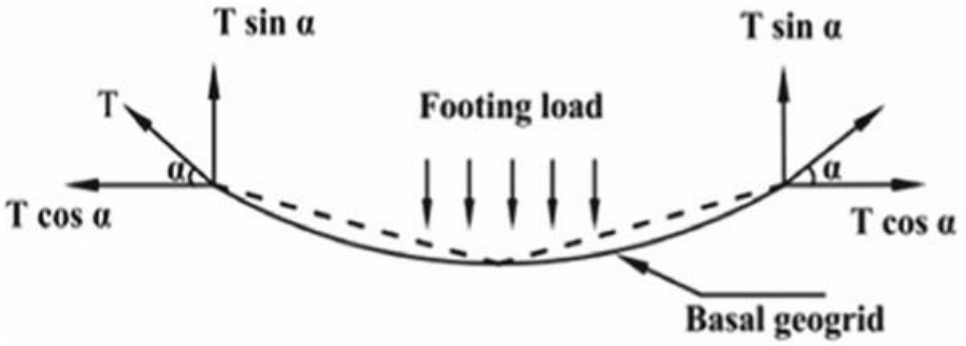


Figure **II-8** Membrane mechanism [20]

Ⅱ-4-3-2 Geonets

Are open grid-like materials formed by two sets of course, parallel, extruded polymeric strands intersecting at a constant acute angle. The network forms a sheet with in- plane porosity that is used to carry relatively large fluid or gas flows.[19]

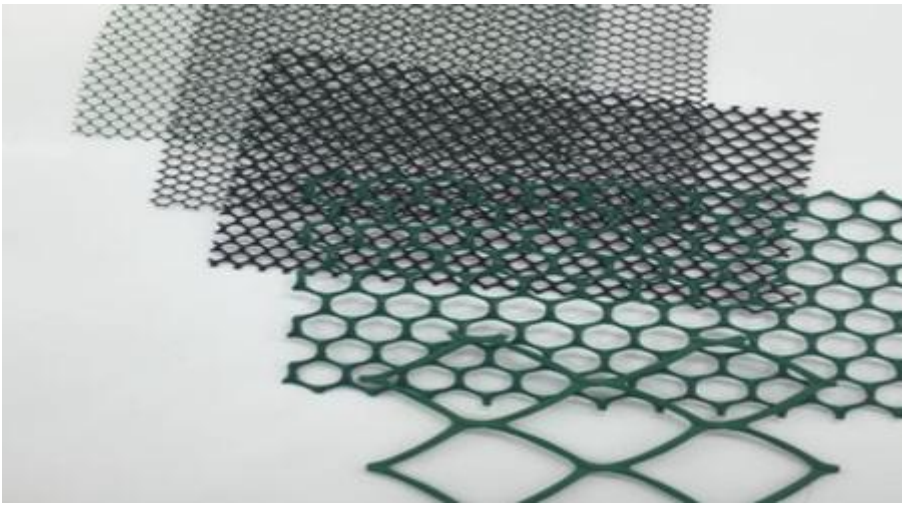


Figure II-9 Geonets Used For Soil Reinforcement. [17]

Ⅱ-4-3-3Geomembranes

Are continuous flexible sheets manufactured from one or more synthetic materials. They are relatively impermeable and are used as liners for fluid or gas containment and as vapor barriers.[18]



Figure II-10 Geomembranes Used For Soil Reinforcement. [15]

Ⅱ-4-3-4Geosynthetic clay liners (GCLs)

Are geocomposites that are prefabricated with a bentonite clay layer typically incorporated between a top and bottom geotextile layer or geotextile bentonite bonded to a geomembrane or single layer of geotextile. [18]



Figure II-11 Geosynthetic Clay Liners Used for Soil Reinforcement. [20]

Ⅱ-4-3-5Geotextile-encased

Are often stitched or needle punched through the bentonite core to increase internal shear resistance. When hydrated they are effective as a barrier for liquid or gas and are commonly used in landfill liner applications often in conjunction with a geomembrane. [20]



Figure II-12 Geotextile-Encased Used For Soil Reinforcement. [17]

Ⅱ-4-3-6 Geocells

Are relatively thick, three-dimensional networks constructed from strips of polymeric sheet. The strips are joined together to form interconnected cells that are infilled with soil and sometimes concrete. In some cases 0.5 m to 1 m wide strips of polyolefin geogrids have been linked together with vertical polymeric rods used to form deep geocell layers called geomattresses. Soil confinement. [20]

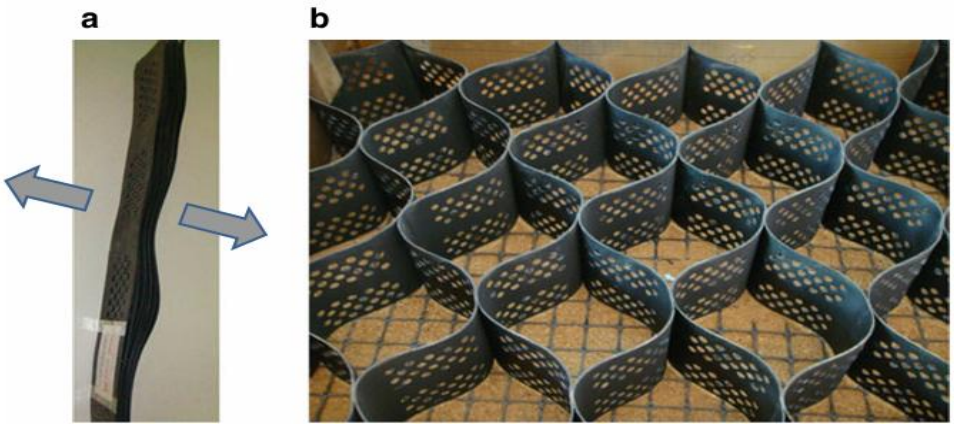


Figure II-13 Photograph of The Geocell: A Folded; B Expanded. [20]

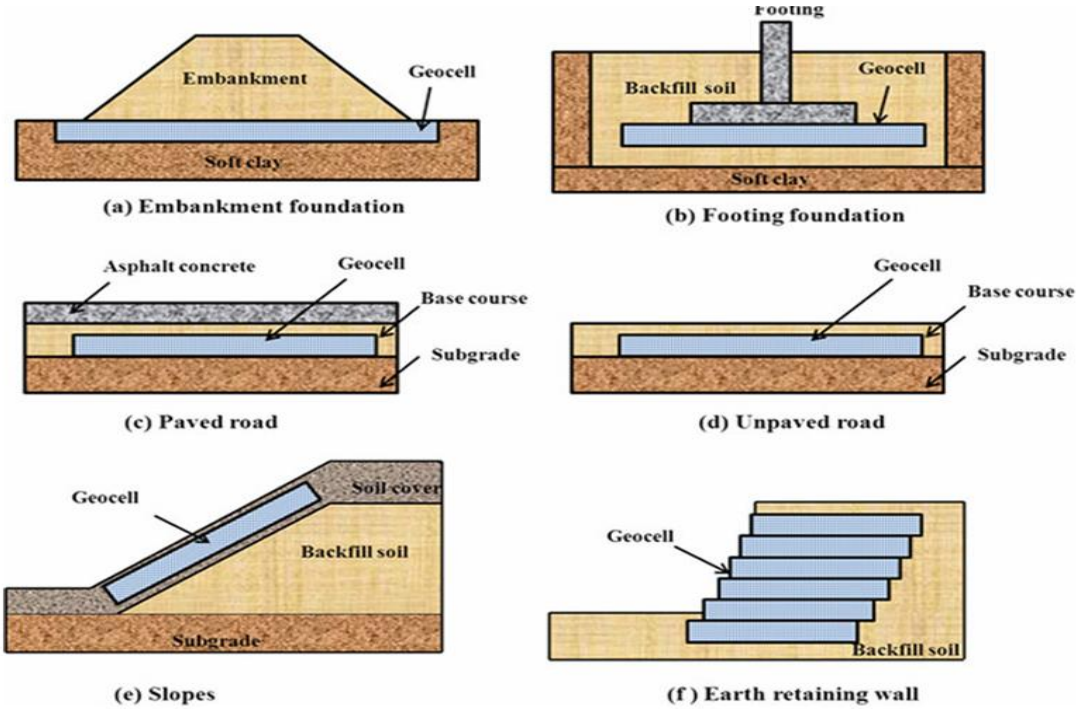


Figure II-14 Different Applications Of Geocells. [20]

Ⅱ-4-3-7 Geofoam

Blocks or slabs are created by expansion of polystyrene foam to form a low- density network of closed, gas-filled cells. Geofoam is used for thermal insulation, as a lightweight fill or as a compressible vertical layer to reduce earth pressures against rigid walls.[20]



Figure II-15 Geofoam Used for Soil Reinforcement. [15]

Ⅱ-4-3-8Geocomposites

Are geosynthetics made from a combination of two or more geosynthetic types. Examples include: geotextile-geonet; geotextile-geogrid; geonet geomembrane; or a geosynthetic clay liner (GCL). Prefabricated geocomposite drains or prefabricated vertical drains (PVDs) are formed by a plastic drainage core surrounded by a geotextile filter.[20]



Figure II-16 Geocomposites Used For Soil Reinforcement. [16]

Ⅱ-4-3-9 Geotextiles

Geotextiles are permeable textile materials made from synthetic polymers such as polypropylene or polyester. They are used in contact with soil, rock, or other geotechnical materials in various civil engineering applications. The term "geotextile" is derived from "geo" meaning earth, and "textile" meaning fabric. These materials are designed to perform several key functions such as reinforcement, filtration, separation, drainage, and protection.

They are available in a variety of forms, including woven, non-woven, and knitted types, each with distinct structural characteristics and suitable for specific applications. The versatility and durability of geotextiles have made them essential components in projects like road construction, slope stabilization, retaining walls, and landfill containment systems.[19]



Figure II-17 Geotextiles Used For Soil Reinforcement. [17]

Ⅱ-4-3-9-1 Functions of Geotextiles: Geotextiles serve multiple engineering functions, often performing more than one function simultaneously:

- **Reinforcement**
  - Geotextiles provide tensile strength to soil systems that are weak in tension.
  - They help to improve load distribution, especially in soft soil foundations.
  - Mechanisms include lateral restraint, confinement of soil, and tensioned membrane support.

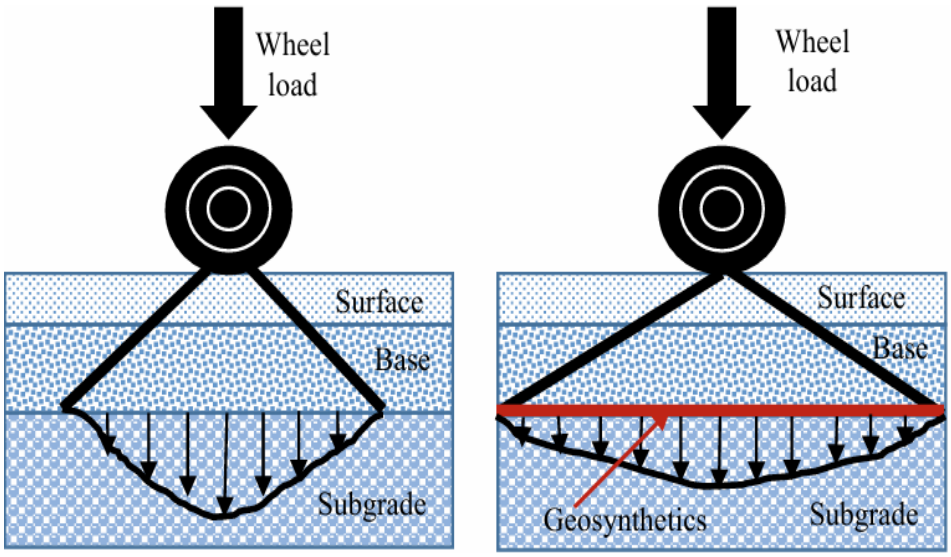


Figure II-18 Reinforcement. [20]

- **Filtration**
  - Geotextiles allow water to pass while retaining fine soil particles.
  - This prevents clogging of drainage systems and maintains long-term functionality.

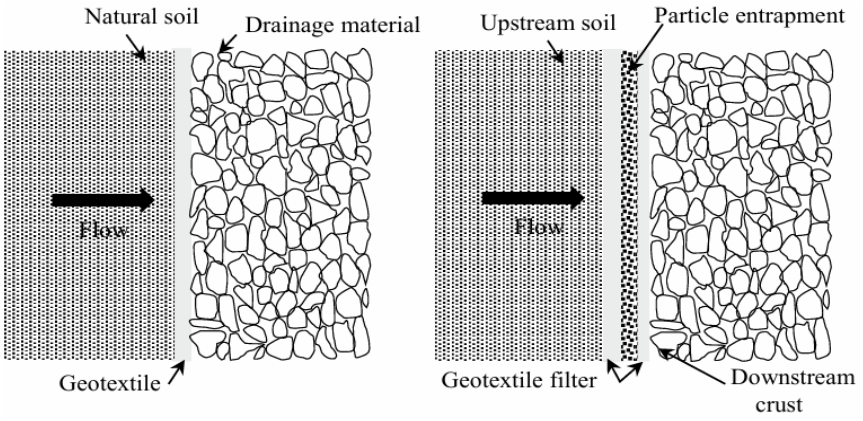


Figure II-19 Filtration. [20]

- **Separation**
  - They prevent the mixing of dissimilar materials (e.g., subgrade soil and aggregate base in pavements).
  - Ensures the integrity and performance of structural layers over time.

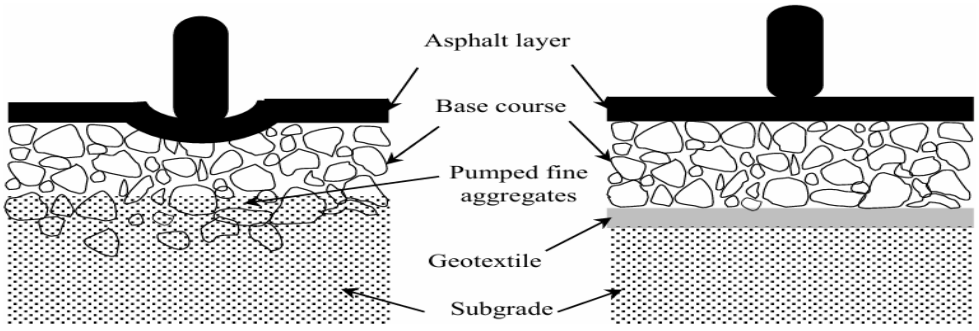


Figure II-20 Separation Functions Of Geosynthetics. [20]

- **Drainage**
  - Geotextiles can transmit water both within the plane and across the plane.
  - Used in vertical and horizontal drainage systems such as around foundations or landfills.

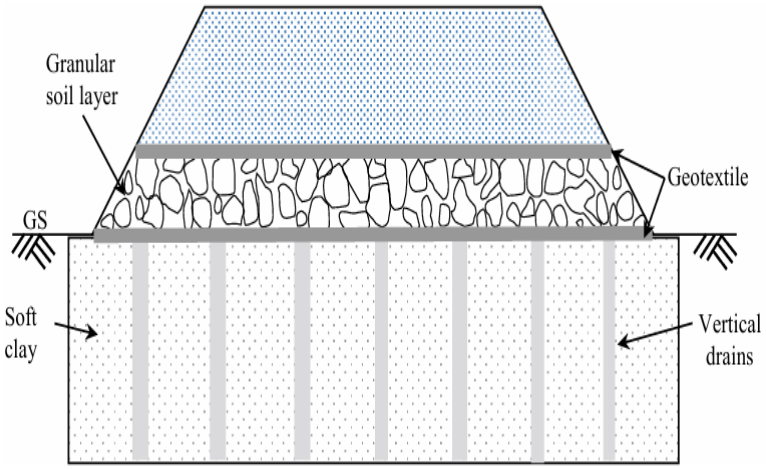


Figure II-21 Drainage.[20]

- **Erosion Control**
  - Used to stabilize soil on slopes, riverbanks, and coastal areas.
  - Promotes the establishment of vegetation and prevents soil loss due to water or wind.

- **Barrier/Protection**
  - Acts as a cushion layer to protect geomembranes in landfill liners or ponds.
  - Absorbs mechanical stresses and prevents puncturing.

Ⅱ-4-3-9-2 Types of Geotextiles

- **Woven Geotextiles**
  - Manufactured by weaving yarns in a systematic pattern.
  - High tensile strength and stiffness.
  - Best suited for reinforcement and separation.

- **Non-Woven Geotextiles**
  - Created by bonding fibers via chemical, thermal, or mechanical methods.
  - Typically have high permeability and excellent filtration properties.
  - Common in drainage and erosion control applications.

- **Knitted Geotextiles**
    - Less commonly used, made by interlocking loops of yarn.
    - Offers a balance between strength and flexibility.[19]

Ⅱ-4-3-9-3Applications of Geotextiles in Engineering

Geotextiles are widely applied in geotechnical, environmental, and hydraulic engineering. Major applications include:

- **Road and Railway Subgrades**: Reinforcement and separation between layers to extend pavement life.
- **Retaining Walls and Reinforced Slopes**: Used as tensile inclusions to provide internal stability.
- **Landfills and Containment Liners**: Used in combination with geomembranes for filtration, protection, and containment.
- **Embankments over Soft Soil**: Acts as a load distribution platform.
- **Drainage Systems**: Serves as filters around drainage pipes, trenches, and geocomposites.
- **Coastal and Riverbank Protection**: Used to stabilize soil and prevent scouring and erosion.[19]

Ⅱ-4-3-9-4 Properties of Geotextiles

Selection of geotextiles for a specific project requires an understanding of their key properties:

- **Physical Properties**
    - Specific gravity
    - Mass per unit area (gsm)
    - Thickness under load
    - Stiffness or flexibility
- **Mechanical Properties**
    - Tensile strength and elongation

- Puncture resistance
- Tear resistance
- Seam strength
- Burst strength
- Creep behavior under long-term loading

- **Hydraulic Properties**

  - Apparent opening size (AOS)
  - Water flow rate/permittivity
  - Transmissivity
  - Resistance to clogging

- **Durability**

  - Resistance to UV radiation
  - Chemical stability in aggressive environments
  - Biological resistance (e.g., against bacterial or fungal attack)
  - Long-term weathering resistance.[19]

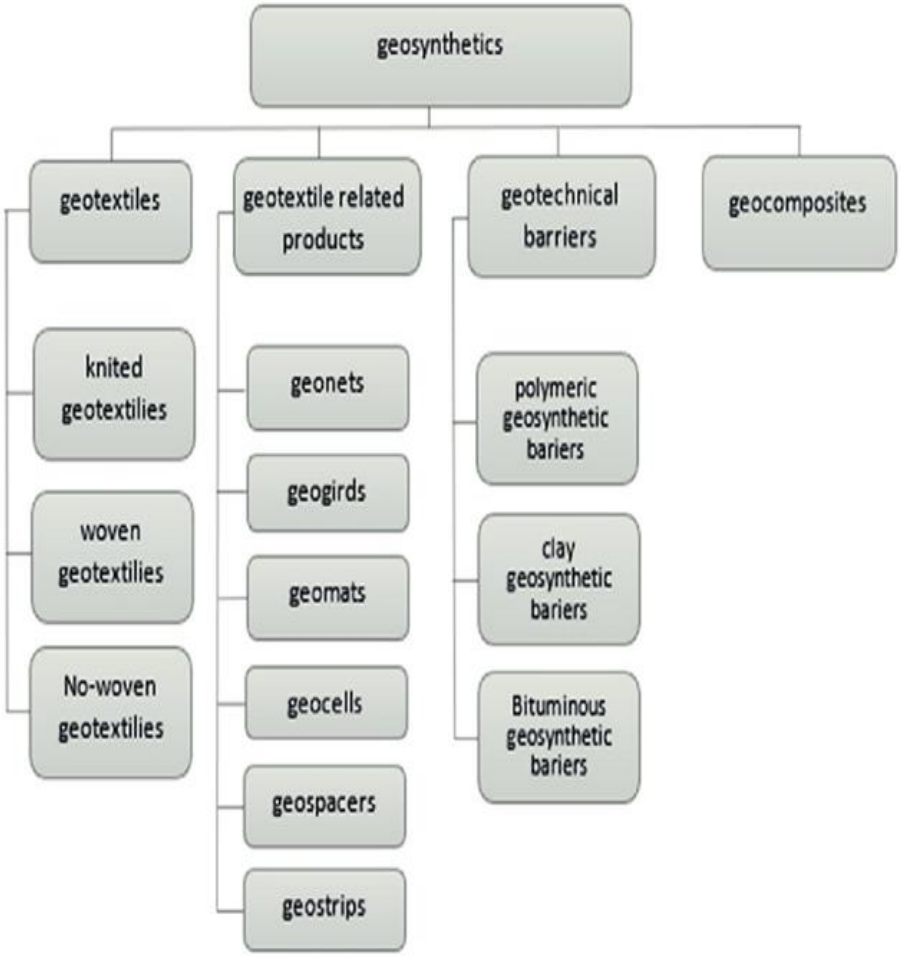


Figure II -22 Classification of Geosynthetics and Their Types.[19]

Ⅱ-5 Conclusion

Through this chapter, we have explored various soil improvement techniques that help increase its bearing capacity. These methods play a key role in ensuring the stability of foundations and the suitability of the soil for construction. However, despite the effectiveness of these techniques, there are cases where they cannot be applied. In the upcoming chapters, we will explore new techniques with a different working mechanism, which can help address situations where traditional methods cannot be used.

Chapter III: Numerical analysis

Ⅲ-1Introduction

This chapter presents the numerical modeling methodology employed in the present study to analyze the bearing capacity of geotextile-reinforced cohesive-frictional soils using PLAXIS 2D. The chapter describes in detail the model geometry, material properties, boundary conditions, loading procedures, mesh configuration, and hydraulic conditions. Additionally, the different calculation phases, deformation analysis, and validation steps are discussed. The goal is to provide a comprehensive understanding of the numerical setup and simulation techniques used to replicate the experimental conditions and investigate the mechanical behavior of reinforced soil foundations under vertical loading.

Ⅲ-2 Geometry

The numerical model developed for this study represents a rectangular soil domain with dimensions of 1000 mm in length and 600 mm in depth. The domain is reinforced with geotextile layers and includes a centrally located rigid strip footing with a width of 100 mm placed directly on the soil surface. The analysis was conducted under plane strain conditions using PLAXIS 2D, reflecting the assumptions made in the experimental setup by Sukmak et al. [21].

This geometric configuration was selected to realistically simulate the mechanical behavior of cohesive-frictional soils and to ensure consistency with the physical model used in the laboratory tests.

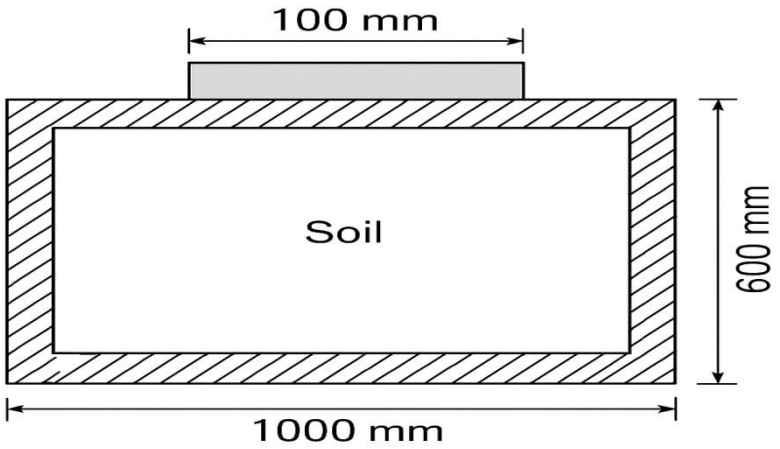


Figure III-1 Geometry of a strip footing resting on a sand layer.



Figure Ⅲ**-2** Model geometry in PLAXIS.

Ⅲ-3Materials

Ⅲ-3-1 Soil Samples

In order to achieve a range of plasticity index (PI) values, mixtures of fine sand and bentonite (montmorillonite) were prepared at six different proportions: 0%, 20%, 40%, 60%, 80%, and 100% bentonite by dry weight, labeled as B0, B20, B40, B60, B80, and B100, respectively. The bentonite used was a commercially available powder, primarily employed as drilling mud in geotechnical applications, and was sourced from Geomechanical Service Co., Ltd., Bangkok, Thailand.

The bentonite consisted of 98% clay and 2% silt. Its liquid limit and plastic limit, measured according to ASTM D4318 using the Casagrande cup and rolling thread methods, were 347% and 33%, respectively.

The sand used in the mixtures was air-dried and passed through a 2.00 mm sieve (No. 10). The pure sand sample (B0) was composed of 98% sand and 2% silt, with an average grain size (D_{50}) of 0.5 mm. The specific gravities of the bentonite and sand were 2.35 and 2.80, respectively. According to the Unified Soil Classification System (USCS), the bentonite was classified as high-plasticity clay (CH), and the sand as poorly graded sand (SP).

(Figure III-3) illustrates the grain size distribution of all mixtures, while (Figure III-4) shows the variations in LL, PL, and PI with increasing bentonite content. A consistent increase in these values was observed as the clay fraction increased. The slope of the PI versus clay content relationship, known as the soil activity, was found to be 3.61, indicating highly active soil.

The mixtures were moistened with water to reach their optimum water content, as determined by standard Proctor compaction tests (ASTM D698). The direct shear test, conducted with a

65 mm-diameter shear box at a shear rate of 0.5 mm/min, was used to determine the shear strength parameters—cohesion (c) and internal friction angle (φ).

(Figure III-5) shows how the strength of the soil changes with the amount of clay. When the clay content increases, the cohesion increases almost in a straight line, but the friction angle goes down in a curved way. For samples with clay content below 60%, a sharp reduction in friction angle was noted, attributed to the lubricating effect of the clay paste. For higher clay contents, this reduction was less pronounced. The B100 sample exhibited the highest cohesion (33 kPa) and the lowest friction angle (0°).

A summary of the physical and mechanical properties of all soil mixtures is provided in (**Table III-1).**[21]

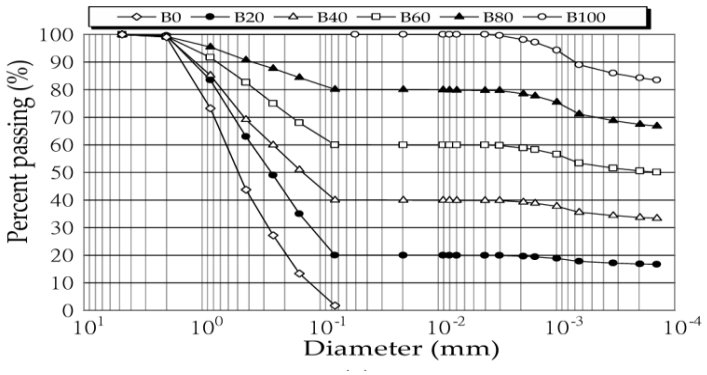


Figure III-3 Grain Size Distribution Curves of All Soil Mixtures.[21]

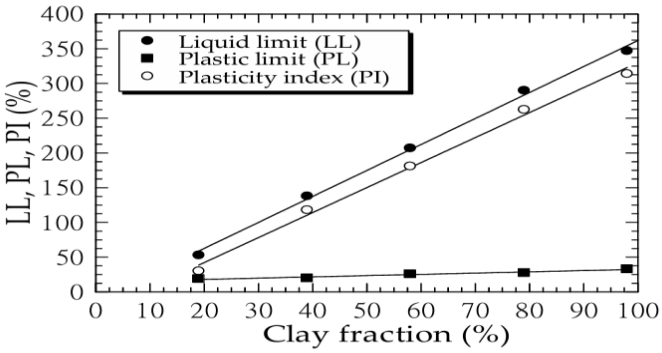


Figure III-4 The Liquid Limit, Plastic Limit, And Plasticity Index for All the Soil Mixtures. [21]

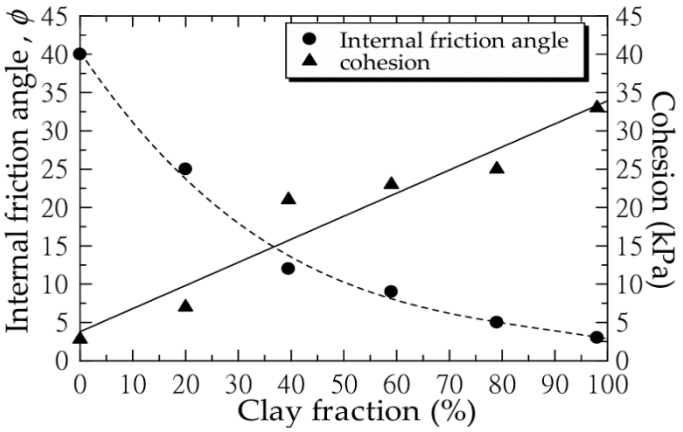


Figure III-5 Relationship Between the Soil Strength Parameters (Friction Angle and Cohesion) And the Amount of Clay in The Soil. [21]

Soils properties

Table III-1 Properties Of Soils.

Soil Mixtures	**B0**	**B20**	**B40**	**B60**	**B80**	**B100**
Total Unit Weight (kN/m^3)	17.66	18.69	17.40	16.17	15.81	14.17
Dry Unit Weight (kN/m^3)	17.14	16.87	15.01	13.32	12.65	10.99
Optimum Water Content (%)	3.0	10.8	16.0	21.4	25.0	29
Liquid Limit LL (%)	-	49	138	207	290	347
Plastic Limit PL (%)	-	19	20	26	28	33
Plasticity Index (PI) (%)	-	30	118	181	262	314
Internal Friction Angle Φ(Degree)	40	30	12	9	5	0
Cohesion (kPa)	2.8	7	21	23	25	33
E (kN/m2)	20,000	17,000	15,000	13,000	8000	5000
ν	0.3	0.3	0.35	0.4	0.4	0.4
ψ(Degree)	10	0	0	0	0	0

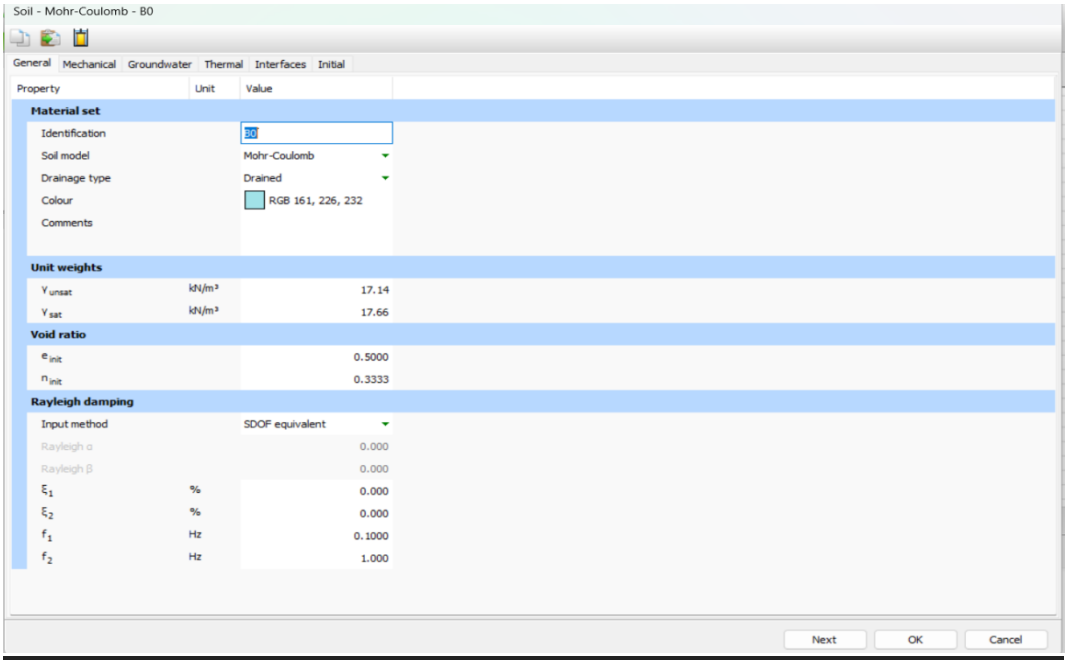


Figure III-6 Input window for general soil data information.

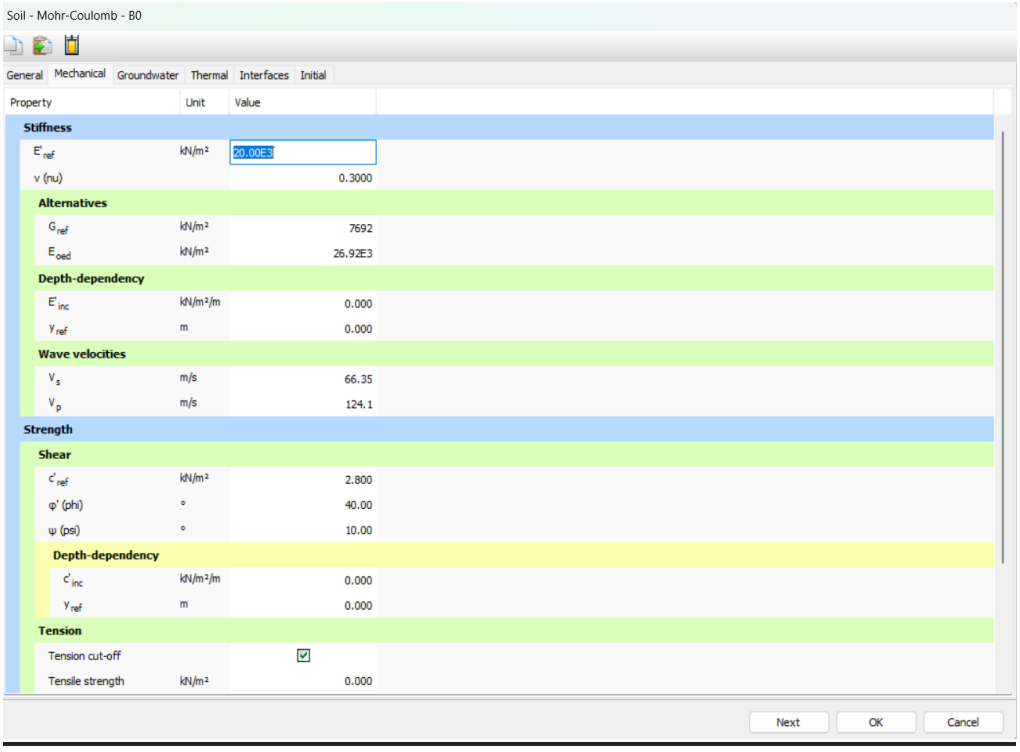


Figure III-7 Input window for mechanical soil data information.

III-3-2Reinforcement Geotextile

In the numerical model, the geotextile reinforcement was simulated using “geogrid” elements in PLAXIS 2D. These structural elements are designed to model the tensile behavior of geosynthetics and require a key input parameter: the axial stiffness (EA). For this study, EA

was set to 200 kN/m based on the manufacturer's specifications and consistent with values reported in the literature.

The geogrid elements were modeled as tension-only materials with no bending stiffness, reflecting the actual mechanical behavior of geotextiles. This approach ensures that the reinforcement only contributes when subjected to tensile forces, which is critical for accurately capturing the interaction between the soil and the reinforcement layers.

Table III-2 Geotextile characteristics.

Materials	**Geotextile**
The axial stiffness (EA)	200 kN/m

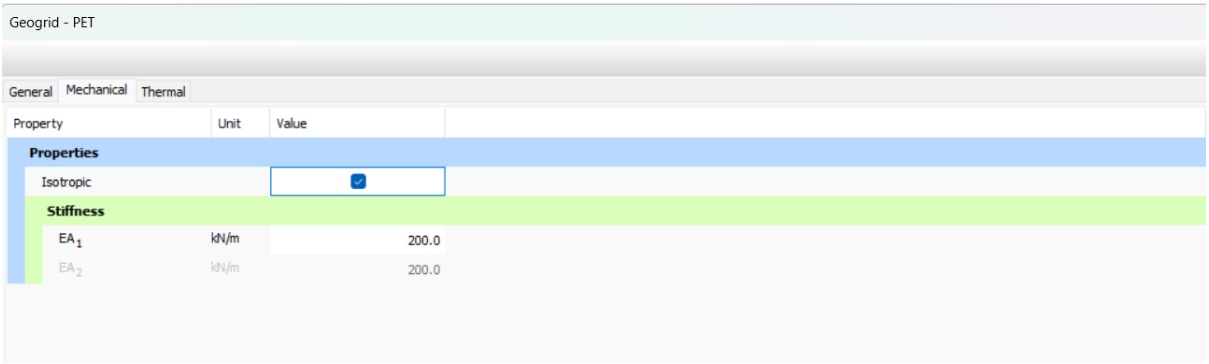


Table III-8 Input window for geotextile data information.

Ⅲ-4Boundary Conditions (Conditions aux limites)

The boundary conditions of the numerical model were carefully defined to ensure realistic simulation of the reinforced soil's behavior under vertical loading, while maintaining numerical stability and eliminating boundary influence on the bearing zone. The vertical sides (right and left) were constrained in the horizontal direction (Ux = 0), allowing vertical displacements while preventing horizontal soil movement. This reflects the plane strain condition adopted in the model.

The bottom boundary of the model was fully fixed in both horizontal and vertical directions ($U_x = U_y = 0$) to simulate a rigid, non-deformable base. Meanwhile, the top surface was left free of constraints, enabling the application of vertical load without numerical distortion and allowing realistic interaction between the footing and the soil surface.

Additionally, the model dimensions (length and depth) were selected large enough to ensure that the imposed boundaries would not interfere with the stress and deformation fields around

the footing. This setup is considered a standard practice in finite element modeling using tools such as PLAXIS 2D.

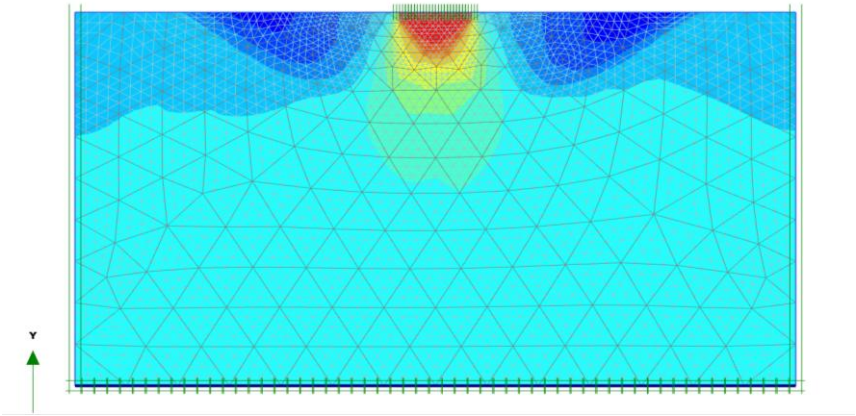


Figure III-9 Generation of boundary conditions.

III-5 Loading (Chargement)

In this study, loading was applied through a rigid strip footing with a width of 100 mm, positioned centrally on the surface of the soil model. The load was implemented as a prescribed vertical displacement corresponding to 10% of the footing width (i.e., 10 mm), which is a commonly accepted failure criterion for shallow foundations.

This displacement-controlled loading method allows for accurate monitoring of the load–settlement behavior and helps determine the ultimate bearing capacity of the reinforced soil. The simulation was carried out in staged construction using PLAXIS 2D, where each phase represents an incremental increase in vertical displacement until the target displacement was reached.

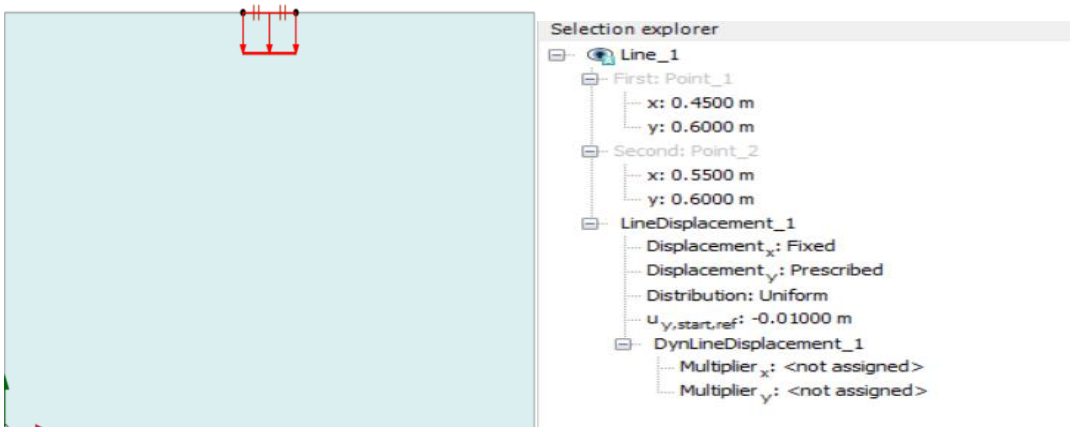


Figure III-10 Prescribed vertical displacement.

Ⅲ-6 Meshing

In the present study, the finite element modeling was conducted using PLAXIS 2D, where the soil domain was modeled under plane-strain conditions. The entire model geometry, including the reinforced soil foundation (RSF), was discretized using 15-noded triangular elements, which provide improved accuracy in capturing stress and deformation fields compared to linear elements.

The mesh density was adaptively refined in areas of interest, particularly around:

- The rigid strip footing (with a width of 100 mm),
- The geotextile reinforcement layers (modeled as geogrid elements),
- And the interfaces between the soil and geotextile, where high stress concentration and relative displacement are expected.

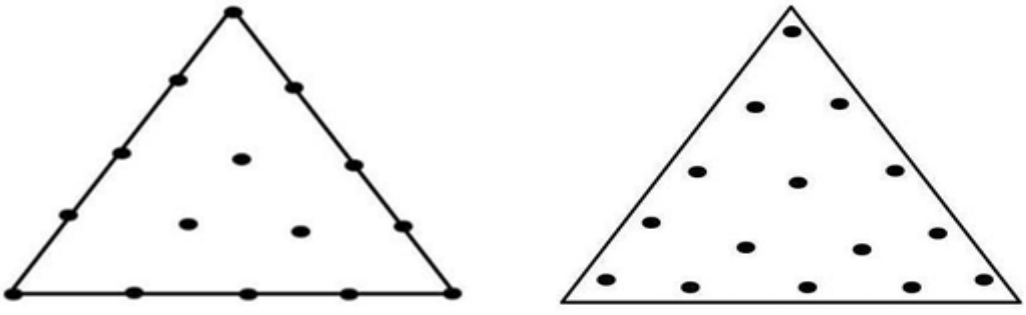
The mesh in the vicinity of the footing and reinforcement was designated as very fine, to accurately capture the load transfer mechanism, development of the stress bulb, and shear zones. In contrast, the regions further from the load application zone were assigned a coarser mesh, maintaining computational efficiency without sacrificing solution stability.

The boundary conditions of the model were defined such that:

- The bottom boundary was fully fixed in both horizontal and vertical directions,
- While the vertical sides were fixed in the horizontal direction but allowed vertical displacement, simulating realistic soil confinement.

The total size of the model box was kept sufficiently large (at least 10B in width and 6B in depth, where *B* is the footing width) to minimize boundary effects, as was also done in the experimental setup.

To ensure accuracy, a mesh convergence analysis was conducted. The final mesh configuration was validated by comparing the numerical results with the experimental data, particularly in terms of bearing stress versus settlement behavior. The good agreement between the two validated the mesh density and element quality used in the simulation.



Triangle with 15 nodes Stress point

Figure III-11 Position of Nodes and Stress Points in Soil Elements.

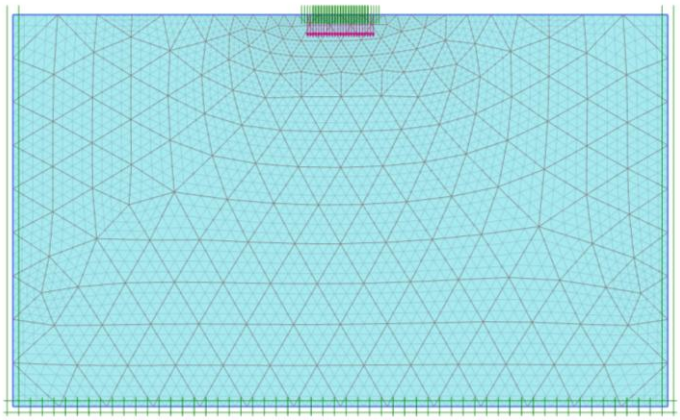


Figure III-12 Mesh Generation.

Ⅲ-7 Hydraulic conditions

Since the study focuses on the behavior of reinforced soil under static loading in dry conditions, the numerical model was developed assuming unsaturated or dry hydraulic conditions. It was considered that the soil contained no groundwater and that pore water pressure did not influence the mechanical behavior during loading. This assumption is consistent with the experimental setup, which was conducted under dry laboratory conditions.

As a result, no flow model or permeability parameters were activated in PLAXIS 2D. The soil was treated as a dry medium, with only mechanical properties being considered. This simplification allows the analysis to focus on the impact of geogrid reinforcement layers on the bearing capacity of the soil, without the complexity introduced by hydraulic interactions. Such assumptions are commonly adopted in laboratory-based geotechnical simulations where moisture is not a dominant factor.

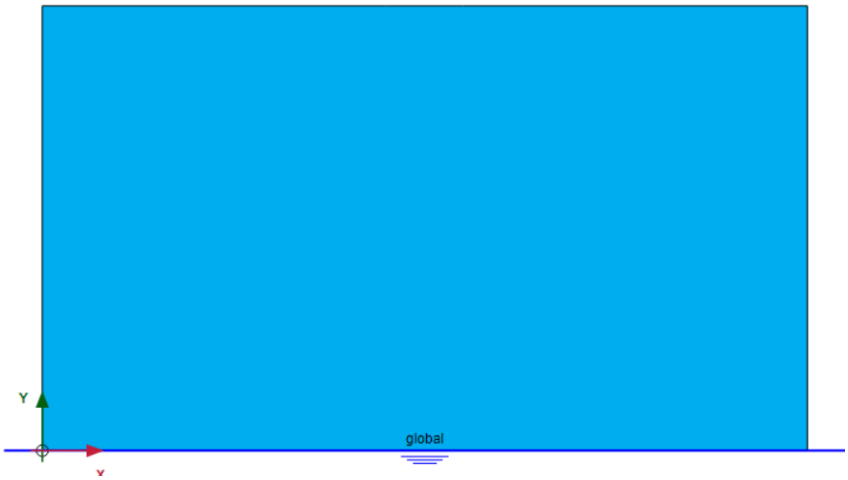


Figure III-13 Hydraulic conditions.

Ⅲ-8 Calculation phases

Ⅲ-8-1 Initial Phase

The initial phase in the numerical modeling is essential for establishing a realistic geostatic stress state in the soil before applying any external load. In this study, the K_0 procedure was adopted to generate the initial stresses, in accordance with the at-rest condition of the soil.

The K_0 procedure is based on the assumption that the soil is in a resting state, meaning it has not yet undergone any deformation due to external loading. The coefficient of earth pressure at rest K_0 is defined as:

$$K_0 = 1 - sin(\Phi)$$

Where Φ is the internal friction angle of the soil. This relation allows the calculation of the initial horizontal stresses from the vertical ones, ensuring a realistic stress distribution in the ground.

The initial stress generation in PLAXIS 2D is performed automatically through the initial phase, where only the self-weight of the materials is considered. This step is essential to ensure the numerical stability of the model and to avoid artificial deformations during the subsequent loading phases.

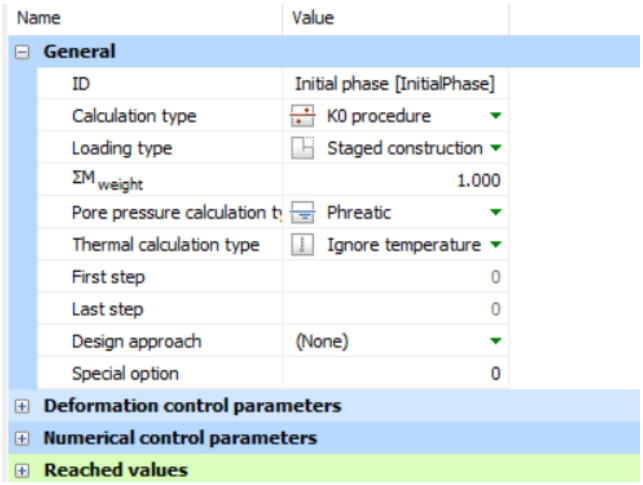


Figure III-14 Set current model phase to the initial phase.

Ⅲ-8-2Type of Analysis – Plastic Calculation

In this numerical study, a plastic calculation type was selected in PLAXIS 2D to evaluate the bearing capacity and failure mechanisms of the soil under strip footing. The plastic analysis enables the simulation of material yielding and permanent deformation, which is essential for assessing the ultimate bearing capacity.

The analysis was carried out using a drained condition for all soil types, assuming slow loading where pore pressure dissipation occurs. The Mohr-Coulomb constitutive model was used to represent the soil behavior, which provides an acceptable balance between simplicity and accuracy for this type of analysis.

The plastic calculation allows the software to capture both the elastic response of the soil during initial loading stages and the plastic behavior as the soil approaches failure. The calculation phase proceeds until the soil fails or the load-displacement curve reaches a stable limit, indicating ultimate bearing capacity.

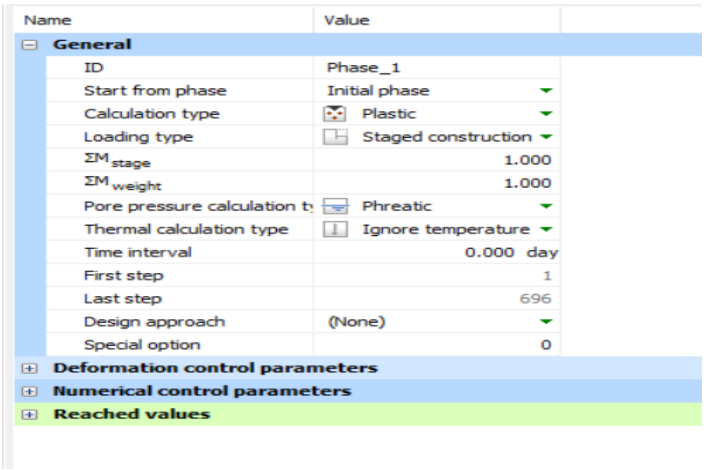


Figure III-15 Set current model phase to the calculated phase.

Ⅲ-8-3Analysis of Mesh Deformation

In this section, the behavior of the soil is examined through three key outputs from the PLAXIS 2D model:

Ⅲ-8-3-1Mesh Deformation: The deformed mesh image provides insight into the overall distortion of the soil domain under applied loading. It highlights areas where strain is concentrated, which can be linked to potential failure surfaces. The (figure III-16) shows the deformed mesh at the end of the plastic calculation phase, magnified 5 times to better visualize the deformation pattern.

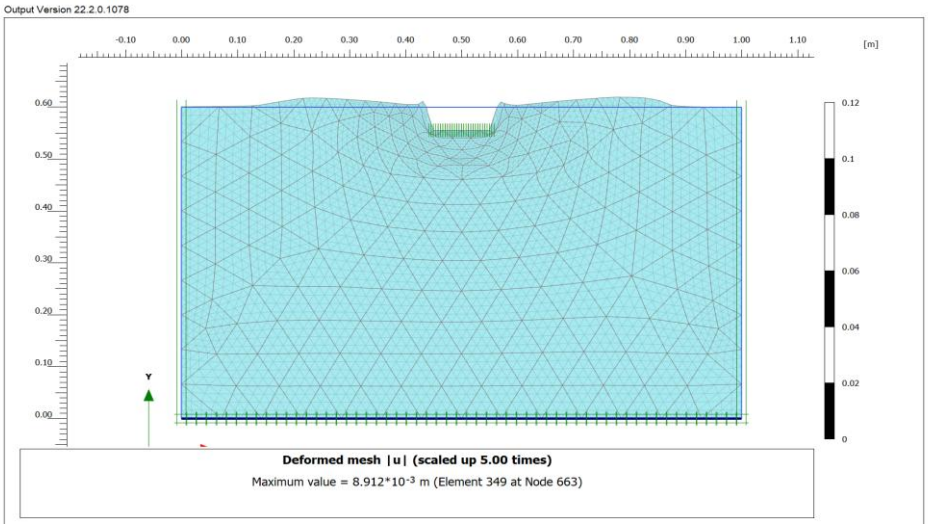


Figure III-16 Deformed mesh.

Ⅲ-8-3-2Total Horizontal Displacement (Ux): The horizontal displacement results illustrate the lateral movement of the soil mass under vertical loading. These displacements help assess the stiffness of the soil system and identify zones where significant lateral spread occurs.

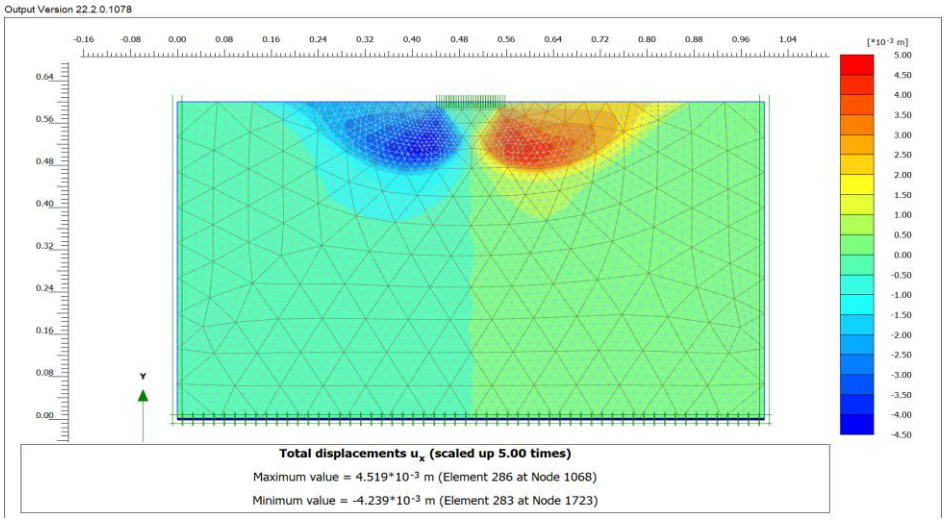


Figure III-17 Total displacements U_x.

Ⅲ-8-3-3Total Vertical Displacement (Uy): The vertical displacement results represent the overall settlement of the soil. They reveal how the soil compresses beneath the foundation and how upward movement may occur at adjacent areas, indicating possible heaving near the edges.

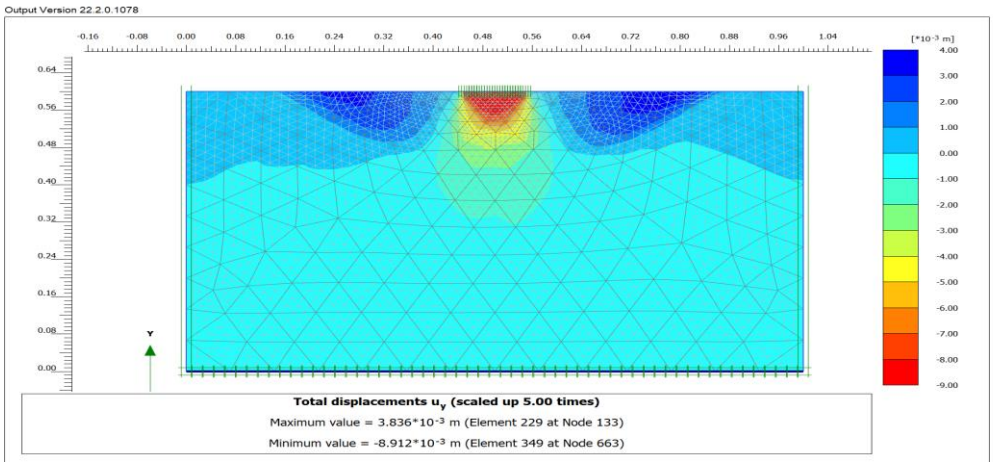


Figure III-18 Total displacements U_y.

Ⅲ-9 Bearing Capacity

In this phase, the goal is to evaluate the ultimate bearing capacity of the shallow foundation by performing a plastic analysis using the finite element method in PLAXIS 2D.

The plastic calculation simulates the gradual loading of the foundation until the soil reaches failure. In this study, the plastic phase was modeled by applying vertical forces incrementally and observing the evolution of displacements and stress states in the soil mass.

As illustrated in (figureIII-19), the soil under the foundation experiences significant vertical and lateral displacements, especially in the central zone. These deformations indicate the beginning of plastic flow, which is critical in assessing the ultimate load-bearing capacity.

In addition, the following figure displays the calculation information window, showing key numerical parameters during this phase:

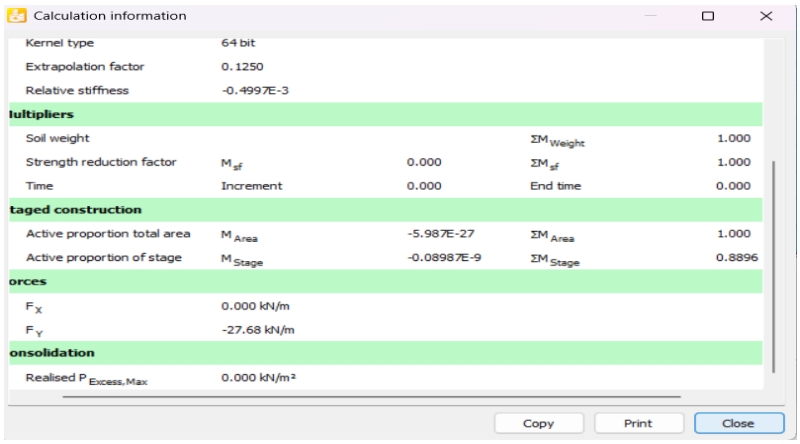


Figure III-19 Calculation information.

We can observe that the vertical force applied is approximately -27.68 kN/m, which corresponds to the maximum load supported by the foundation before the onset of failure. The strength reduction factor M_{SF} is equal to 1.0, indicating no reduction in strength during this phase, confirming that it is a plastic analysis rather than a safety factor reduction analysis.

Furthermore, the ultimate bearing capacity q_u can also be computed manually using the simple relation:

$$q_u = F_y / A$$

Where **Fy** is the applied vertical pressure and A is the loaded section area.

This offers a quick hand-calculation check alongside the detailed finite-element result.

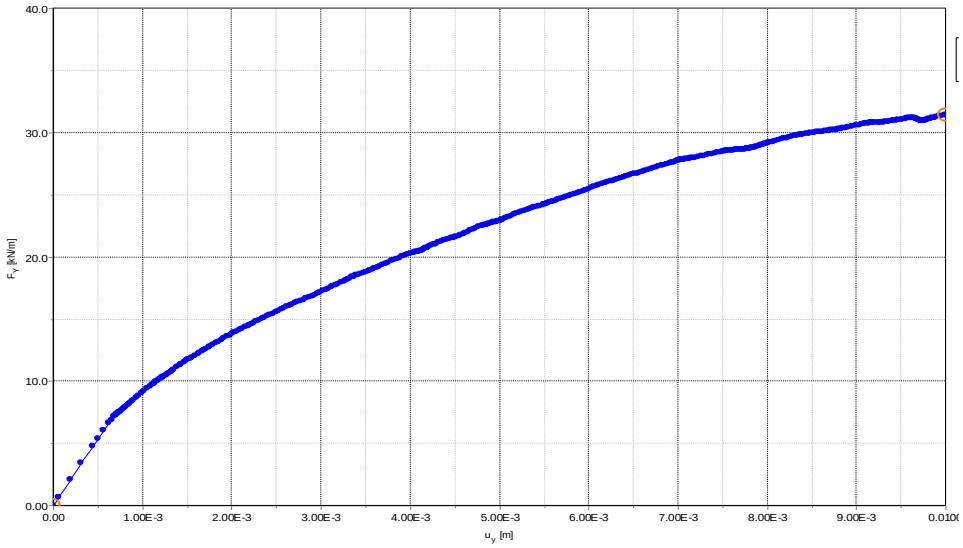


Figure III-20 Load–Settlement curve of the footing (PLAXIS 2d)

Ⅲ-10Validation by Comparing Plaxis and Terzaghi Results

To validate the numerical model created in Plaxis, a comparison was carried out between the bearing capacity values obtained from PLAXIS simulations and those calculated analytically using Terzaghi's bearing capacity formula. The table below summarizes the results for different soil compositions ranging from B0 (pure sand) to B100 (pure clay).

$$q_u = 1/2 * \gamma B * N_{\gamma'} + C * N_{C'} + \gamma * D * N_{q'}$$

Example:

Soil B80: γ=15.81KN/m^2 C=25KPa Φ=5 (degree) N_C'=6.74 $N\gamma'$=0.074

$$q_u = 0.5 * 15.81 * 0.1 * 0.074 + 25 * 6.74$$

$$q_u = 168.6KPa$$

Table III-3 Comparison between numerical and analytical bearing capacities for unreinforced soil.

Soil Type	Q_u (PLAXIS) [kPa]	Q_u (Terzaghi) [kPa]
B40	202.1	181.53
B60	188.6	154.96
B80	166.6	168.6
B100	165.3	188.1

The results show that the bearing capacity values from PLAXIS are consistently lower than those obtained using Terzaghi's method. This discrepancy is expected, as Terzaghi's formula provides an idealized theoretical estimation that does not account for several real-life factors such as mesh discretization, material non-linearity, and plastic behavior considered in the PLAXIS model.

Despite the differences, the general trend observed in both methods is similar: the bearing capacity decreases with the increase in clay content. This confirms the consistency of the Plaxis results and validates the reliability of the numerical approach used.

Ⅲ-11 Conclusion

In this chapter, a comprehensive numerical model was developed using PLAXIS 2D to simulate the load-bearing behavior of shallow foundations on cohesive-frictional soils. The modeling process included the definition of geometry, material properties, boundary conditions, loading method, mesh configuration, and hydraulic assumptions.

The model was validated through comparison with Terzaghi's analytical bearing capacity equation for unreinforced soil, and the results showed good agreement, confirming the reliability of the numerical approach.

The established model provides a solid foundation for the upcoming parametric study, where the influence of geotextile reinforcement on soil performance will be systematically investigated in the next chapter.

Chapter Ⅳ: Parametric study

Ⅳ-1Introduction:

This chapter presents a comprehensive numerical study aimed at evaluating the improvement of bearing capacity of shallow foundations through different geotextile reinforcement strategies.
The investigation is conducted using PLAXIS 2D software, focusing on various soil types ranging from pure sand (B0) to pure bentonite (B100).

Initially, the natural behavior of the soils without reinforcement is analyzed to establish a reference.
Subsequently, several reinforcement methods are applied:

- Simple horizontal geotextile layers (Series C)
- Full Wraparound technique with identical internal and external soils (Series D)
- Full Wraparound with a strong internal B0 core (Series E)
- Full Wraparound with full encapsulation using B0 internally and above (Series F)

In addition to analyzing soil behavior and reinforcement techniques, the study also investigates the influence of key reinforcement parameters, namely:

- the embedment depth to footing width ratio (U/B),
- the reinforcement width to footing width ratio (W/B),
- the vertical spacing to footing width ratio (H/B),
- And the number of geotextile layers (N).

These parameters are systematically varied to assess their impact on the performance of reinforced shallow foundations.

The goal is to identify the most effective strategy for enhancing bearing capacity, especially in weak soils, and to understand the key factors controlling the soil–reinforcement interaction.

Table IV-1 Details of numerical programs.

Investigation Cases	Reinforcement Layout Configurations	Test Series	Soil Ground	Filled Soil	Reinforcement Layout Configurations	Test Series
numerical investigations	Unreinforced soil	A	B0, B20, B40, B60, B80, B100	-	-	-
	Horizontal planar reinforced soils	B-1	B0	-	N = 1, W/B = 6	U/B = 0.1, 0.3, 0.5, 1 and 2
		B-2		-	N = 1, U/B = 0.3	W/B = 2, 3, 4, 5 and 6
		B-3		-	N = 2, U/B = 0.3, W/B = 3	H/B = 0.1, 0.25, 0.5, 0.7
		B-4		-	W/B = 3, H/B = 0.5	N = 1, 2, 3 and 4
	Horizontal planar reinforced soils	C-1	B0	-	U/B = 0.3, W/B = 3, H/B = 0.5	N = 1, 2, 3 and 4
		C-2	B20	-		
		C-3	B40	-		
		C-4	B60	-		
		C-5	B80	-		
		C-6	B100	-		
Numerical investigations	Full wraparound ends of geotextile	D-1	B0	B0	U/B = 0.3, W/B = 3, H/B = 0.5	N = 2, 3 and 4
		D-2	B20	B20		
		D-3	B40	B40		
		D-4	B60	B60		
		D-5	B80	B80		
		D-6	B100	B100		
	Full wraparound ends of geotextile with filled-in sand	E-1	B20	B0	U/B = 0.3, W/B = 3, H/B = 0.5	N = 2, 3 and 4
		E-2	B40			
		E-3	B60			
		E-4	B80			
		E-5	B100			
	Full wraparound ends of geotextile reinforcement with filled-in sand and sand backfill	F-1	B20	B0	U/B = 0.3, W/B = 3, H/B = 0.5	N = 2, 3 and 4
		F-2	B40			
		F-3	B60			
		F-4	B80			
		F-5	B100			

Ⅳ-2Effect of Soil Nature (Series A)

In this section, we investigate the effect of soil composition on the ultimate bearing capacity of a shallow foundation. The study is based on a series of numerical simulations conducted using PLAXIS 2D. Six different soil mixtures were considered: B0, B20, B40, B60, B80, and B100. These mixtures represent different proportions of sand and bentonite. The objective of Series A is to analyze how the mechanical properties of the soil—specifically cohesion and internal friction angle—affect the load-bearing behavior of the foundation. The bearing capacities obtained from each simulation are compared, and relevant curves are presented to support the discussion and interpretation of the observed trends.

Ⅳ-2-1 Results and Discussion

TableIV-2 Ultimate Bearing Capacity Vs Soil Type.

Soil Type	Internal Friction Angle (°)	Cohesion (kPa)	Ultimate Bearing Capacity (kPa)
B0	40	2.8	276.8
B20	30	7.0	254.4
B40	12	21.0	202.1
B60	9	23.0	188.6
B80	5	25.0	166.6
B100	0	33.0	165.3

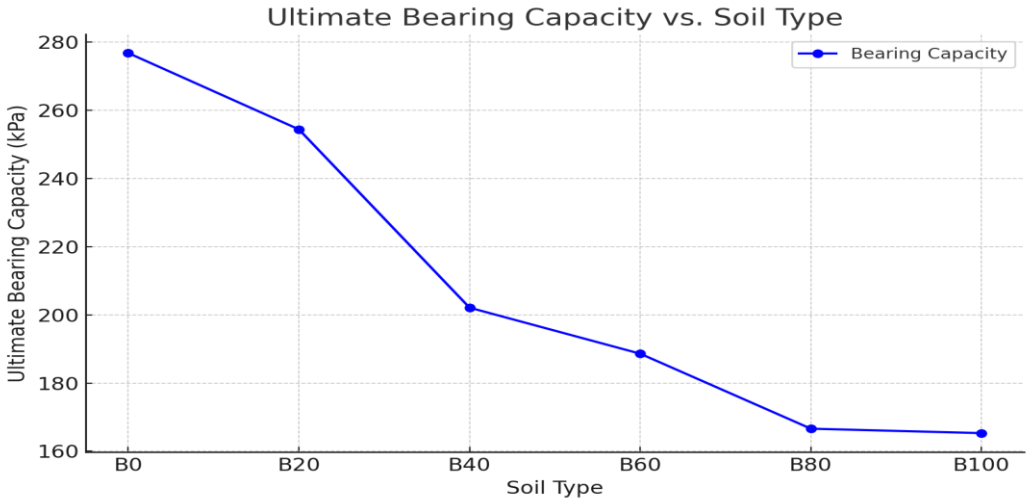


Figure IV-1 Ultimate bearing capacity vs soil type.

This figure illustrates the relationship between ultimate bearing capacity (in kPa) and soil type, which appears to be categorized using a B-value classification system .The numerical results from Series A reveal a clear trend in how soil composition affects the ultimate bearing capacity. The soil type B0, which consists of pure sand, exhibited the highest bearing capacity. This can be attributed to its relatively high internal friction angle and low cohesion.

As the proportion of bentonite increased in the mixtures (from B20 to B100), the bearing capacity gradually decreased. For instance, the mixture B100, composed entirely of bentonite, showed the lowest capacity among all tested soils. This is due to the fact that while cohesion increases with more bentonite content, the internal friction angle significantly drops, reducing the soil's ability to resist shear under the footing.

These observations align with the shear strength behavior of cohesive-frictional soils, where both parameters—cohesion and friction angle—play critical roles. The simulations clearly show that a high internal friction angle, as in B0 and B20, contributes more significantly to the overall bearing capacity than cohesion alone. This behavior is illustrated in the load-settlement curves and stress distribution patterns, where dense granular soils demonstrate sharper resistance to settlement compared to fine, clay-rich soils.

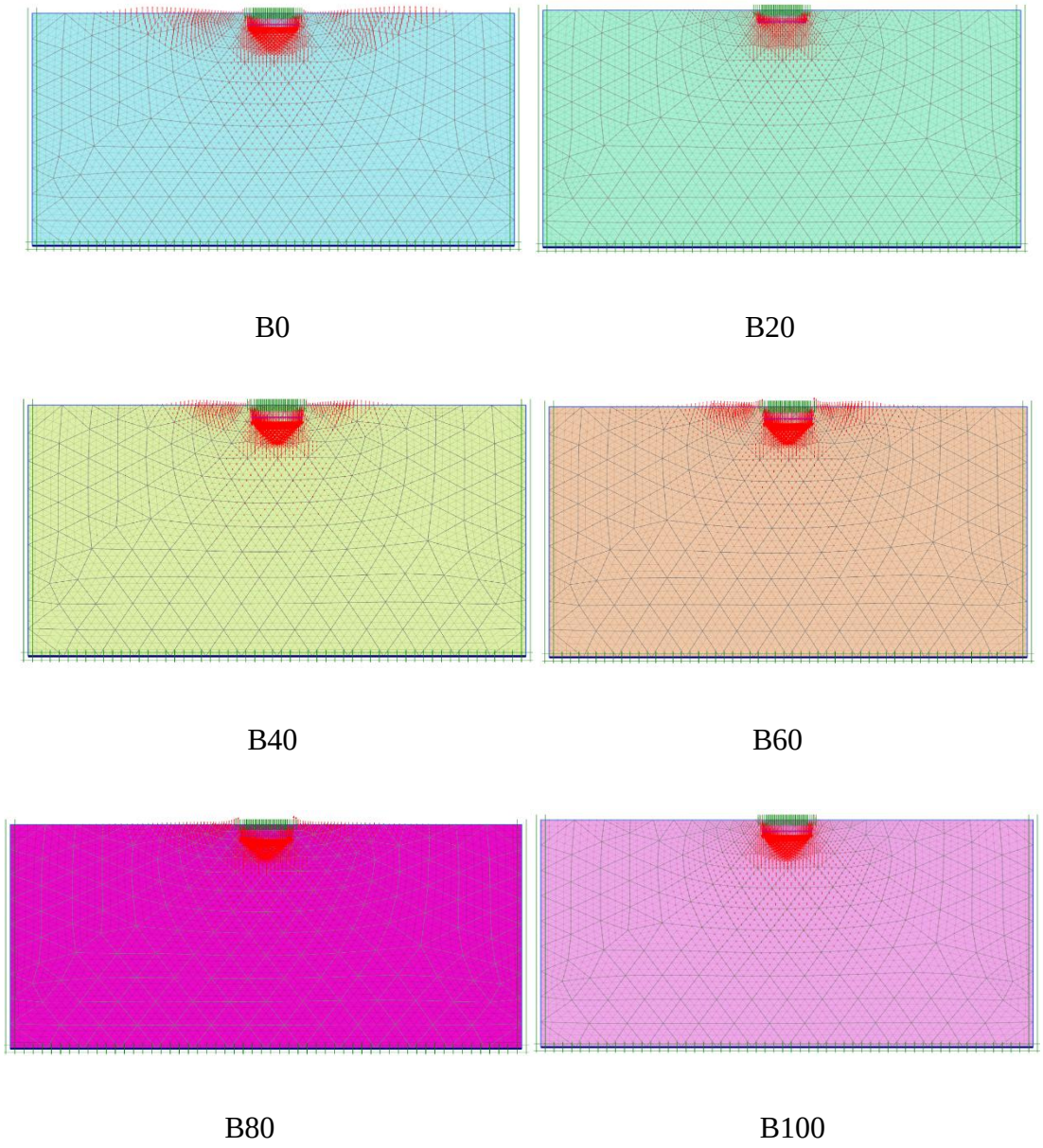


Figure IV-2: Distribution of deformation for different soil types.

Ⅳ-3Effect of Reinforcement – Series B:

In this section, the effect of geotextile reinforcement on the bearing capacity of shallow foundations is examined. Numerical simulations were carried out using PLAXIS 2D to evaluate how different reinforcement configurations improve the load-bearing behavior of sandy soil (B0).

The analysis focused on varying the key reinforcement parameters:

- **U**: the depth of the first reinforcement layer from the footing base,

- **W**: the width of the geotextile layer, and
- **H**: the vertical spacing between reinforcement layers.

The purpose of this series is to identify the optimal reinforcement configuration that yields the maximum improvement in bearing capacity. Each parameter was varied systematically while keeping the others constant, and the corresponding ultimate bearing capacities were compared using load–settlement curves and bearing capacity ratios.

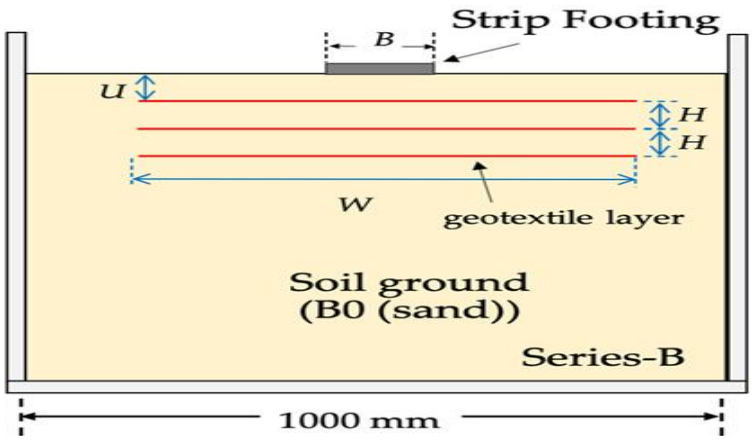


Figure IV-3 Reinforcement Layout Configurations for Numerical Investigations.[21]

IV-3-1 Series B1 – Effect of Reinforcement Depth (U/B):

IV-3-1-1Results and Discussion

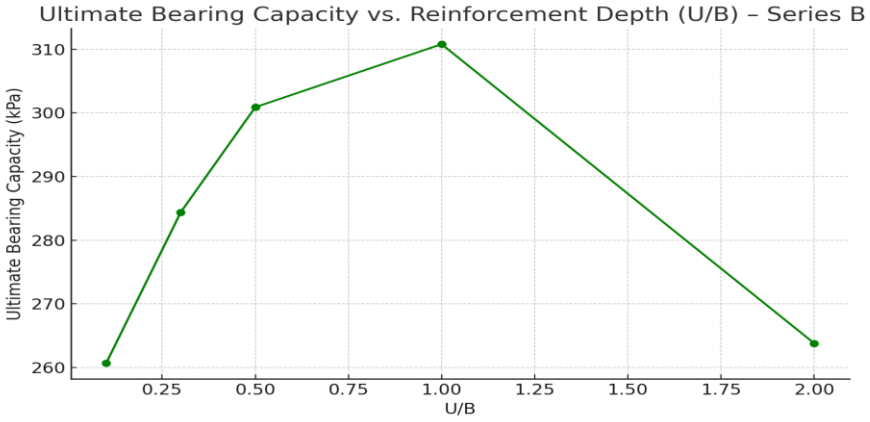


Figure IV-4 Relationship between bearing stress with various parameters of (u/b).

This graph illustrates the relationship between ultimate bearing capacity (kPa) and the reinforcement depth ratio U/B. In this part of the study, the influence of the reinforcement depth (U), expressed as a ratio to the footing width (U/B), on the ultimate bearing capacity of a shallow foundation was investigated. A single geotextile layer was used, and numerical simulations were conducted in PLAXIS 2D for five different embedment depths: U/B = 0.1, 0.3, 0.5, 1.0, and 2.0. The results show a clear trend: the bearing capacity increases with U/B, reaching a peak value of 310.8 kPa at U/B = 1.0. However, the result at U/B = 0.5 is also significantly high, reaching 300.9 kPa, which is very close to the maximum. This suggests that although U/B = 1.0 gives the highest value, selecting U/B = 0.5 is more efficient and cost-effective, since it provides nearly the same performance with a shallower reinforcement depth—reducing excavation and material use. Therefore, U/B = 0.5 can be considered the optimal choice from both technical and economic perspectives.

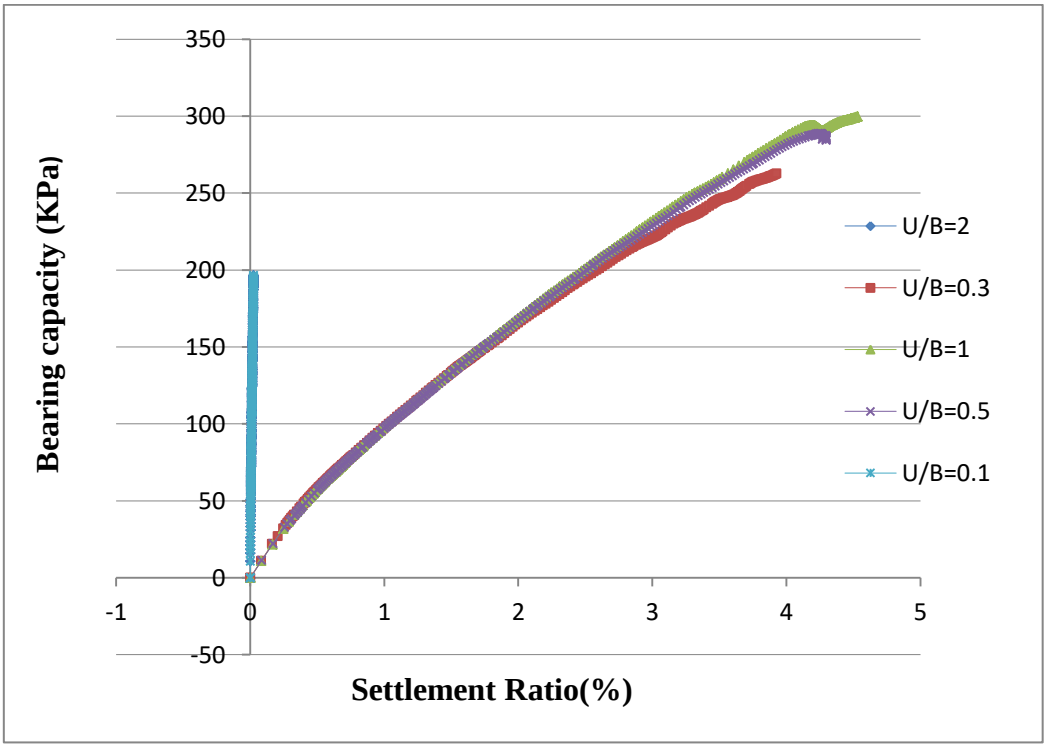
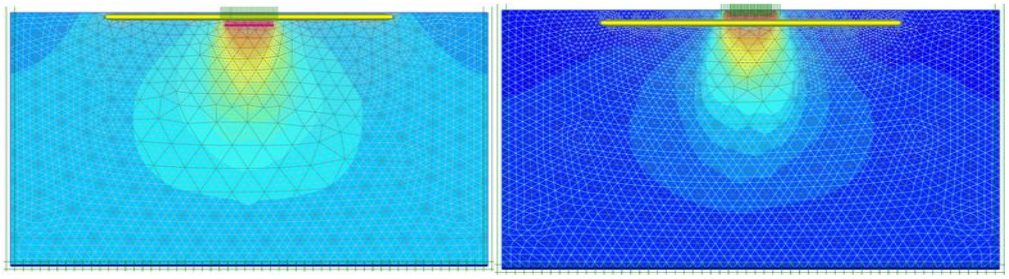
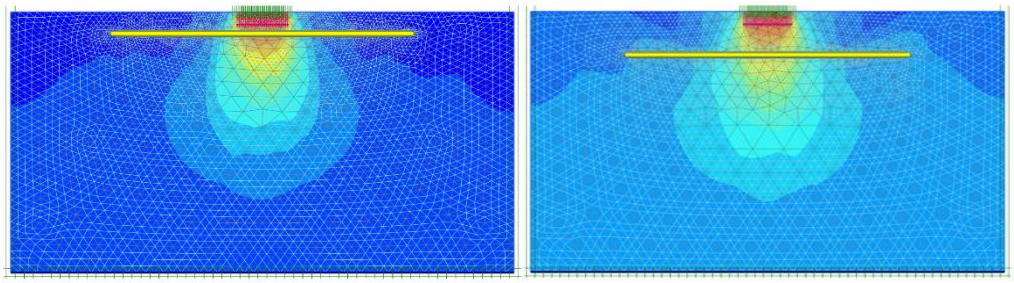


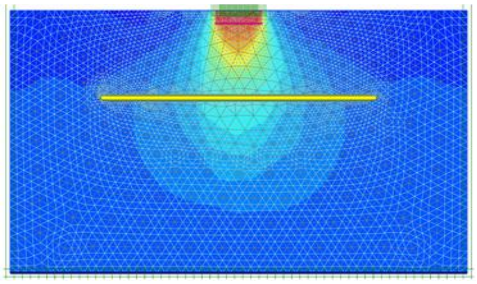
Figure IV-5 Relationship Between Bearing Stress And S/B Ratio with Various Parameters of U/B



U/B=0.1 U/B=0.3



U/B=0.5 U/B=1



U/B=2

Figure IV-6 Effect Of U/B Ratio on Stress Distribution Below the Footing.

Ⅳ-3-2Effect of Geotextile Width (W) (Series B2):

Ⅳ-3-2-1Results and Discussion:

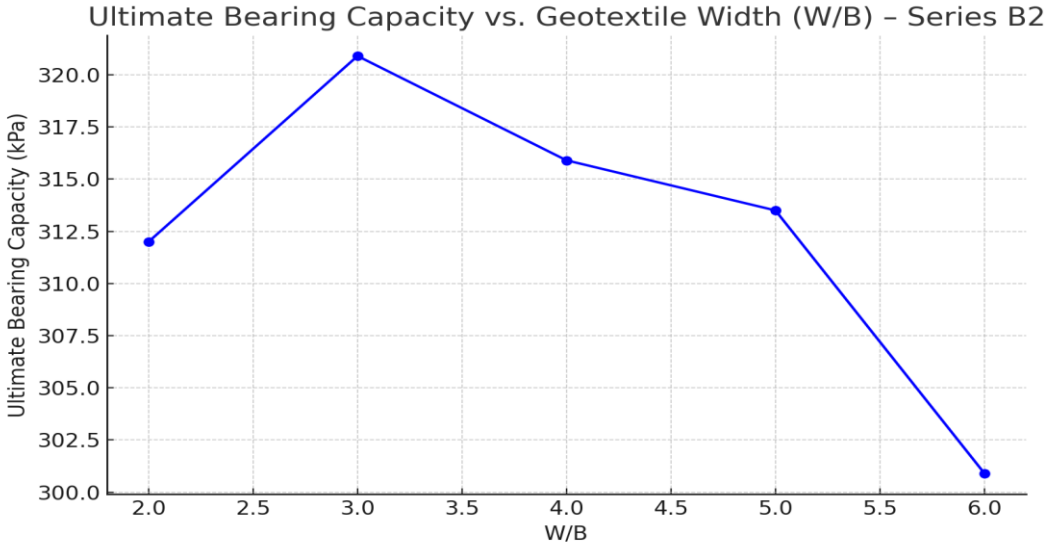


Figure IV-7 Relationship Between Bearing Stress with Various Parameters Of (W/B).

This graph illustrates the relationship between ultimate bearing capacity (kPa) and the geotextile width ratio W/B, where W represents the width of geotextile reinforcement and B likely represents the foundation width. The reinforcement was placed at a constant depth of U = 0.5 m, and the width was varied across the following values: 0.2 m, 0.3 m, 0.4 m, 0.5 m, and 0.6 m, corresponding to W/B ratios of 2 to 6.

The results obtained from PLAXIS 2D simulations show that the bearing capacity increases with reinforcement width up to W = 0.3 m, where it reaches a maximum value of 320.9 kPa. Beyond this width, the capacity slightly decreases, indicating that additional width does not contribute significantly to further improvement. Therefore, W = 0.3 m (W/B = 3) appears to be the most efficient reinforcement width in this configuration.

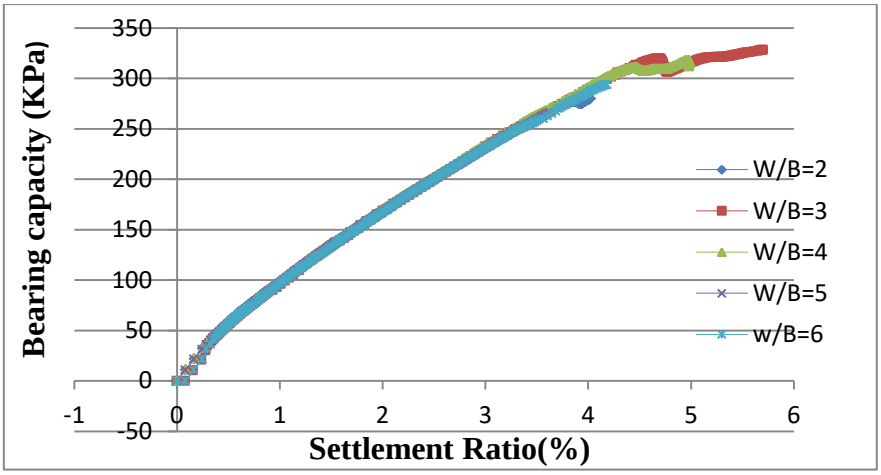
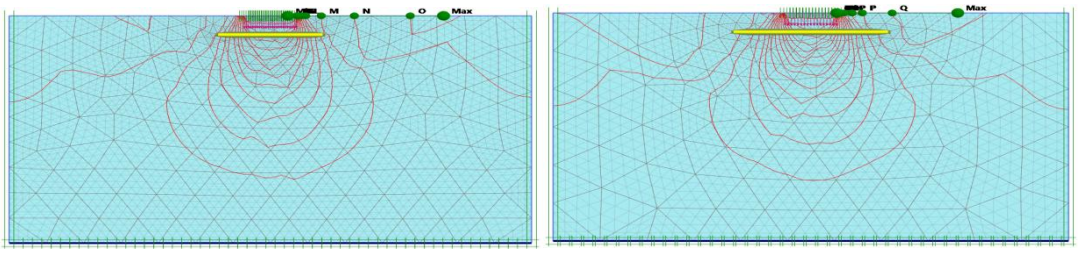
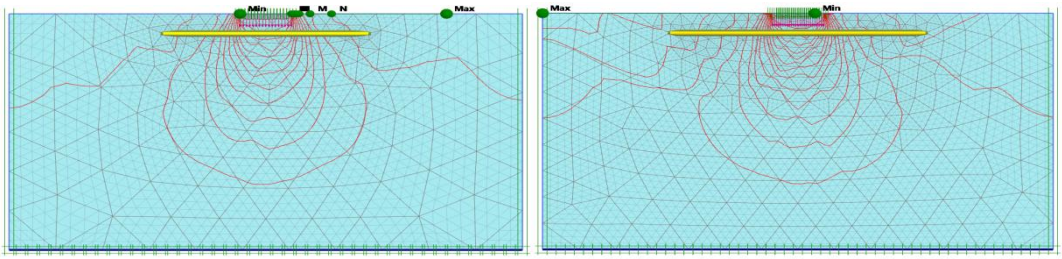


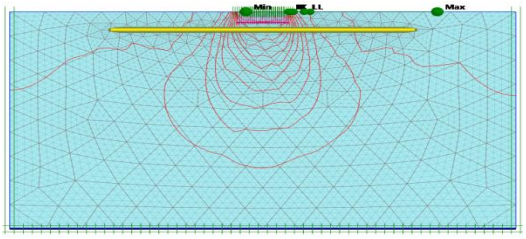
Figure IV-8 Relationship Between Bearing Stress And S/B Ratio with Various Parameters Of W/B



W/B=2 W/B=3



W/B=4 W/B=5



W/B=6

Figure IV-9 Effect of Geotextile Length (W/B) On Deformation Patterns in Reinforced Soil.

Ⅳ-3-3 Effect of Vertical Spacing Between Reinforcement Layers (H/B) -Series B3

Ⅳ-3-3-1 Results and Discussion:

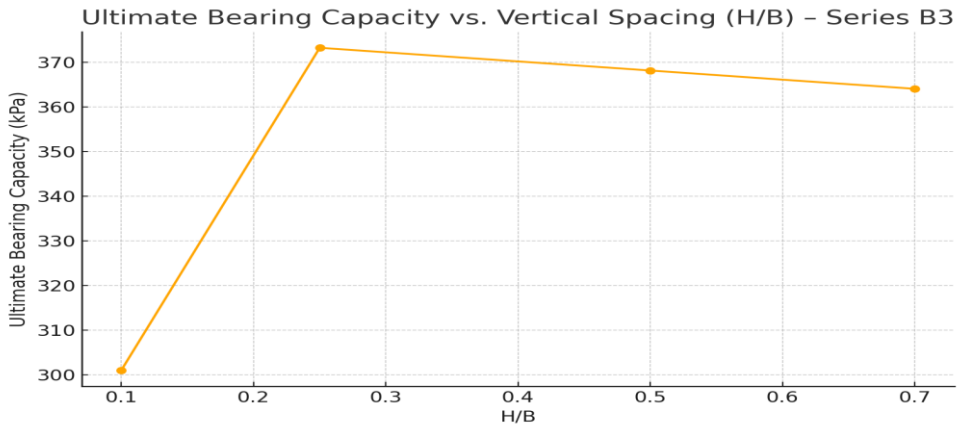


Figure IV-10 Relationship Between Bearing Stress with Various Parameters Of (H/B).

This graph illustrates the relationship between ultimate bearing capacity (kPa) and the vertical spacing ratio H/B for Series B3, where H represents the vertical spacing between reinforcement layers and B likely represents the foundation width. The distance between the layers was expressed as a ratio to the footing width (H/B), and four values were tested: 0.1, 0.25, 0.5, and 0.7.

The results indicate that the maximum bearing capacity was achieved at H/B = 0.25, reaching a value of 373.3 kPa. As the spacing increased beyond this point, a slight decrease in bearing capacity was observed. When the spacing was too small (H/B = 0.1), the performance was also lower. This suggests that an optimal spacing exists where the interaction between reinforcement layers is maximized, and in this case, it corresponds to H/B = 0.25.

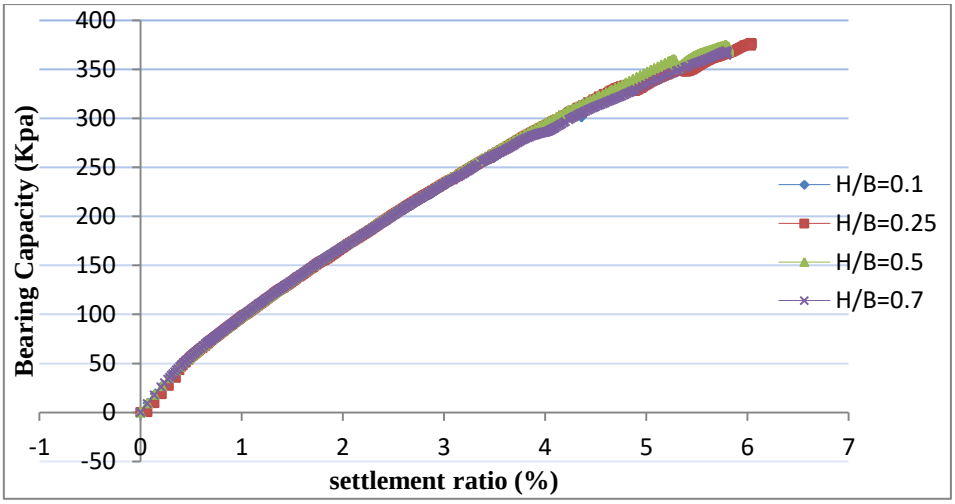
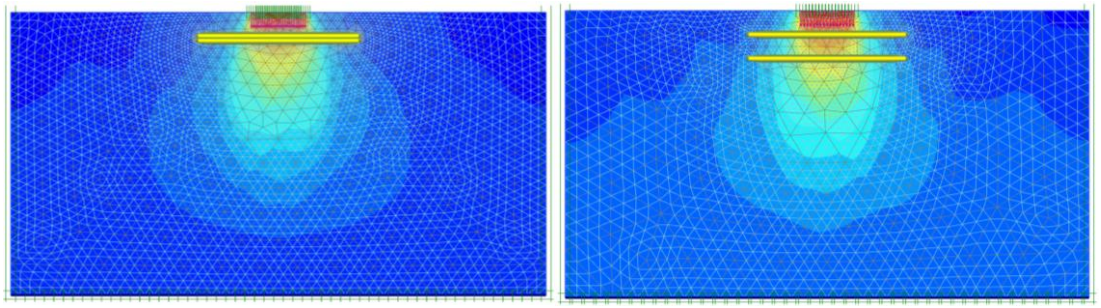
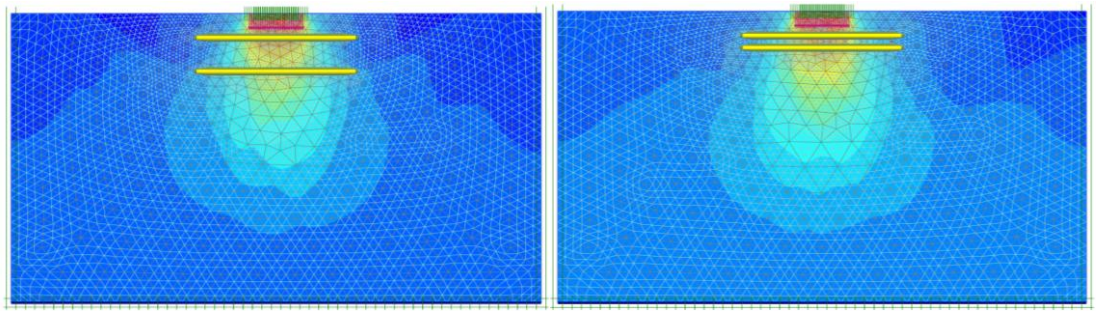


Figure IV-11 Relationship between bearing stress and S/B ratio with various parameters of H/B



H/B=0.1 H/B=0.25



H/B=0.5 H/B=0.7

Figure Ⅳ-12 Effect Of H/B Ratio on Stress Distribution Below the Footing.

Ⅳ-3-4 Series B4

IV-3-4-1 Results and Discussion

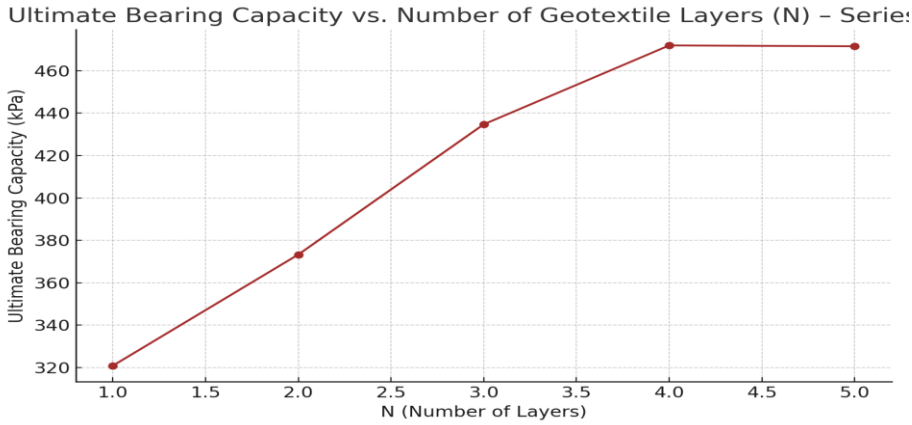


Figure IV-13 Relationship Between Bearing Stress with Various Parameters Of (N).

This section analyzes the influence of the number of geotextile layers (N) on the ultimate bearing capacity of a shallow foundation.

All other parameters, including soil type and reinforcement configuration, were kept constant while only the number of layers was varied from 1 to 5.

The results show that the bearing capacity increases significantly with the number of reinforcement layers.

The capacity rose from 320.9 kPa with a single layer to a maximum of 471.9 kPa at N = 4. However, when a fifth layer was added (**N = 5**), the increase was negligible, and the capacity slightly dropped to 471.5 kPa.

This reduction is explained by the geotechnical behavior of the reinforced soil: the fifth layer is likely located outside the failure zone (zone of rupture lines), which means it no longer interacts effectively with the stress paths or shear zones that develop under loading.

As a result, the fifth layer fails to mobilize significant tensile force, and its contribution becomes minimal.

Therefore, adding more than four layers leads to increased cost without practical benefit. The optimal solution is to limit the number of layers to four, which ensures full interaction within the critical failure zone and maximizes the reinforcement efficiency.

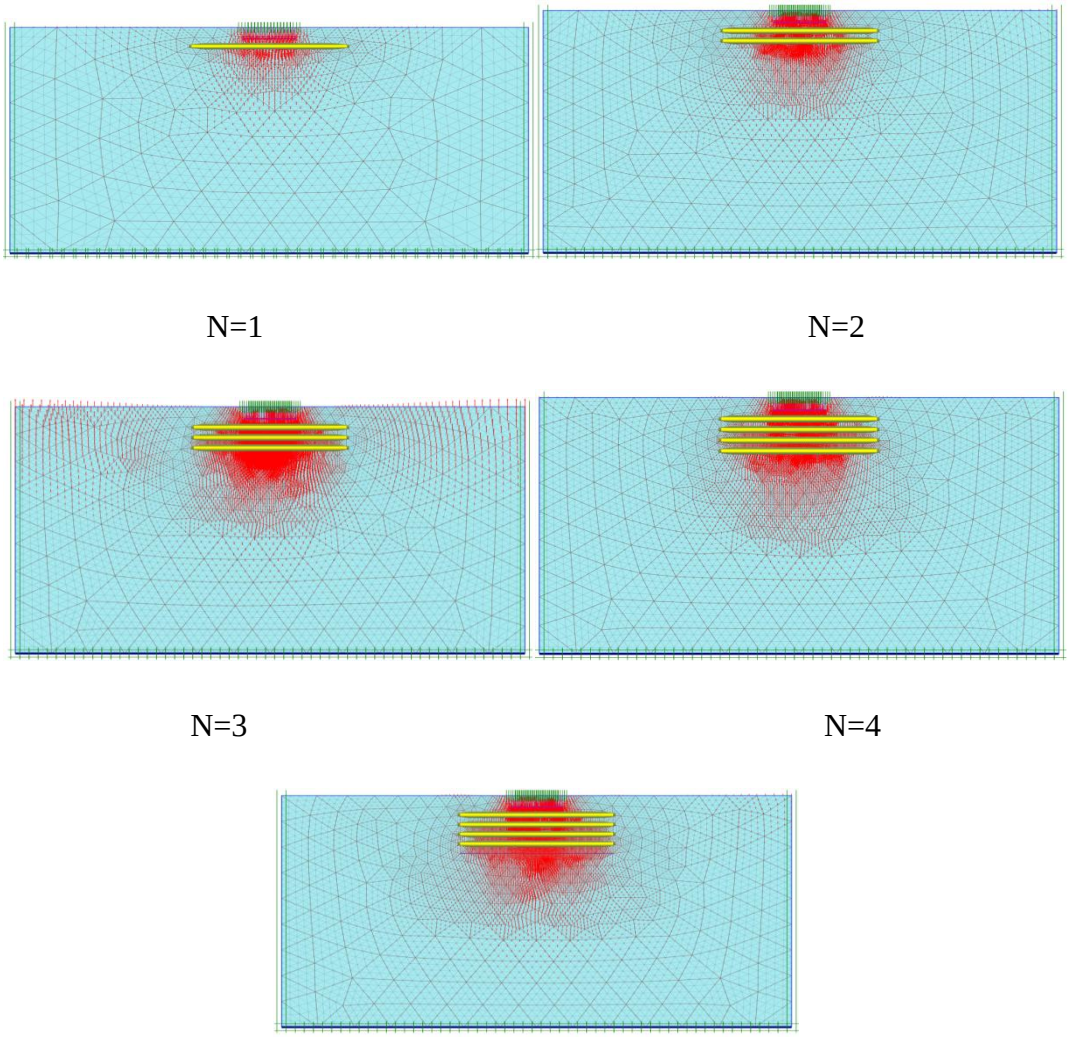


Figure IV-14 Effect of Geotextile Layer Number (N) On Soil Reinforcement Efficiency.

Ⅳ-4 Series c:

Reinforced soils using geotextile.

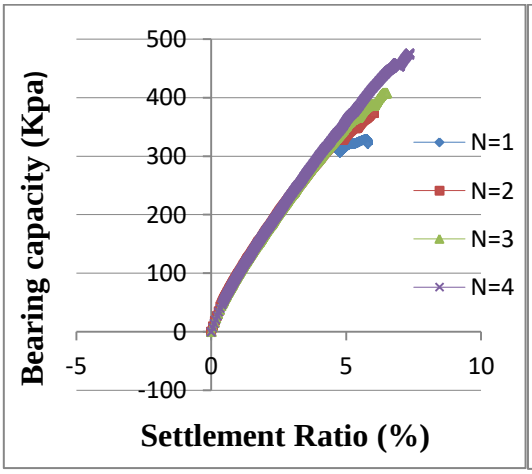
To ensure a fair comparison, all reinforcement parameters were fixed based on the optimal configuration obtained from previous series, especially Series B, using the following values: U/B = 0.5, W/B = 3, H/B = 0.5 (all values in meters).

A simple horizontal reinforcement method was adopted, where one to four layers of planar geotextile were placed beneath the strip footing, without altering the shape or arrangement of the reinforcement.

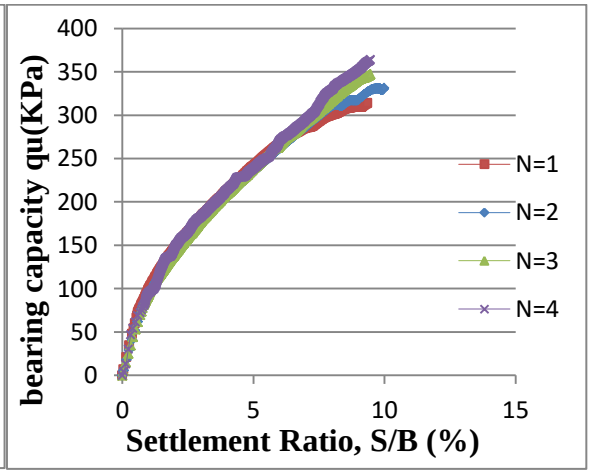
Six different soil types were considered in this study: B0, B20, B40, B60, B80, and B100, each characterized by specific mechanical properties.

To comprehensively evaluate the performance, each soil type was tested under four reinforcement scenarios: with one, two, three, and four horizontal geotextile layers. The objective was to assess how the soil's properties interact with horizontal reinforcement and how the number of layers affects the ultimate bearing capacity for each soil type.

Ⅳ-4-1-1Results and Discussion:



B0



B20

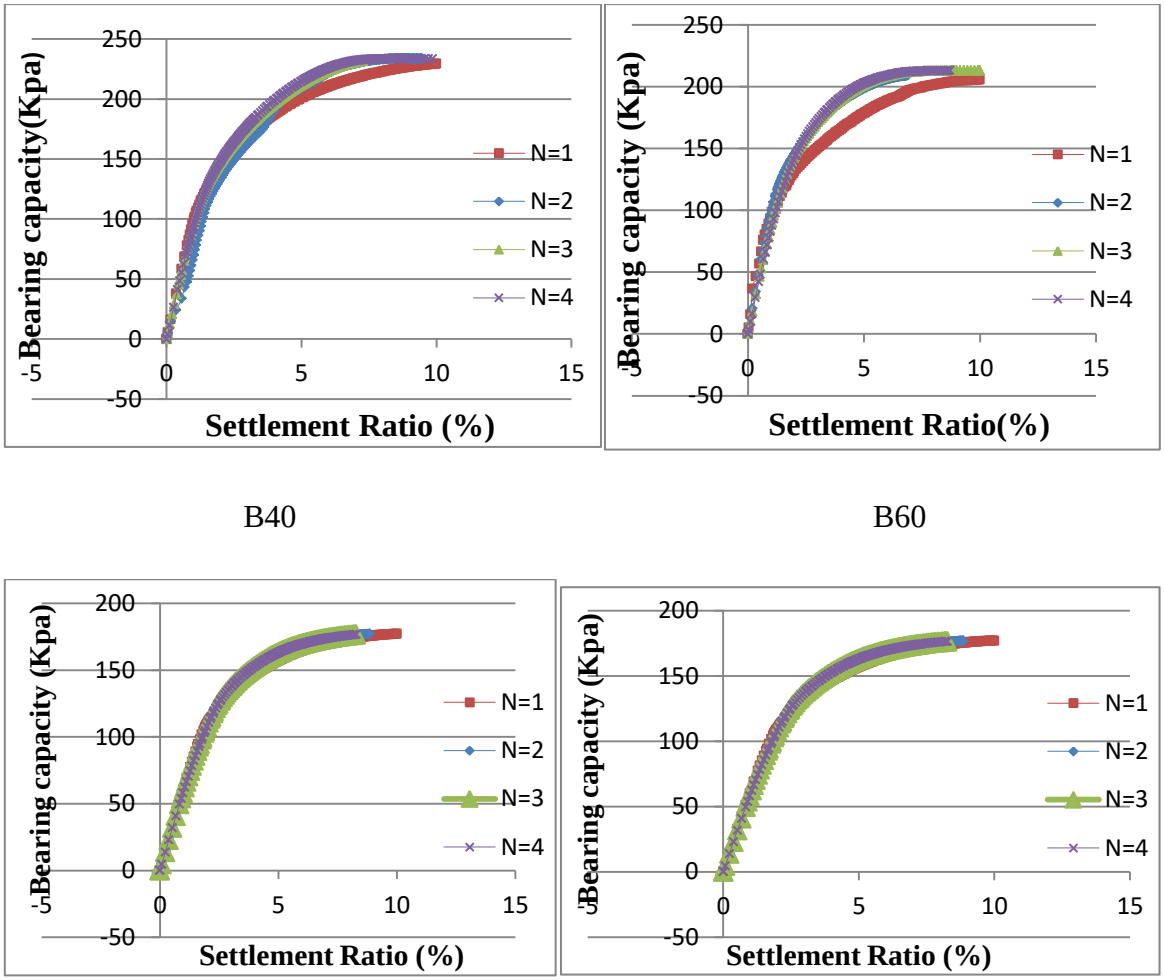


Figure IV-15 Simulated Bearing Stress Results Of Strip Footing Resting On Different Soils Reinforced With Different Reinforcing (Series C)**.**

The results show that the ultimate bearing capacity increases progressively with the number of geotextile layers across all soil types. This trend is more pronounced in stronger soils (e.g., B0 and B20), where the reinforcement effect is more efficiently mobilized, leading to significant improvements in load-bearing performance.

In contrast, for weaker soils such as B80 and B100, the increase in bearing capacity becomes less significant after the second or third layer. This suggests that excessive reinforcement in such soils may lead to diminishing returns, where additional layers do not contribute proportionally to the capacity increase.

Notably, the best results were obtained for B0 with four reinforcement layers, reaching a maximum value of 471.9 kPa, while B100 showed a limited increase, reaching 174.6 kPa with the same configuration.

These findings indicate that the effectiveness of reinforcement is highly dependent on the soil's mechanical properties, and that the optimal number of geotextile layers should be tailored to the soil type in order to achieve a balance between performance and cost-efficiency.

Ⅳ-5 Series D:

In this part of the study, the focus is placed on evaluating the effect of the reinforcement configuration using the Full Wraparound method.

This technique involves enclosing the reinforced soil within a rectangular geotextile wrap, created by joining two flexible geotextile sheets. The internal and external soils are identical in each case, ensuring consistency across the experimental conditions.

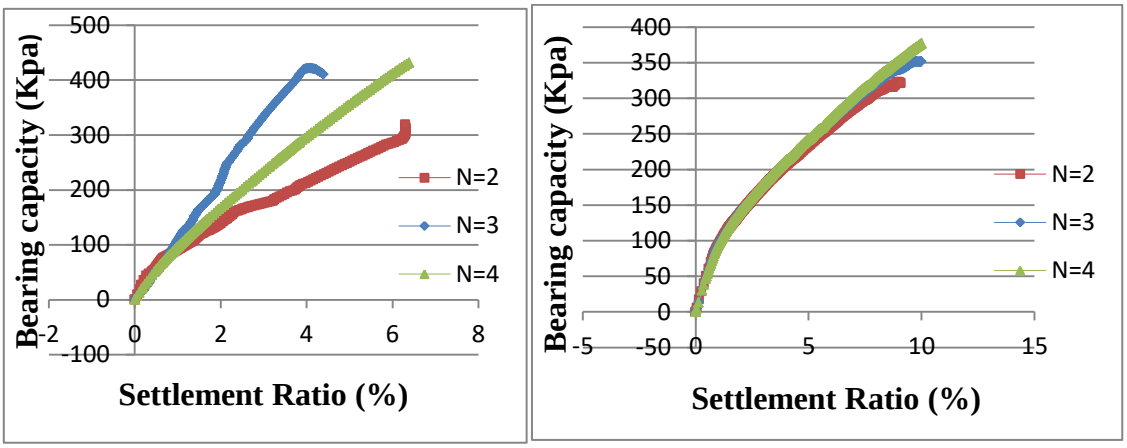
The Full Wraparound forms a closed box filled with the same soil used for the surrounding medium, allowing both lateral and bottom confinement. This enhances the interaction between the geotextile and the soil and improves the system's overall stability and bearing capacity.

For each soil type (B0, B20, B40, B60, B80, B100), several reinforcement configurations were tested by varying the number of rectangular geotextile units (or “boxes”):

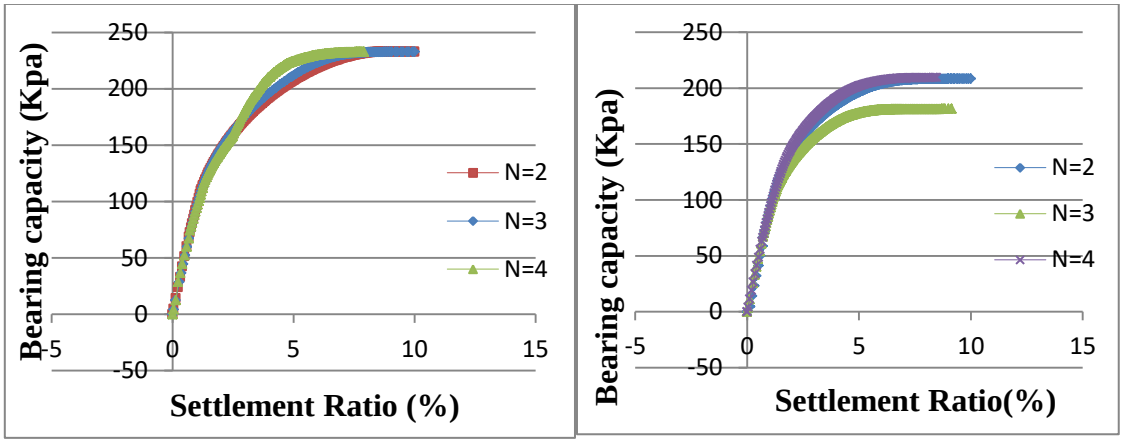
- one box (single unit),
- two boxes,
- and three boxes.

Each configuration simulates a teamwork concept, where the number of units reflects the level of reinforcement collaboration. The objective is to study how the number of geotextile boxes influences the ultimate bearing capacity of the foundation system under different soil conditions.

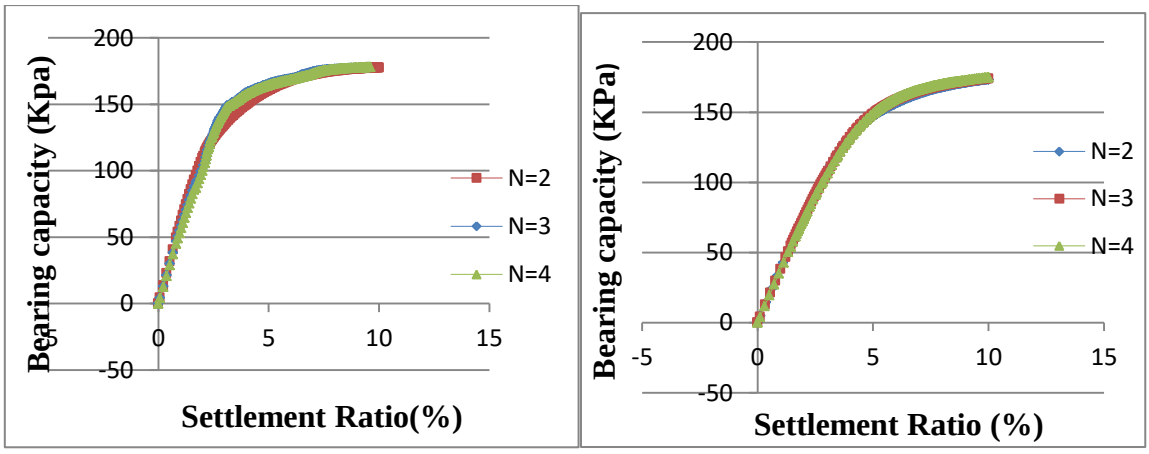
Ⅳ-5-11Results and Discussion:



B0 B20



B40 B60



B80 B100

Figure IV-16 Simulated Bearing Stress Results Of Strip Footing Resting On Different Soils Reinforced With Different Reinforcing (Series D).

The results indicate a significant improvement in bearing capacity when the Full Wraparound method is applied, especially in stronger soils such as B0 and B20. The difference between unreinforced and reinforced conditions is particularly noticeable in B0, where the bearing capacity increases from 176.8 kPa (unreinforced) to 527.8 kPa with four geotextile layers—almost a tripling of the performance.

In moderate-strength soils like B40 and B60, the increase is present but more limited. For example, B40 improves from 202.1 kPa to 239.8 kPa, while B60 goes from 188.6 kPa to 209.5 kPa, indicating a diminishing return as the soil becomes less responsive to confinement.
For weaker soils such as B80 and B100, the reinforcement still yields improvement, but the effect is marginal compared to stronger soils. This suggests that Full Wraparound is most effective when the soil has sufficient stiffness to mobilize the confinement, and its benefit decreases as the soil becomes softer.

Overall, the results confirm that the Full Wraparound system can substantially enhance the bearing capacity, especially in soils with good mechanical properties, making it a viable and efficient reinforcement technique in geotechnical engineering.

Ⅳ-6 Series E (Full Wraparound with B0 Core):

In this phase of the study, the Full Wraparound reinforcement method is applied again, with one key modification:

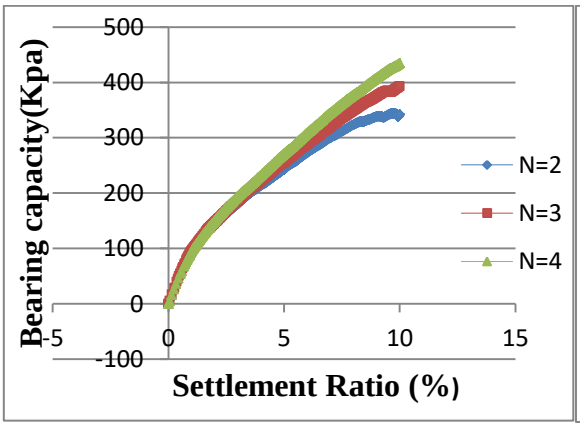
the inner fill of the geotextile box is fixed as B0 soil, while the outer surrounding soil varies depending on the case (B20, B40, B60, B80, B100).

This approach is based on the results from the previous series, which demonstrated that B0 consistently produced the highest bearing capacity among all soil types.
By using B0 as the internal material inside the geotextile confinement, the goal is to transfer its superior performance characteristics to the surrounding weaker soils.

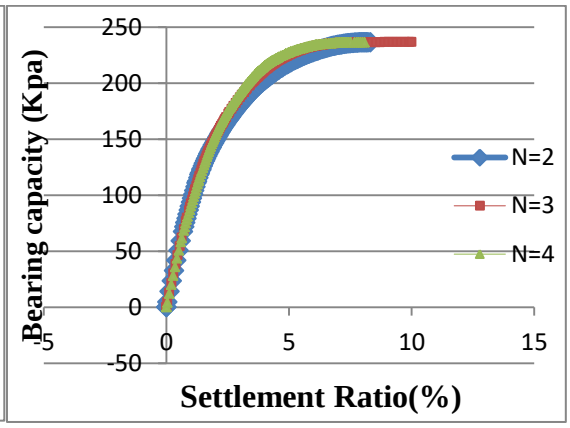
The vertical geotextile wrap is designed to mobilize tensile strength, contributing to the overall system stability by resisting lateral deformations and anchoring the inner material.

This series investigates whether the bearing capacity of weak and moderate soils can be significantly improved by using high-quality fill (B0) inside the reinforcement system, simulating a real-world engineering enhancement strategy.

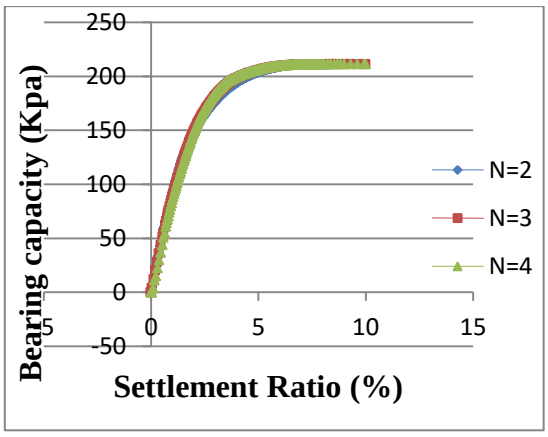
Ⅳ-6-1 Results and Discussion:



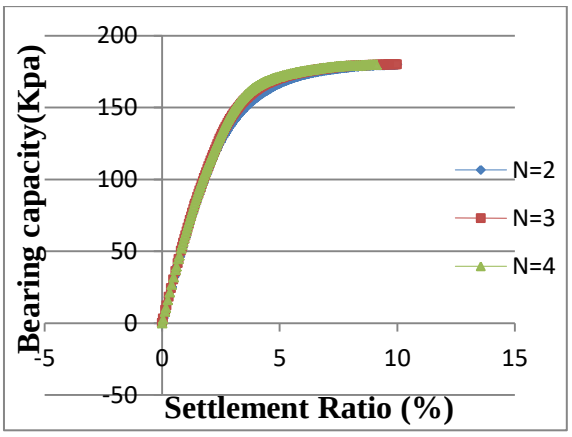
B20



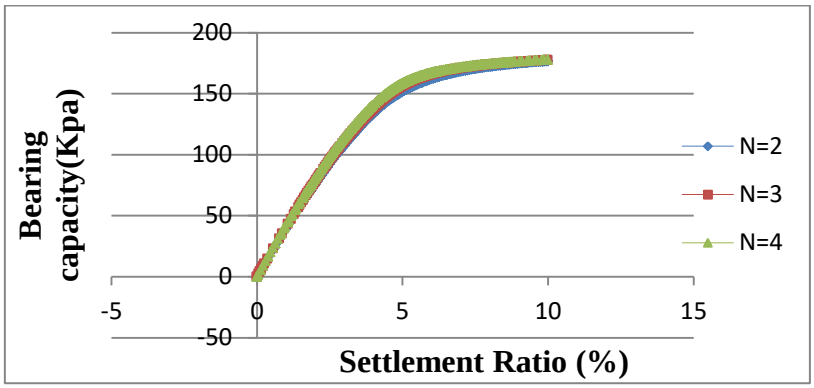
B40



B60



B80



B100

Figure IV-17 Simulated Bearing Stress Results Of Strip Footing Resting On Different Soils Reinforced With Different Reinforcing (Series E).

The results from Series E show only a slight improvement in the bearing capacity of the soils studied when using a B0 soil core within the Full Wraparound reinforcement. Compared to the results from Series D, this improvement was not substantial or as significant as expected. Although B0 had demonstrated excellent performance in previous series, using it as the internal fill was not sufficient to drastically enhance the behavior of weaker surrounding soils. The data indicate that the reinforcement effect remained limited, and the interaction between the geotextile and the outer soil was not strongly activated in most cases. Based on these findings, it can be concluded that simply using a strong core material like B0 is not enough to significantly improve the performance of weak surrounding soils. Therefore, in the next series, additional modifications to the reinforcement method will be explored to further enhance the bearing capacity.

IV-7 Series F (Full Wraparound with Full Encapsulation)

In this final reinforcement configuration, the Full Wraparound method is implemented with complete encapsulation of the reinforced zone.

The geotextile enclosure fully surrounds the internal fill, not only from the sides and bottom, but also from the top. This creates a tightly confined and fully enclosed box system.

The internal fill is composed entirely of B0 soil**,** while the surrounding soil varies across different cases **(**B20, B40, B60, B80, B100**).**

Additionally, B0 soil is also placed above the geotextile wrap, simulating a real scenario where strong material overlays a weaker foundation zone.

This configuration was inspired by findings from previous series, which showed that B0 soil consistently yielded the highest bearing capacity**.**

The objective of Series F is to determine whether the superior behavior of B0 can be transferred and imposed onto weaker soils, by enclosing them in a high-performance system that maximizes tensile resistance through full confinement.

Ⅳ-7-1Results and Discussion:

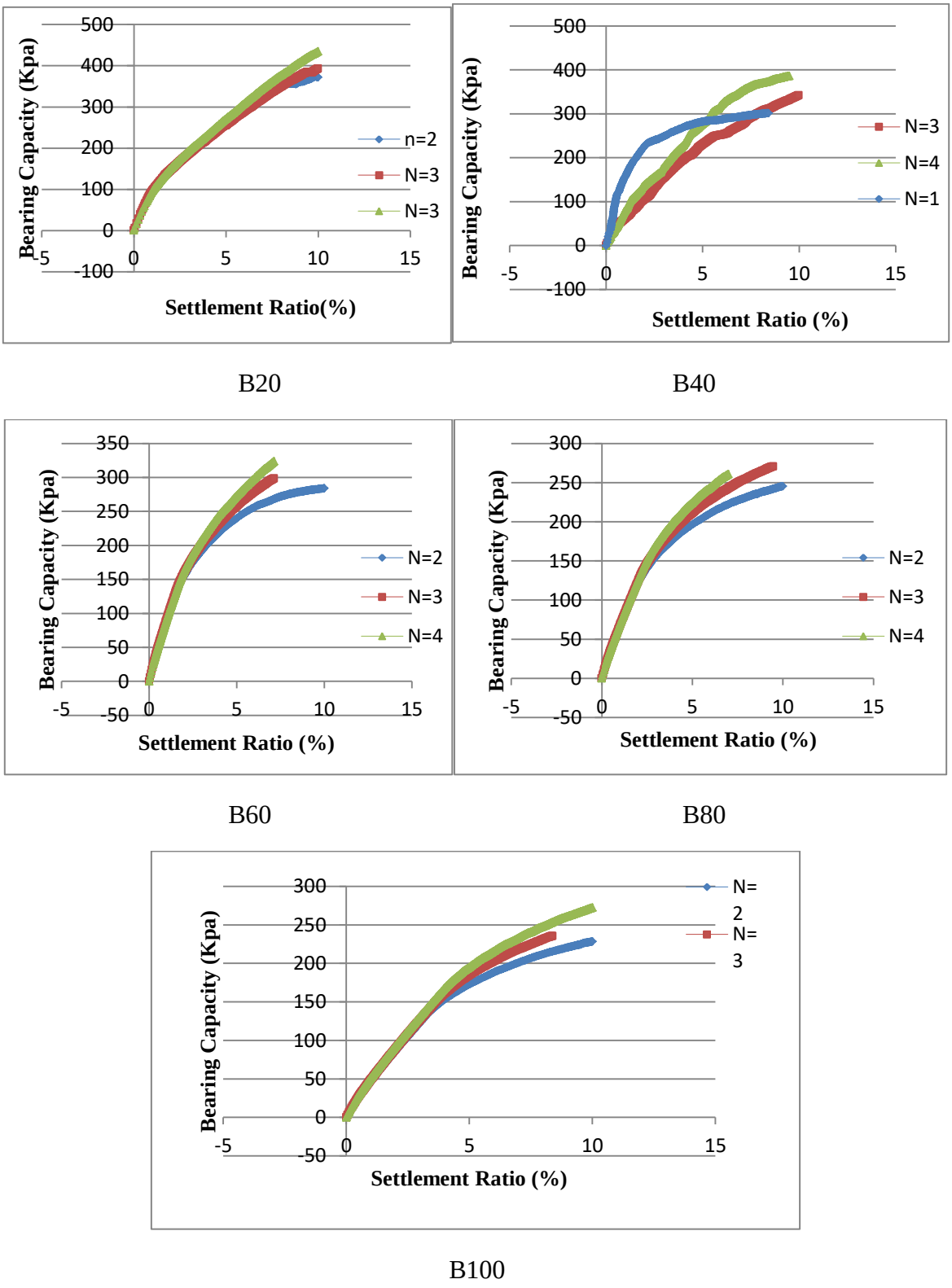
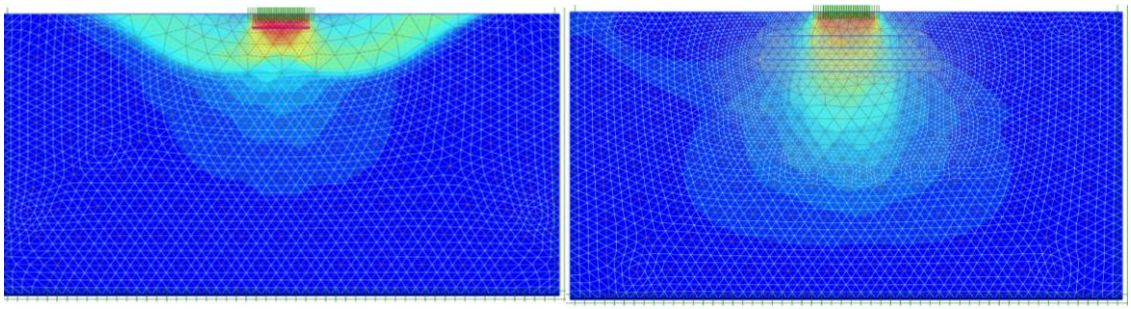


Figure IV-18 Simulated Bearing Stress Results Of Strip Footing Resting On Different Soils Reinforced With Different Reinforcing (Series F).

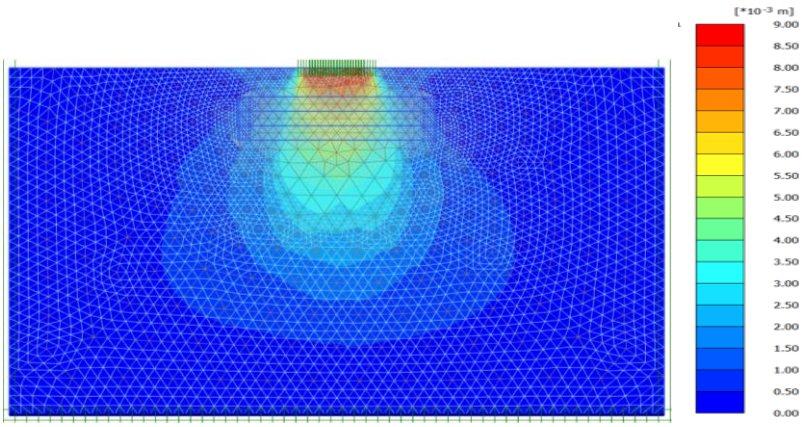
The results from Series F indicate a significant increase in bearing capacity across all soil types when the Full Wraparound system is applied with complete encapsulation — including top confinement using B0 soil.

This configuration proved to be highly effective, as the presence of strong B0 soil both inside and above the geotextile wrap allowed for better stress distribution and more efficient mobilization of tensile strength within the reinforcement.

Compared to the previous series, the results of Series F show the highest bearing capacities overall, confirming that the Full Wraparound method, when applied properly and completely, can significantly improve the behavior of weak soils.

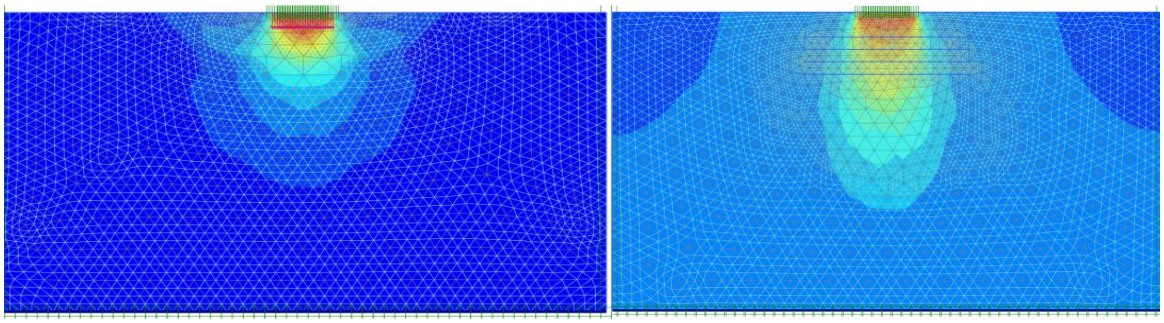


Series A Series C

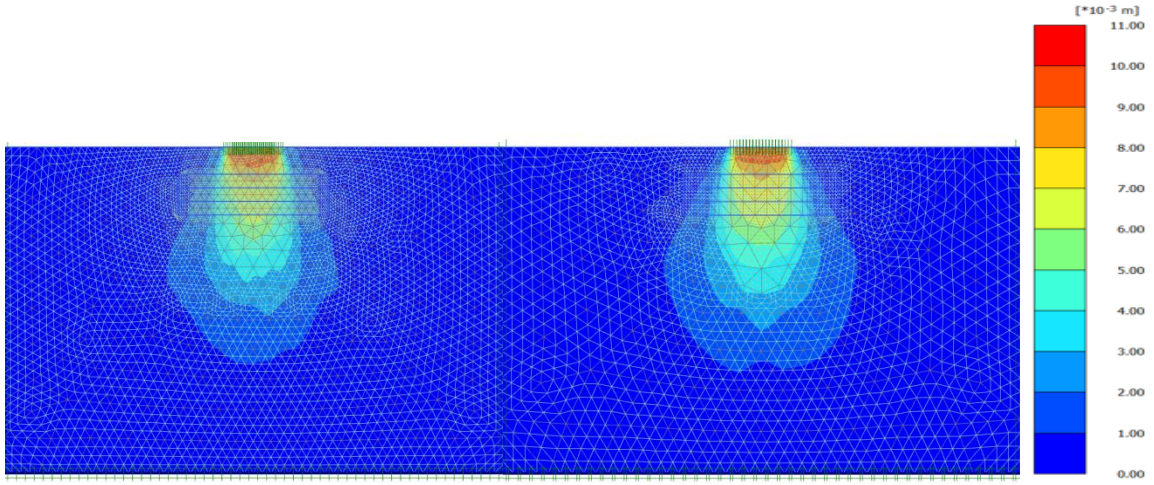


Series D

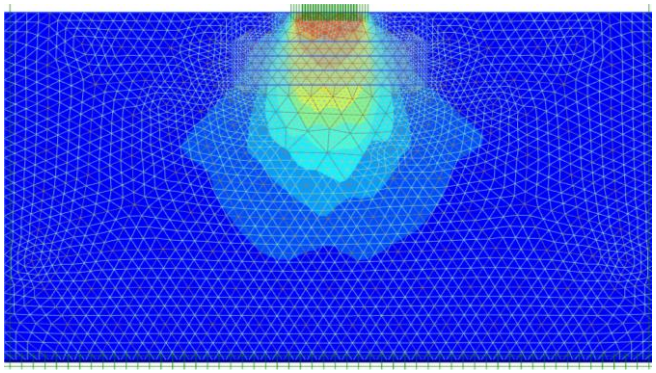
Figure IV-19 Simulated Stress Distribution Results Are Presented For Three Cases: (A) Unreinforced B0 Soil, (B) B0 Soil Reinforced Using Series C, And (C) B0 Soil Reinforced Using Series D, With N = 4 And A Settlement Ratio (S/B) Of 10%.



Series A **Series C**

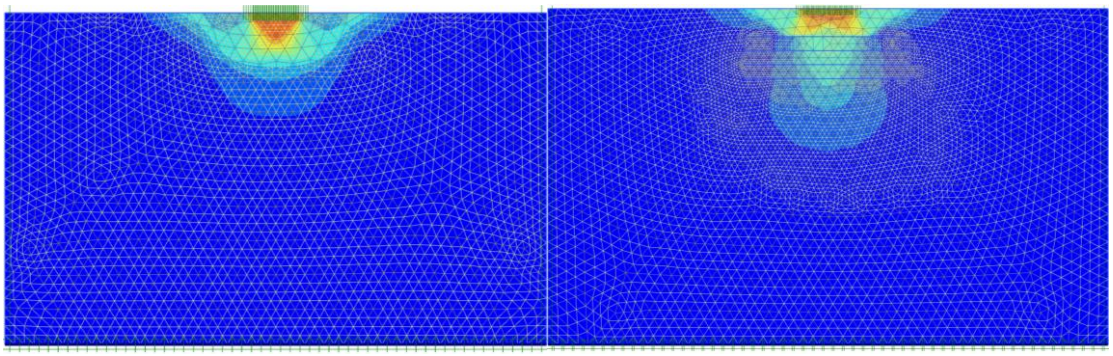


Series D **Series E**

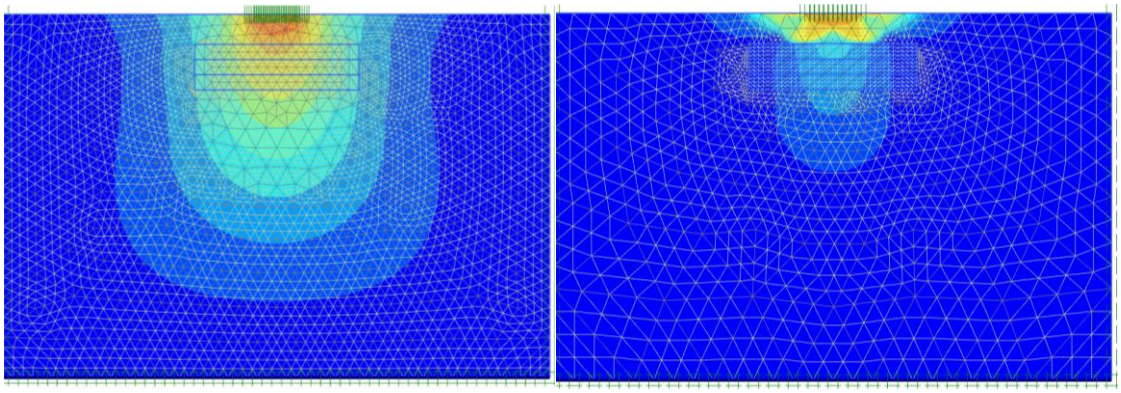


Series F

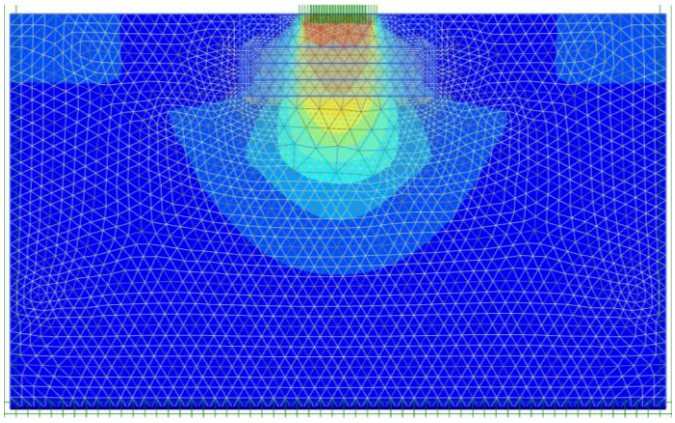
Figure IV-20 Stress Distribution for The Following Cases: (A) Unreinforced B20 Soil, (B) B20 Reinforced with Series C, (C) B20 Reinforced with Series D, (D) B20 Reinforced with Series E, and (E) B20 Reinforced with Series F. All Cases Correspond to N = 4 And A Settlement Ratio (S/B) Of 10%.



Series A Series C



Series D Series E



Series F

Figure IV-21 Stress Distribution for The Following Cases: (A) Unreinforced B40 Soil, (B) B40 Reinforced with Series C, (C) B40 Reinforced with Series D, (D) B40 Reinforced with Series E, and (E) B40 Reinforced with Series F. All Cases Correspond to N = 4 and A Settlement Ratio (S/B) Of 10%.

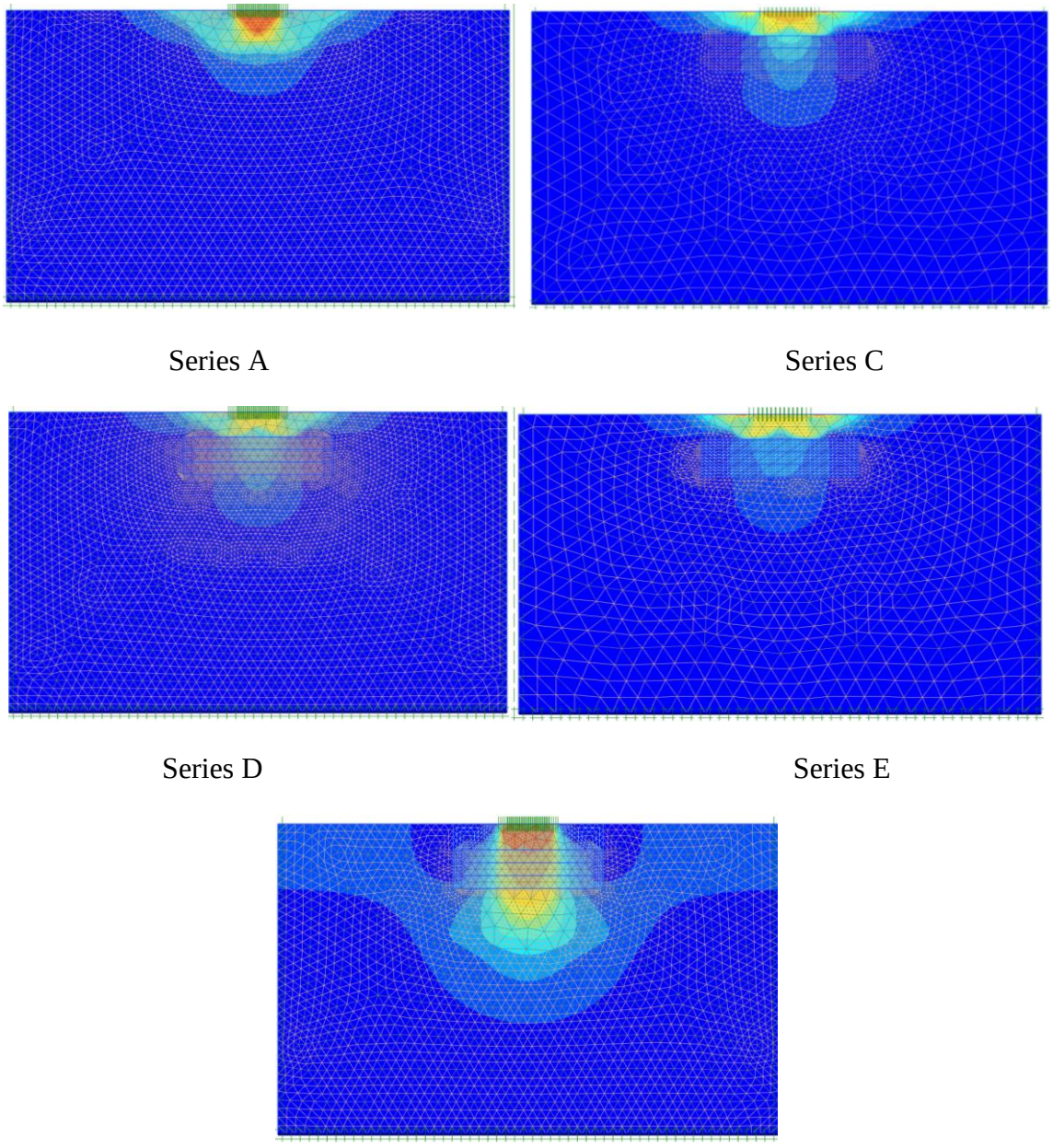


Figure IV-22 Stress Distribution for The Following Cases: (A) Unreinforced B60 Soil, (B) B60 Reinforced with Series C, (C) B60 Reinforced with Series D, (D) B60 Reinforced with Series E, and (E) B60 Reinforced with Series F. All Cases Correspond to N = 4 and a settlement Ratio (S/B) Of 10%.

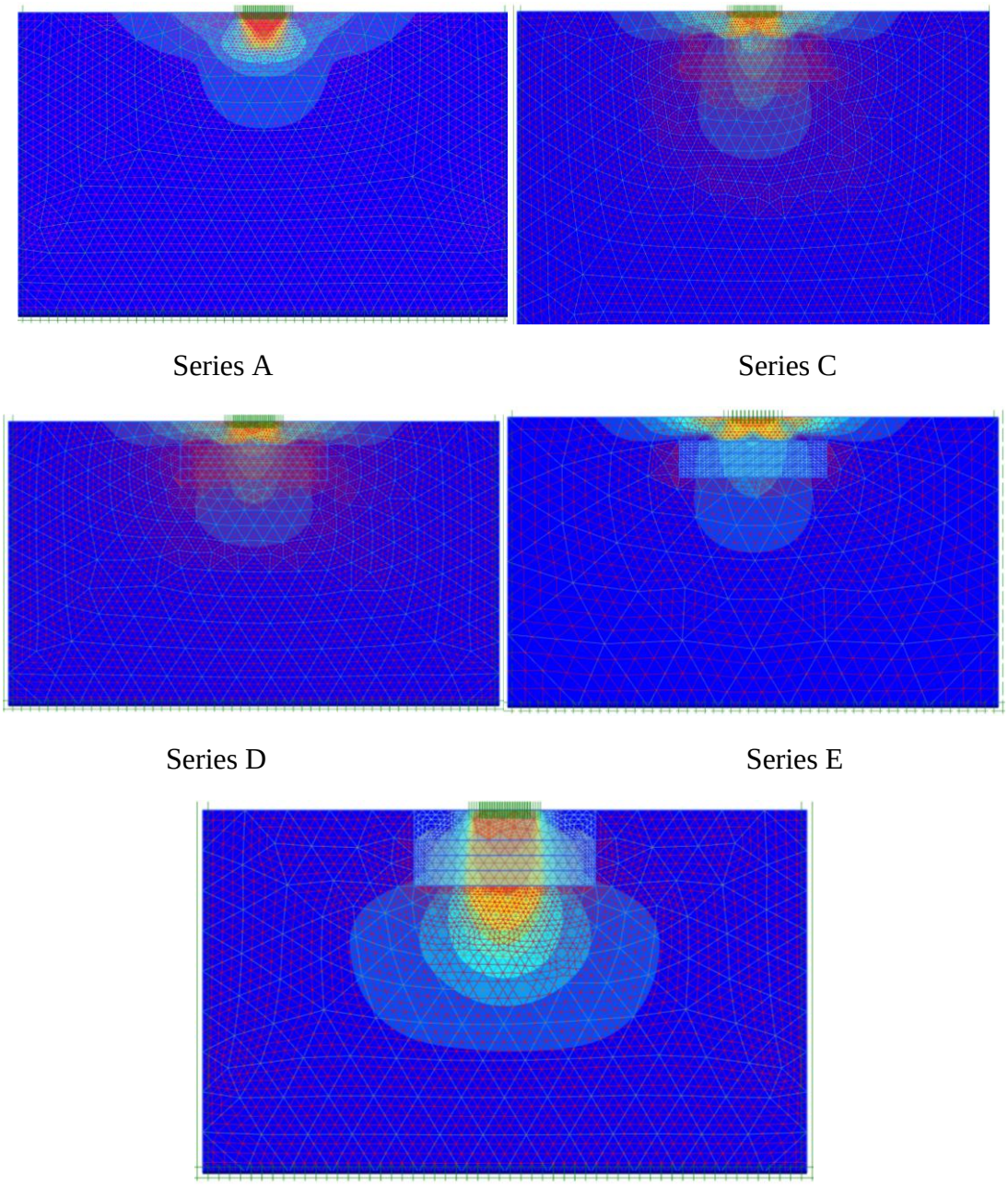


Figure IV-23 Stress Distribution for The Following Cases: (A) Unreinforced B80 Soil, (B) B80 Reinforced with Series C, (C) B80 Reinforced with Series D, (D) B80 Reinforced with Series E, and (E) B80 Reinforced with Series F. All Cases Correspond to N = 4 and a settlement Ratio (S/B) Of 10%.

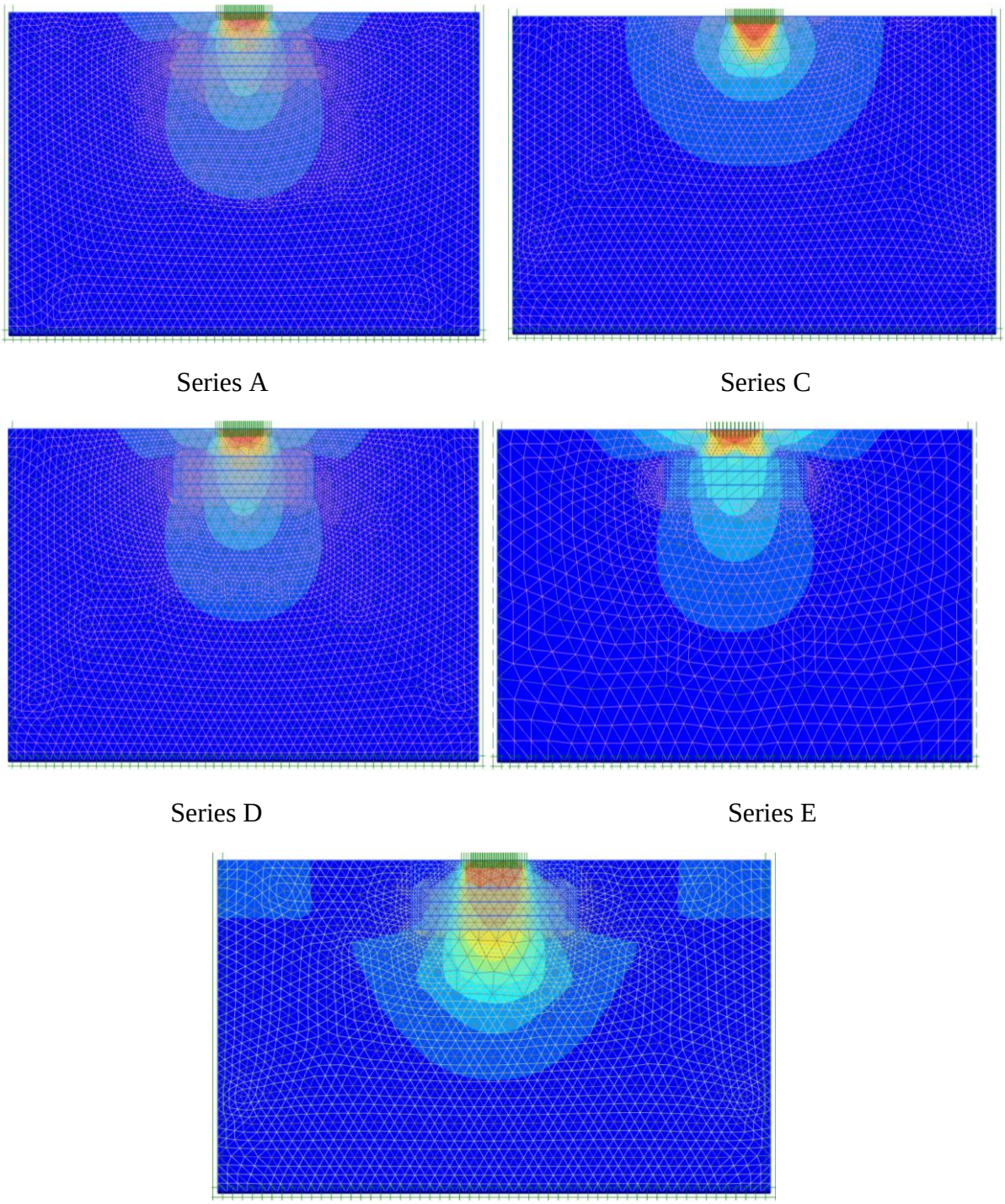


Figure IV-24 Stress Distribution for The Following Cases: (A) Unreinforced B100 Soil, (B) B100 Reinforced with Series C, (C) B100 Reinforced with Series D, (D) B100 Reinforced with Series E, and (E) B100 Reinforced with Series F. All Cases Correspond to N = 4 and a settlement ratio (S/B) Of 10%.

Ⅳ-8 Conclusion

The numerical simulations carried out in Chapter 4 clearly demonstrate that geotextile reinforcement can significantly improve the ultimate bearing capacity of shallow foundations, especially when the reinforcement is properly designed and fully confined.

Among the techniques evaluated, the Full Wraparound method with complete encapsulation (Series F) produced the best results, maximizing the interaction between the geotextile and the soil mass.

Using B0 soil as the internal and top fill further enhanced performance by increasing stress distribution efficiency.

It is concluded that:

- Reinforcement is most effective when tensile forces are fully mobilized through proper confinement.
- The choice of soil properties (strong internal core) and reinforcement arrangement (complete wrapping) plays a critical role.
- Over-reinforcement without careful planning can lead to diminishing returns.

These findings provide practical insights for the optimized design of reinforced shallow foundations in geotechnical engineering applications.

General Conclusion

General Conclusion

This master's thesis has presented a comprehensive numerical investigation into enhancing the bearing capacity of Cohesive-Frictional soils through geotextile reinforcement, with particular emphasis on the Full Wraparound technique. The research methodology progressed from a rigorous theoretical framework to sophisticated numerical analysis using PLAXIS 2D software, systematically evaluating multiple soil types and reinforcement configurations.

The findings unequivocally demonstrate the significant advantages of geotextile reinforcement—particularly the Full Wraparound method—compared to conventional horizontal reinforcement techniques. This innovative approach, which completely encapsulates the soil mass from all sides including the upper surface, proved remarkably effective in enhancing bearing capacity, even in substantially weak soil conditions. A principal benefit of this methodology is its capacity to reduce required foundation dimensions, thereby enabling more compact structural designs without compromising structural integrity or safety factors.

Furthermore, the technique exhibits considerable economic viability as a cost-effective alternative to deep foundation systems or more complex soil improvement methodologies. Through identification of optimal parameter ranges—including reinforcement depth (U), width (W), vertical spacing (H), and number of layers (N)—this study establishes a robust framework for designing reinforced soil foundations that maximize both efficiency and economy.

In conclusion, this research makes a significant contribution to geotechnical engineering by introducing and validating a novel, practical reinforcement technique. It advocates for the implementation of advanced numerical modeling to develop innovative, space-efficient, and economical foundation solutions for structures built on weak or marginal soils.

References

- [1] Prasad, S. K. (n.d.). *Bearing Capacity of Soil: Terzaghi's Theory & Definitions*. StudyLib. Retrieved May 13, 2025, from https://studylib.net/doc/8477708/bearing-capacity-of-soilstudylib.net
- [2] Ambo University, Department of Civil Engineering. (n.d.). Soil mechanics II: Lecture notes [Lecture notes]. Ambo University, Institute of Technology.
- **[3]** Das, Braja (2007), Principles of Foundation Engineering (6th ed.), Stamford, CT: Cengage Publisher
- [4] Sahani, B. (n.d.). *Foundation Engineering* [Lecture notes]. GITAM Deemed to be University. Retrieved May 13, 2025, from https://gitam.ac.in/wp-content/uploads/2024/03/BS-Sahani-Fe-note.pdf
- [5] Das, B. M. (2007). *Principles of Foundation Engineering* (6th ed.). Stamford, CT: Cengage Learning.
- [6] Das, B. M. (2007). *Principles of Foundation Engineering* (6th ed.)
- [7] Budhu, M. (2011). Soil mechanics and foundations (3rd ed.). John Wiley & Sons.
- [8] Coduto, D. P. (2001). *Foundation Design: Principles and Practices*. Prentice Hall.
- [9] Densification. (n.d.). *Dynamic Compaction 101: The Ultimate Guide for Beginners*.
- [10] Akhtar, S. (2018). *Dynamic Compaction*. Indian Institute of Engineering Science and Technology, Shibpur. Retrieved from
- [10] Liao, W., & Whitman, R. V. (1986). *Dynamic compaction of cohesionless soils*. Journal of Geotechnical Engineering, 112(8), 1001–1017.
- [12]Hamakareem, M. I. (2019). *Dynamic Compaction: Advantages, Purposes, and Uses*. The Constructor.
- [13] Gaafer, M., Bassioni, H., & Mostafa, T. (2015). *Soil improvement techniques*. *International Journal of Scientific & Engineering Research, 6*(12), 217–222. Retrieved
- [14] The Constructor. (n.d.). *How to Select Soil Improvement Method Based on Soil Types?*
- [15] Das, B. M., & Sobhan, K. (2017). *Principles of geotechnical engineering* (9th ed.). Cengage Learning.
- [16] Han, J. (2015). *Principles and Practice of Ground Improvement*. John Wiley & Sons.

- [17] SKDAV Polytechnic. (n.d.). Soil reinforcing techniques [PDF]. https://www.skdavpolytech.ac.in/lecture_files/soil_reinforcing_techniques_(1)_1649587227.pdf
- [18] Gul, M. F. G. b. H. G., Baki, S. S. B. H., Kamis, H. B., & Othman, N. A. B. M. (n.d.). Literature review: Soil reinforcement [Unpublished manuscript].
- [19] Balcos, M. F. M. (2018). Geotextiles [Unpublished individual project paper]. Department of Civil Engineering, De La Salle University.
- [20] Koerner, R. M. (2005). Overview of geosynthetics (6th ed.). Geosynthetic Institute.
- [21] Sukmak, G., Sukmak, P., Horpibulsuk, S., Hoy, M., & Arulrajah, A. (2021). Load bearing capacity of cohesive-frictional soils reinforced with full-wraparound geotextiles: experimental and numerical investigation. Applied Sciences, 11(7), 2973.